Molecular and functional characterization of lysophospholipase like proteins in *Plasmodium falciparum* as novel drug targets

Thesis submitted for the award of degree of

Doctor of Philosophy

To

Jawaharlal Nehru University

New Delhi, India

By

Pradeep Kumar

Parasite Cell Biology Group

International Centre for Genetic Engineering and Biotechnology

New Delhi, India

2020

INTERNATIONAL CENTRE FOR GENETIC ENGINEERING AND BIOTECHNOLOGY

ICGEB Campus, Aruna Asaf Ali Marg,
New Delhi - 110 067, India
http://www.icgeb.org

Tel. : 91-11-26741358/61
91-11-26742357/60
91-11-26741007
Fax : 91-11-26742316
UIN NO.: 0717UNO00161UNZ
E-mail : icgeb@icgeb.res.in

Certificate

This is to certify that the research work embodied in this thesis entitled **"Molecular and functional characterization of lysophospholipase like proteins in *Plasmodium falciparum* as novel drug targets"**, submitted for the award of degree of Doctor of Philosophy, is the bona fide work of Pradeep Kumar conducted at Parasite Cell Biology Group, International Centre for Genetic Engineering and Biotechnology, New Delhi, India. This work is original, and no part of this thesis has been submitted for the award of any other degree or diploma to any other university.

Dr. Asif Mohmmed
Group Leader
Parasite Cell Biology
ICGEB, New Delhi

Dr. Asif Mohmmed
(Supervisor)
Parasite Cell Biology Group
ICGEB
New Delhi-110067
India

Director

2020

Prof. Dinakar M. Salunke
(Director)
Structural Immunology Group
ICGEB
New Delhi-110067
India

DECLARATION

I hereby declare that the research work embodied in this thesis entitled **"Molecular and functional characterization of lysophospholipase like proteins in *Plasmodium falciparum* as novel drug targets"** has been carried out by me under the supervision of Dr. Asif Mohmmed at the Parasite Cell Biology Group, International Centre for Genetic Engineering and Biotechnology, New Delhi, India.

Date:

Pradeep Kumar
Ph.D. student (Candidate),
Parasite Cell Biology Group,
ICGEB, New Delhi 110067,
India

DEDICATED

TO

MY FAMILY

Acknowledgements

The submission of my thesis gives me immense pleasure, satisfaction, and a unique sense of accomplishment despite many difficulties and troubles that came in its way. On this moment of submission of my PhD thesis, I would like to thank all the people who have contributed and inspired me during my doctoral study.

First, I would like to express my deep sense of gratitude to my mentor, **Dr. Asif Mohmmed** for providing me an opportunity to work with him. I am indebted to his constant guidance, encouragement, enthusiasm. He is always enthusiastic and encouraging about science, his constructive comments, positive attitude greatly helped me during my Ph. D tenure. His insights into the field of parasite biology made me realize and understand the subject in a broader perspective. I also thank him for his care and consideration.

I would like to express deep regards and gratitude to **Dr. Pawan Malhotra**. Sir's ever enthusiastic approach and passion for scientific research has always been a source of great inspiration for his ever-willing guidance and interest in the progress of this study. His words and name for me, '*Chotu Jaat*' will always be dear to me and reminder of his cheerful aura.

I wish to thank director of ICGEB **Prof Dinakar M. Salunke** for giving me an opportunity to pursue PhD in the exceptional working atmosphere at ICGEB and providing excellent experimental facilities. I would like to thank **Dr. Renu Tuteja** for her unconditional support and treating me as a part of her group. I have debt of gratitude for my doctoral committee members **Dr. Dhiraj Kumar** and **Dr. Dinesh Gupta** for their continuous guidance essentially required for the accomplishment of my thesis work.

I also extend my acknowledgements to **Dr. Inderjeet Kaur** for acquisition of mass spectrometry samples. My sincere thanks to the entire technical

staff of ICGEB, who have helped me to the best of their capabilities. I am grateful to **Purnima mam** for teaching and helping me with the confocal microscope with an ever-consistent smile and patience. I would like to thank the animal house staff members **Ashok ji, Rakesh ji, Munna ji** and **Patra ji** for their efforts and helping me in handling mice and rabbits. May God forgive me for sacrificing the life of all those animals. I am grateful to the financial, academic, and technical support of the ICGEB. The support and concern of **Mayank sir, Sachin sir**, and **Pratibha mam** during all these years at ICGEB have been indispensable.

Thanks to **Narender ji** for maintaining our entire lab and providing all the resources required for research work.

I would like to thank all the present and past members of **AM group**; Sumit Sir, Asad Sir, Shaifali Ma'am, Dipto Sir, G.D Sir, Mudassir Sir, Azhar Sir, Vandana Maam, Shweta, Monika Narwal, Shilpi Jain, Priya Arora, Omair, Muzahid, Sheetal, Vivek, Pooja, Harsheeta, shantanu, Aakansha, Pranay and Areej for providing a lively, intellectual and supportive environment. I would also like to thank all members of the **PM group**: Ekta Saini, Ashutosh Sir, Asif Sir, Kalam Sir, Gourab Sir, Aditya, Priya, Sadaf, Vaibhav, Rashmita, Osama, Iqbal, Noah, Mohit Sir, Khushboo Maam, Tarushikha, Shreyansh, Gautam Sir and **RT group**; Manish, Tarique, Suman, Vipin, Moaz, Farhana, Rahena, Isha and many more who came and left in between for countless day to day help during these years.

I am highly indebted to my lab mates for everything starting from work cooperation to being problem solvers in every aspect of my life. I owe special thanks to **Mudassir (Muddu) Sir** for being a great senior, a special friend and most importantly for his encouragement and ever serene attitude during our discussions even the once on negative results (*Koi ni dobara krte hein*). He is the most patience personality I have ever seen in

my life. I will always remember his words about our lab '*Tote tum Jannat me ho'*.

Special thanks to **Azhar Sir** for sharing his protocols, special tricks, and scientific discussions. He is the first person I looked for whenever I got stuck and most of the time, he had answers to all my queries. Special thanks to him for handing my cultures during my home visits and endless scientific discussions with you were a treat.

Asad sir deserves a special mention for giving me his working bench and most importantly handling and managing the whole lab with so much patience. I would like to thank **Dipto Sir** 'comedian' of the group for making all of us laugh our heart out even during the most serious situations. I am grateful to **Vandana Mam** for teaching me culture basics. I would like to thank **Shweta Singh** for her cheerful good morning greetings and our silly fights. I would like to acknowledge **Sheetal** for our non-scientific long conversations, **Priya Arora** for helping me in my research work, **Vivek Nair** for his love and specially for PUBG matches. I am fortunate for having lovely and best juniors; **Shilpi** and **Muzahid**.

Special Thanks to **Shilpi** (*Baby Boss*) a student, a friend and even a kid for her cheerful company and silly queries.

I am grateful to **Monika Narwal** *(The Silent Sneezer)* for being my friend. She is one of the most mentally strong personality I have seen. She taught me how to survive during the tough times. I will remember her for her comment 'Kuch Bhi' on my weird and silly jokes and making tea for me during my thesis writing days.

Contributions of **Sadaf Shehzad** for help in bioinformatics work is gratefully acknowledged.

I take this opportunity to thank my seniors Haroon, Niharika, Rajan, Dileep, Nishat, Shabnam, for their help, support, and suggestions. I have been lucky to be blessed with exemplary juniors in Prakhar, Mamta Yadav, Vipul Swarup, Ganesh, Swati, Vivek Sharma, Raman, Anju, Iqra, Saeed, Charu, Hasan, Ankit. I thank them for their constant hellos and cheerful smiles throughout my PhD period which gave me a reason to smile every day. Special thanks to **Mamta Yadav** for bringing home made Haryanvi food (Churma, lassi and Bajre ki roti) which I missed during my stay here and **Charli** for her cheerful personality.

Friendship is not a big thing- It is a billion little things. I have been fortunate to find some extremely good friends *'My Buddies'* with whom I spent most of the time outside the lab. I would thank all my friends from the bottom of my heart: Ashish Subba *(laughing Budda),* Bhabesh *(Chao)* Manish (Mani), Ekta Saini (Neta Ji), Sandeep Kaushik *(Sundi), Kashif (Saxena), Niharika (Nikki, Lombdi), Jaspreet Kaur (Jassi), Afreen, Veena ji, Garima Verma, Sneha, Keshav Saini, Rokeb.*

I would like to thank **Subba, Mani bhai** and **Chao** for being my room partners and bearing my cranky nature during this journey. I feel blessed to have you all in my life and thankful to you guys for our weekend parties during our initial phase of Ph.D. I can say, that was the best time of my PhD tenure and I will cherish those lovely and cheerful moments throughout my life.

I would like to thank **Sundi,** a brother from another mother, a friend for over a decade now, for his unconditional love and care. He is the person whom I can call in the middle of night (my 4 AM friend) and he has always been there whenever I needed him, and I know he will be there for me in future as well.

I am extremely fortunate to have **Kashif Mohmmed (Saxena)** as my friend. He is also one of the most good-hearted persons I have met. I owe him for handing me over his nano (dhanno) whom I exploited and learned driving.

I would like to thank **Ekta Saini**, my greatest support during these years. She is the most selfless and caring person I have ever met. I am indebted to her for her unconditional love and untiring support and care. She is one of the few people I look for in a crowd to share my joy and sorrow. I am thankful to her for providing me lab reagents and bearing with me for all these years. Special thanks to her for making delicious food during the lock-down period. I am forever in her debt for keeping me from falling when I was about to give up. Words fail me to describe how grateful I am to have her as a friend. I would just like to say thanks for being there.

Special thanks to **Anjali behen,** a friend, a guardian, a sister for providing a sparkling company and a full-time support system which has helped me to get a better understanding of the outside world and remain sane during this entire time.

I feel fortunate and special to get travel grants from **ICMR, DBT, Molecular Parasitology Meeting (MPM2019)** and **Molecular approaches to Malaria meeting (MAM2020),** for travel support for attending several conferences during my PhD around the globe (France, USA, Australia). My sincere thanks **Haroon Kalam, Muddu Sir** and **Sachin Khurana** for their wonderful hospitality during my visits to USA and Australia.

I would like to special acknowledge for my **PUBG ke mareej** (Killwish, Mogambo, Kancha, Shakal, Vasooli, Gabbar, Khush, Nashedi Kashif, Jageera, Komolika, Someone and Nakita). Their company in this game helped me relieving my stress during the tough times.

I thank **UGC**, for granting me the UGC-JRF Fellowship to carry out my PhD work at ICGEB. The financial support provided by UGC, Govt. of India in the form of JRF and SRF is duly acknowledged.

I dedicate this thesis to my family who has been with me through the thick and thin and everything in between. My parents who bought me into this world and provided me with everything I could I ever need. They believed in me and let me make my own way. I am thankful to my brother (**Sumer Singh**) and bhabhi (**Monika Nandal**) for their love and care. They made me an independent person but have always been there for me. Their belief in me has always carried me forward when I thought of quitting. I can never have enough words to describe how much I love them and how grateful I am to have them as my support system. Thankyou Maa, Papa, Bhai, Bhabhi and Jashan, Rishika and Rahul for everything, your unconditional love has been my greatest strength.

At the end, I would like to apologize to those whom I could not accommodate in this note, but I would like to express my heartfelt gratitude to all those who went unmentioned in this note of acknowledgement.

Abbreviations

Aa	amino acid
Ab	Antibody/antibodies
Amp	Ampicilline
ATCC	American Type Culture Collection
APS	Ammonium per sulfate
bp	Base pairs
BSA	Bovine serum albumin
cDNA	Cytoplasmic DNA
CHAPS	3-[(3-cholamidopropyl) dimethylammonio]-1-propanesulfonate
cm	centimeter
C-terminal	Carboxy terminal
DAB	Diamino benzidine
DD	Degradation domain
DNA	Deoxyribose nucleic acid
dNTPs	Deoxynucleoside triphosphate
DTT	Dithiothreitol
EDTA	Ethylenediaminetetraacetic acid
ELISA	Enzyme-linked immunosorbent assay
ER	Endoplasmic reticulam
FACS	Fluorescence activated cell sorter
FBS	Fetal Bovine Serum
FITC	Fluorescein isothiocyanate
FKBP	FK506 binding protein
FV	Food vacuole
FAs	Fatty acids

GFP	Green fluorescent protein
HA	Hemagglutinin tag
hDHFR	Human dihydrofolate reductase
His	Histidine
hr	hour(s)
HRP	Horse radish peroxidase
Hsp	Heat shock protein
HPI	Hours post invasion
IPTG	Isopropyl β-D-thio-galactopyranoside
IgG	Immunoglobulin G
kDa	Kilo Dalton
kb	Kilo base pairs
L	Litre
LB	Luria-Bertani
LPLs	Lysophospholipases
LPC	Lysophosphatidylcholine
M	Molar
mAb	Monoclonal Antibody
µF	micro-Farad
µg	micro-gram
µl	micro-litre
µm	micro-metre
min	minute(s)
mg	milli-gram
ml	milli-litre
mM	milli-molar
mRNA	messenger RNA

MSP1	Merozoite Surface protein 1
N	Normal
ng	nano-gram
Ni-NTA	Nickel-Nitriloacetic acid
nm	nanometre
N-terminal	Amino terminal
Ω	Ohm
OD/OD_{600}	Optical density/ Optical density at 600nm
O/N	Overnight
ORF	Open reading frame
PAGE	Polyacrylamide gel electrophoresis
PBS	Phosphate buffered saline
PBST	Phosphate buffered saline with Tween 20
PCR	Polymerase chain reaction
PV	Parasitophorous vacuole
PVM	Parasitophorous vacuolar membrane
i-RBCs	Infected red blood cells
RBCs	Red blood cells
rpm	Revolutions per minute
SDS	Sodium dodecyl sulphate
TE	Tris-EDTA
TEMED	N, N, N', N' - Tetramethylethylenediamine
V	Volt
WHO	World Health Organization

Table of Contents

Chapter 1 Introduction

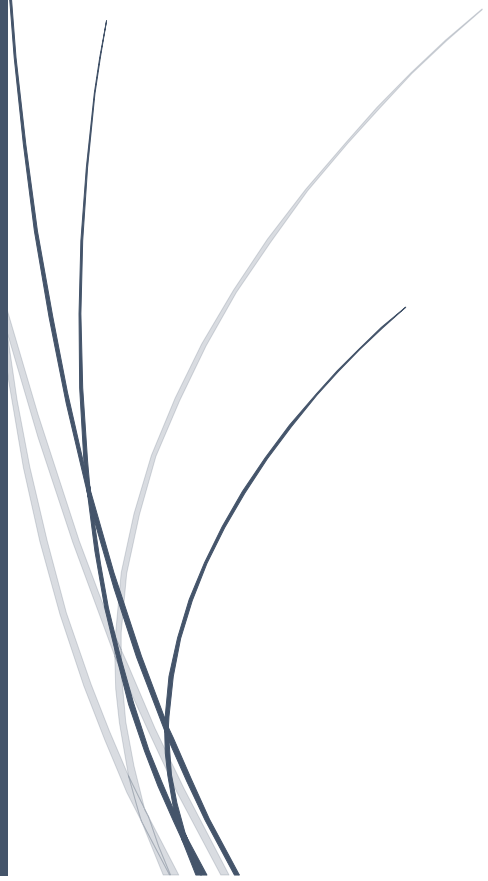

1. Introduction and Objectives

Malaria is a vector transmitted parasitic disease which remains to be major medical problem in tropical and sub-tropical areas of the world; malaria leads to ~500,000 to 1 million deaths globally every year (Hay et al., 2010; O'Brien et al., 2015; WHO, 2019). Absence of efficient vaccine along with the rapid spread of drug resistant parasites strains, made it imperative to discover and validate new drug-targets against the disease. Understanding of key metabolic pathways essential for parasite survival remains to be the pre-requisite to identify unique and potent drug targets in the parasites. The pathological symptoms of malaria are caused by recurrent blood stage asexual cycles of the parasite in host erythrocytes. Different parasite development stages during the asexual life cycle involve extensive lipid synthesis, modification of host cell membrane, and biogenesis membrane needed for parasite division and propagation (Botte et al., 2013; Dechamps et al., 2010). This high demand of lipids/phospholipids required for extensive membrane synthesis is fulfilled by scavenging from the host milieu, degradation, modification as well as through *de novo* synthesis. Indeed, it has been shown that asexual blood stages parasite can both scavenge and synthesize up to 300 different lipid species for their growth and proliferation (Gulati et al., 2015). The Phospholipids, including phosphatidylcholine (PC), phosphatidylethanolamine (PE), and phosphatidylserine (PS), are the major structural components of the membranes. In addition, recent studies have shown that phospholipid by-products also act as signalling molecules to control differentiation and development process in the parasite (Bobenchik et al., 2013; Pessi et al., 2004; Witola et al., 2008). PC is shown to be the major phospholipid in *Plasmodium* membranes during both liver stage and intra- erythrocytic schizogony, suggesting its importance for parasite multiplication. The parasite possesses *de novo* phospholipid synthesis machinery, Kennedy pathway, CDP-DAG pathway, which is capable of assembling and synthesizing PA, DAG, CDP-DAG lipid precursors as well as major phospholipid classes PC, PE, PS, PI, PG, CL using precursors lyso-lipids (Ramakrishnan et al., 2013). *P. falciparum* blood stages notably relies on the scavenging of lysophosphatidylcholine (LPC), to utilize its polar head phosphocholine to fuel *de novo* synthesis of the major membrane lipid of the parasite, (Bhanot et al., 2005; Kilian et al., 2018; Wein et al., 2018).

Since LPC plays an important role in parasite development and differentiation, enzymes involved in its hydrolysis are considered as attractive targets for antimalarial development (Hanada et al., 2002). In summary, *P. falciparum* blood stage parasites relies on the scavenging of phospholipids/FA/lysolipids from host as well as on the metabolic pathways for degradation and reassembly of the phospholipid building blocks (FA, polar heads, lysolipids). This catabolism of lipid metabolites from the host must involve phospholipases to manipulate the scavenged lipids and generate the proper lipid moieties. Indeed, parasite contains several phospholipases, harbouring α/β hydrolase domain, including a family of lysophospholipase (LPL) (Flammersfeld et al., 2018). The LPLs play key role in recycling of lipids by hydrolysis of acyl chains from lysophospholipids, which are the intermediated in metabolism of membrane phospholipids.

In the present study, we have biochemically and functionally characterized three LPLs in *P. falciparum*: *Pf*LPL3, *Pf*LPL4, and *Pf*LPL20. In first part of the research work, we studied the enzymatic properties of these proteins. All these targets were expressed as recombinant proteins which showed characteristic LPL activities. The activity assay standardised here was used later for compounds library screening. In the second part of the thesis, we utilized reverse genetic approaches, metabolic and lipidomic analysis, as well as transcriptomic analysis to assess functional role of these targets. Generation of gene knock-out parasite cell line is the direct approach for gene function analysis; however due to several technical challenges in disruption of essential genes in *P. falciparum* blood stages, novel tools have been developed for gene functional analysis, which include the transient knock-down of target gene using degradation domain or ribozyme tagging (de Azevedo et al., 2012; Prommana et al., 2013). We have used DD-GFP and GFP-*glmS* ribozyme system for C-terminal tagging of the native *PfLPL* genes for endogenous localization as well as transient down-regulation of *Pf*LPL protein during the parasite blood stages. The GFP targeting showed *Pf*LPL3 to be localized in parasitophorous vacuole as well as extending into the tubulovesicular network space during the trophozoite and schizont stages. Transient knock-down of *Pf*LPL3 caused decrease number of schizont development as well as decreased number of merozoites generated in each schizont. To further assess mechanistic details of *Pf*LPL3 function, we performed lipidomic analyses,

which showed that parasites lacking *Pf*LPL3 displayed fluctuations in fatty-acids, phospholipids, and neutral lipids contents. Overall, we show that *Pf*LPL3 plays essential role in lipid homeostasis linked with generation of fatty acids required for parasite growth as well as for the membrane synthesis during the schizogony.

We utilized *glm*S mediated knock-down of another phospholipase *Pf*LPL20 to understand its functional role in the parasite. In *Pf*LPL20 depleted parasites, transcript levels of the enzymes of SDPM pathway (Serine Decarboxylase-Phosphoethanolamine Methyltransferase) were altered along with significant increment in levels of phosphocholine; these results show upregulation of an alternate pathway to generate the phosphocholine that can be utilized for PC synthesis through Kennedy pathway. Our study highlights presence of alternate pathways for lipid homeostasis/membrane-biogenesis in the parasite; these data could be useful to design future therapeutic approaches targeting phospholipid metabolism in the parasite.

In the third part of the thesis, we identified specific inhibitors for validated drug targets for *Pf*LPL3. *In-vitro* activity assay-based screening of MMV "Malaria Box" identified specific inhibitors of *Pf*LPL3 enzymatic activities with potent parasiticidal efficacies, these compounds can be further developed into new antimalarials targeting lipid homeostasis machinery in the parasite.

OBJECTIVES

Overall aim of the project is biochemical and functional characterization of *Plasmodium falciparum* lysophospholipases with a view to validate these as novel drug targets for malaria and identify specific inhibitors for these enzymes.

To fulfill the above-mentioned goals of this project, we have laid out the following specific objectives for the study.

1. To understand functional significance of selected lysophospholipases of *P. falciparum* by gene knockout/ knock-down approaches.
2. To understand role of selected lysophospholipases in lipid homeostasis in the parasite.
3. To characterize biochemical activities of these lysophospholipases.
4. To identify specific inhibitors of enzyme activities of selected lysophospholipases as lead candidates that can be developed as new antimalarials.

Chapter 2

Review of Literature

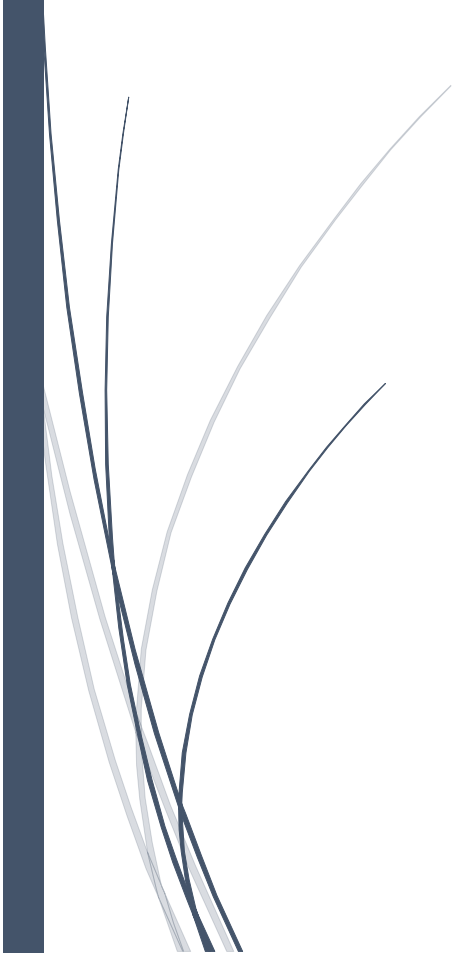

2. Review of Literature

2.1 Malaria: An enduring challenge

Malaria, the vector-borne infectious disease caused by protozoan parasite is found in more than 80 countries worldwide. This is the major life-threatening disease in humans and particularly rampant in tropical and subtropical regions of the world. According to the World Health Organization (WHO), more than 228 million cases of malaria happened worldwide in 2018 out of this, approximately 213 million cases were from African region. This parasitic disease caused 405000 deaths globally and the most vulnerable group is the children aged under 5 years. An estimated 272000 children died in 2018 due to malaria (WHO, 2019). Poor economy of tropical and subtropical countries results in a weak infrastructure and poor health care system responsible for high mortality there. Malaria is caused by the protozoan parasite and is transmitted by the female Anopheles mosquito. Disease incidences are linked to poverty, natural disaster hence depends on the environmental factors in terms of altitude, vegetation, climate, and implementation of control measures (Abdullah and Karunamoorthi, 2016; O'Brien et al., 2015). There are approx. 200 species in genus *Plasmodium* which further divided into many subgenera. At least 10 of them can infect humans but malaria is majorly caused by four *Plasmodium* species: *P. falciparum*, *P. vivax*, *P. malariae* and *P. ovale*.

P. falciparum and *P. vivax* are mainly responsible for the malaria burden worldwide. According to WHO malaria report 2019, *P. falciparum* is responsible for more prevalent malaria cases in WHO African region (99.7%) in 2018, as well as WHO Eastern Mediterranean Region (71%), WHO Western Pacific Region (65%), WHO South-East Asia Region (50%). Globally, 53 % of the *P. vivax* burden is in WHO South-East Asia Region, with majority in India (47%) and major parasite in the WHO region of the American, representing 75% malaria cases. *P. malariae* and *P. ovale* also have global distribution but the incidence is relatively low. *P. ovale* cases mainly occurred in Southeast Asia and Africa. The natural host of the *P. kowlesi* are macaques, however it is able to infect humans as well; and its high morphological similarities resulted in misdiagnosed as *P. malariae* initially in Malaysia which has its high burden (Singh et al., 2004).

2.2 Life Cycle of *Plasmodium falciparum*

Plasmodium life cycle is complicated and involves two hosts. At the end of the 19th century, it was believed that inhalation of dirty water leads to malaria. Different scientists had different opinions about the causative agent of malaria. Several biologists Patrick Manson (Manson, 1894), Koch, King (King, 1883), and Lavern (Laveran, 1884) developed the theory that mosquito bites may cause malaria. Later in 1898, Ronald Ross, in his experiments of 4 sparrows and a weaver bird, observed parasites in their blood after the biting of the infected mosquito (Manson, 1898). He demonstrated for the first time that the protozoan can infect two different hosts to complete its life cycle. Later in 1902 and 1907 Ronald Ross and Laveran, were awarded Nobel prize in physiology or medicine for their work, respectively.

Life cycle of the malaria parasite is quite conserved across the *Plasmodium* lineages that are infectious for mammals (Figure1). Life cycle starts when an infected mosquito bites human and takes a blood meal. During this, it injects sporozoites into the human skin and these sporozoites enter the blood stream to reach liver. This temporal location helps them to evade the host immune system and lymphatic system (Amino et al., 2006; Tavares et al., 2013). Sporozoites cross the sinusoidal barrier to reach and enter hepatocytes (Tavares et al., 2013). Next, parasite undergoes asexual reproduction to form thousands of daughter merozoites known as merosomes (Mota et al., 2001). The duration of the exoerythrocytic cycle is species dependent. Some parasite species, such as *P. ovale* and *P. vivax* can undergo the latency by forming hypnozoites instead of schizonts. These hypnozoites are non-replicating form which helps in the long-term survival of the parasite and responsible is for the relapses. In the cell, parasite completes its life cycle inside a double membrane structure known as the parasitophorous vacuole. There are two options for the hepatocytes released merosomes; either they can go to the exoerythrocytic cycle again or they can infect the RBC to complete their erythrocytic cycle. Parasite does not show any clinical symptoms during the liver stage cycle, so this phase is known as silent phase.

The merozoites invade the RBCs to complete the asexual blood-stage cycle and form schizont which produces up to 32 merozoites. The duration of the erythrocytic cycle again is species-dependent and can vary from 24 to 72 hours (24 hours in case of *P. knowlesi*, 48 h in case of *P. falciparum*, *P. vivax* and *P. ovale* and 72 h in *P. malariae* infection). The erythrocytic cycle is mainly responsible for malaria symptoms and leads to a high parasite burden which causes severe disease. Interestingly *P. vivax* restricted itself to the reticulocytes which represents only 1-2 % of the total RBCs. The sexual cycle begins when some of the merozoites commit for sexual progeny, that is the gametocytes which take several days to mature. These mature forms of the gametocytes are taken up by the mosquito and both male and female gametocytes egress from the RBCs to differentiate into microgametes and macrogametes respectively inside the midgut of the mosquito (Sologub et al., 2011). They both fuse to form the zygote which transforms into the ookinete. The ookinete can cross the midgut wall and form oocyst. At this stage, a parasite undergoes asexual replication again and forms thousands of the sporozoites. These sporozoites are released into the hemolymph of mosquito. These sporozoites reach the salivary glands of the mosquito and are transmitted to a new human host when mosquito takes a blood meal.

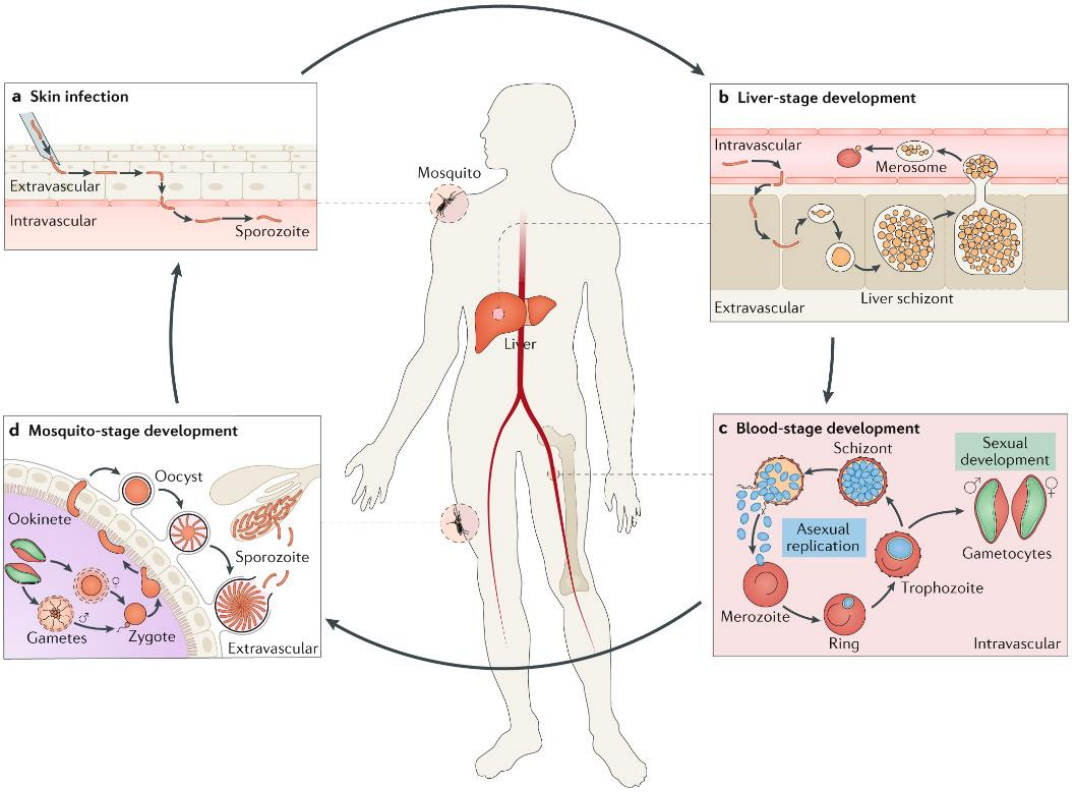

Figure 1: *Plasmodium falciparum* Life cycle: Life cycle of *P. falciparum* showing different stages in human host and mosquito: (A) Skin infection; (B) Liver stage development; (C) blood stage development; (D) Mosquito stage development. Source: (Venugopal et al., 2020)

2.3 Anti-malarial drugs and drug resistance

Several antimalarials drugs have developed for malaria therapy. Based on their chemical properties, anti-malarial drugs can be classified into 5 categories: -

1. **Antifolates:** Pyrimethamine (PYR), Cycloguanil (CYC), Sulfadoxin (SDX)
2. **Napthoquinones:** Atovaquone (ATQ)
3. **Aryl-amino alcohols:** Quinine (QN), Lumefantrine (LMF), Mefloquine (MFQ)
4. **4-aminoquinolines:** Chloroquine (CQ), Amodiaquine (AQ), Piperaquine (PPQ), Pyronaridine
5. **Antibiotics:** Clindamycin, Doxycycline
6. **Endoperoxides:** Artemisinins

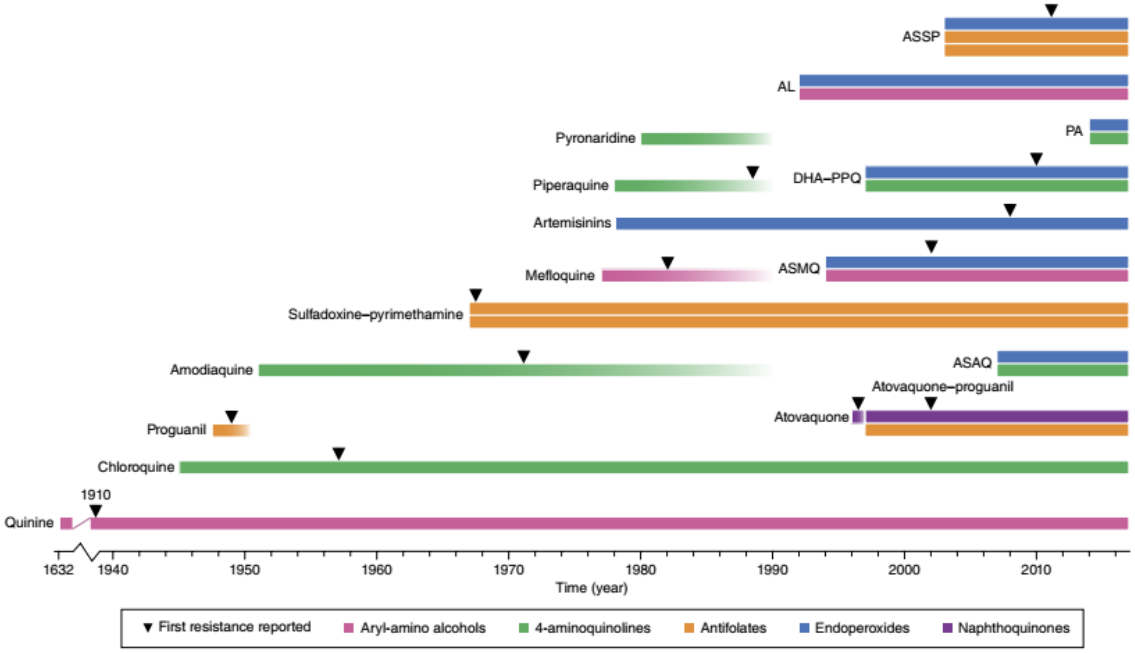

Figure 2: Development of drug resistance in *Plasmodium* against major antimalarials and the emergence of drug resistant parasite strains for each drug is shown. Source: (Blasco et al., 2017)

Quinine: Natives of Venezuela and Bolivia have been aware of the antipyretic properties of the "quina-quina" (cinchona bark) (Kaufman and Ruveda, 2005) and it was the Peru Indians who serendipitously discovered the antimalarial properties of cinchona bark (Roberts, 1989). In 1820, two French chemists Pierre Joseph Pelletier and Jean Bienaime Caventou successfully isolated the active compound from the cinchona bark and named it "Quinine". Further, during World War II chloroquine, chloroguanide (proguanil/atovaquone) were introduced, and eventually amodiaquine and pyrimethamine came in. Although quinine has many side effects like rashes, vertigo, nausea, tinnitus, abdominal pain, and vomiting but still quinine and its derivates have been used to cure malaria for a long time. However, resistance has been reported for quinine.

Chloroquine: In the early twentieth century, due to emergence of resistance, quinine was replaced by chloroquine. Chloroquine was discovered by the Germans and was extensively used during World War II. This drug was acted as a gold standard drug for malaria treatment until its resistance emerged in 1960. The resistance against CQ developed in different regions of the world independently and subsequently spread over the world.

Today, most of the field isolates are resistant to chloroquine, despite that CQ is still used as first line drug for the treatment of *P. vivax.*

Proguanil and Atovaquone: Later, Proguanil and Atovaquone were developed as new antimalarials, but their resistance came within a year of their use. Both are used in combination under the brand name of Malarone®. It is mainly used for chloroquine-resistant parasite treatment. (Gardiner et al., 2009; Jefford, 2001).

Artemisinin: In 1967, during the Vietnam war, Chinese scientists were under pressure to develop new antimalarials, as their soldiers were developing the chloroquine resistant malaria. They started 'Project 523' secretly under the guidance of Tu Youyou. By 1970, they had screened over 2000 traditional recipes on mice and finally, in 1972, they were successfully isolated the malaria killing compound from the leaves of sweet wormwood (*Artemisia annua*) plant. Currently, the Artemisinin (ART) and its derivatives are playing an important role as first-line antimalarials. ART and its derivatives have highest potent activity at the trophozoite stage of the asexual blood stage parasite (ABS). At the metabolically most active trophozoite stage, hemoglobin is degraded in the parasite and most of the reactive heme (Fe2+) is sequestered in hemozoin crystals as Fe3+ dimers. Still, some reduced form of heme is present in the parasite which activates the ART and this activated ART is lethal for the parasite. It results in the oxidative stress by alkylation of the biomolecules such as proteins, lipid and heme, thereby causing cellular damages (Blasco et al., 2017; Tilley et al., 2016). Artemisinin and its derivatives (ARTs) were first used independently but their short half-life and incidences of resistance led to the introduction of the artemisinin-based combination therapy (ACT). ACTs involve all the ART derivatives (artemether, artesunate, or dihydroartemisinin / DHA) with enhanced pharmacological properties that can reduce the parasite load up to 10,000-fold in 48 hours.

Mechanisms of resistance against major antimalarials

Plasmodium falciparum infection begins with the entry of sporozoites in the hepatocytes and proceeds to the most fatal stage i.e. asexual blood stage (ABS) before developing into the transmissible sexual stages. The ABS parasites are mainly responsible for the disease

symptoms and experience maximum drug pressure. So, there are more chances to develop resistance at this stage as we have observed in case of major antimalarials **(Figure3)**.

The compounds of antifolates group (PYR, CYC, SDX) kill the parasite by effecting its pyrimidine synthesis pathway and the mutations in two crucial enzymes dihydrofolate reductase (DHFR) and dihydropteroate synthetase (DHPS) is responsible for the resistance against PYR, CYC and SDX respectively. Electron transport chain is key which provides electrons for the *de-novo* pyrimidine biosynthesis via ubiquinone-dependent dihydroorotate dehydrogenase (DHODH). Atovaquone (ATQ) hampers the mitochondrial function (Biagini et al., 2006; Fry and Pudney, 1992) by inhibiting the *bc1* complex (Srivastava et al., 1997) of the mitochondrial electron transport chain and a single point mutation in the cytochrome b subunit (CYTb) is responsible for the resistance.

Some aryl-alcohols, including QN, and most of the 4-aminoquinolines (CQ, AQ, PPQ, PND) accumulate in the food vacuole, binds to the reactive heme, and interfere with its detoxification. Point mutations in the transporters such as *Pf*MDR1 and *Pf*CRT are determinants of resistance to these antimalarials. Resistance to PPQ is also related to the mutation in the *Pf*CRT gene, however, in the PPQ resistant parasite's food vacuole, expression of the hemoglobinase plasmepsin 2 and 3 (PM2/PM3) was found to be increased.

The ARTs have an inherent disadvantage of having very short half-life *in-vivo*, so these are used in combination with longer half-life partner drugs such as mefloquine, lumefantrine, piperaquine, amodiaquine, pyronaridine or sulfadoxine-pyrimethamine, in ART-based combination therapies (ACTs). The resistance for the ART is primarily due to mutation in the K13- Propeller protein.

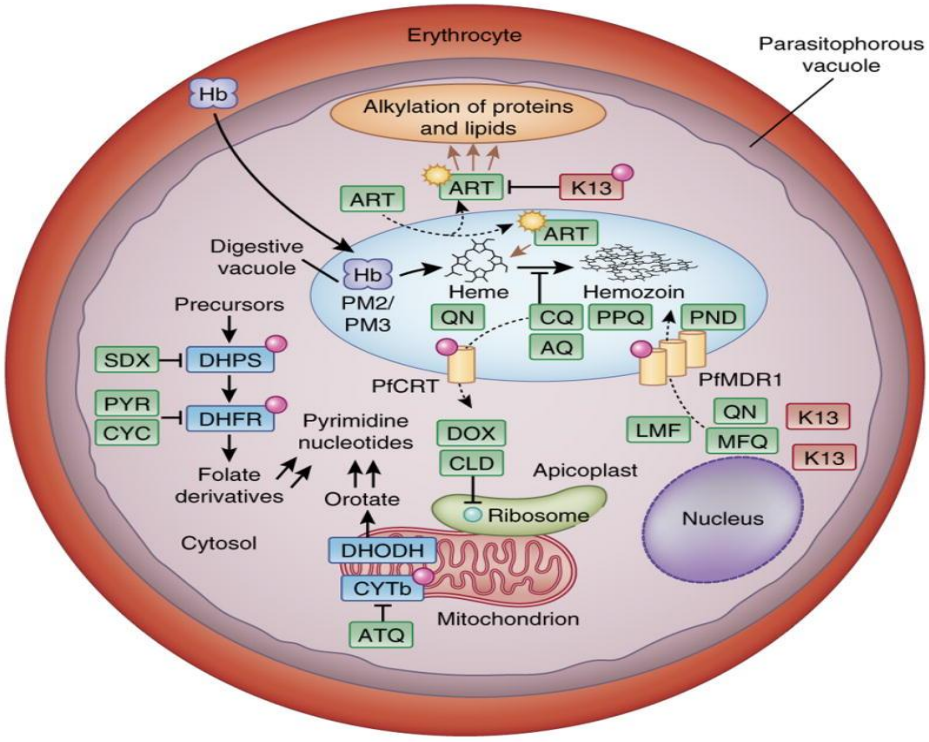

Figure 3: Diagram showing the major anti-malarials and their mechanism of action in the parasite: Most of the anti-malarials targets heme detoxification pathway in food vacuole, electron transport chain, pyrimidine, or folate synthesis pathway. Source: (Blasco et al., 2017)

2.4 Lipid Metabolism in *Plasmodium falciparum*

Lipids function as signaling molecules, as an important component of membranes and as a source of metabolic energy (van Meer et al., 2008). Inside the host cell, malarial parasite replicates rapidly. It requires lipids to support membrane biogenesis, PVM expansion, organelle development and to survive and maintain the lipid homeostasis in the parasite (Prudencio et al., 2006). These demands can be fulfilled by scavenging the host cell lipid, as well as *de novo* synthesis of fatty acids (Dechamps et al., 2010; Ralph et al., 2004; Wein et al., 2018) and phospholipid synthesis.

2.4.1 Fatty acid synthesis (Type FASII) pathway

Every Apicomplexan member has apicoplast, an organelle that was acquired by the parasite via secondary endosymbiosis of the cyanobacteria (McFadden et al., 1996). Apicoplast is

indispensable for the parasite as it harbors some of the very crucial pathways of the parasite such as FASII pathway, an iron-sulfur cluster assembly pathway, isoprenoid precursor synthesis pathway and a part of heme synthesis. Higher eukaryotes use type I fatty acid synthetase (FASI) in which fatty acid synthesis is catalyzed by a single protein having various domains. Although *Plasmodium* is a eukaryote, it has a type II fatty acid synthetase system (FASII) in which each step of the pathway is carried out by a discreet enzyme (Waller et al., 1998).

The FASII pathway in apicoplast starts with the import of phosphoenolpyruvate (PEP) from the parasite cytoplasm and through a cascade of reactions involving 10 different enzymes results in the formation of saturated fatty acid having eight or more carbon length (Botte et al., 2013; Ramakrishnan et al., 2012; Sharma et al., 2007). Different genetic approaches have been used to gene deletion or knock-down for FASII pathway genes to understand the functional importance of the pathway. The whole FASII pathway is mainly divided into three different steps; **preparation phase** in which the imported PEP is converted into acetyl-CoA (Lim et al., 2010), **initiation phase** in which acetyl-CoA is converted into malonyl-ACP and acetoacetyl-ACP (Goodman and McFadden, 2007), which serve as carbon donor for elongation phase and **elongation phase** in which fatty acid chain grows by two carbon per turn (Goodman and McFadden, 2007; Sharma et al., 2007). The essentiality of fatty acids for the parasite makes FASII pathway enzymes a good drug target.

2.4.1.1 Preparation Phase of FASII pathway:

Plastidic phosphate transporters (pPTs): FASII pathway starts with the transportation of the PEP in exchange of inorganic phosphate inside the apicoplast by the transporters. *P. falciparum* has two pPTs localized in the outer and the inner membrane of the apicoplast (Mullin et al., 2006). *In- vitro* assays have shown that these pPTs prefer PEP with high affinity over DHAP (dihydroxyacetone phosphate) and 3-phosphoglycerate (Lim et al., 2010). In contrast to *Plasmodium, T. gondii* have only one pPT and electron microscopy studies showed that it can be present in multiple membranes of apicoplast (DeRocher et al., 2012; Fleige et al., 2007; Karnataki et al., 2007). *P. berghei* knockout studies suggested

that the inner membrane pPTs are essential for the blood stage parasites however, the knockout parasites cannot attribute phenotypically to the loss of FASII pathway suggesting the role of the inner membrane pPTs in the DOXP pathway (Maeda et al., 2009). The outer membrane pPTs deficient *P. berghei* parasites showed defect at the mosquito and the liver stage.

Pyruvate kinase II: PKII is involved in the second step of the preparation phase responsible for the conversion of PEP into pyruvate and ATP molecule. In *P. falciparum* two PK; PKI and PKII are present which are responsible for the generation of the pyruvate in the cytoplasm and the apicoplast respectively (Fleige et al., 2007; Maeda et al., 2009). Importance of these enzymes is yet to be established by knock-down /deletion studies however PKII, is the only enzyme which is responsible for generation of the energy in the apicoplast and generates pyruvate for both DOXP and the FASII pathways. Thus, PKII is likely to be a good drug candidate for the malaria parasite.

Pyruvate dehydrogenase complex (PDH): PDH is an α-keto dehydrogenase family member having four subunits (E1α, E1β, E2, and E3) and requires lipoic acid as a co-factor. The four polypeptide subunits assemble with NAD+ and thiamine pyrophosphate to form functional domain which catalyzes the pyruvate conversion into acetyl-CoA and carbon-dioxide. In *P. berghei*, genetic knockout of this gene showed defects at the late liver stage parasites (Nagel et al., 2013; Pei et al., 2010), however, PDH deficient parasites were arrested before the sporozoite development in *P. falciparum* (Cobbold et al., 2013; Waller et al., 2003), which suggested that the human and the rodent parasites differ in their fatty acid synthesis pathway.

2.4.1.2 Initiation phase of FASII pathway:

Acetyl-CoA carboxylase (ACC): This is the first step of the initiation phase. ACC is composed of three domains and are either multifunctional or dissociative enzymes depending on whether their domains are encoded by a single gene or multiple genes. In *Plasmodium falciparum* ACC are the multi-functional enzymes which catalyze the acetyl-CoA using biotin as cofactor and results in the generation of the malonyl-CoA. Studies have shown that *Plasmodium* ACC can be blocked by the aryloxyphenoxypropionate (fop)

and cyclohexanedione (dim) herbicides (Louie et al., 2010; Waller et al., 2003). However, the FASII pathway dispensability for the parasite at this stage indicates the off-target activity of fop and dim.

Malonyl-CoA:ACP transacylase (FabD): Next step of the initiation phase involves formation of malonyl-ACP via a transfer of malonyl group from malonyl-CoA to ACP. This step is catalyzed by FabD, which is the least characterized enzyme of the FASII pathway.

Acyl-carrier protein (ACP) and Acyl-carrier protein synthetase (ACPS): ACP is one of the most crucial enzymes of the FASII pathway which is required almost at every step after the FabD. ACP plays a crucial role in both initiation and elongation phases. It binds to the different substrates by binding to fatty acids via phosphopantetheine and helps in shuttling of substrates for different enzymes. *Pf*ACP is not yet characterized well, most of the studies have been done on *T. gondii*. *In-vitro* and complementation studies have also been done in *E. coli* to functionally characterize the *Pf*ACP (Prigge et al., 2003; Sharma et al., 2007; Waters et al., 2002). Genetic studies in *T. gondii* have shown defects in the apicoplast in *Tg*ACP depleted parasites. These studies in *T. gondii* demonstrate that ACP is essential for the parasite and makes it a good target for drug development.

Initially, ACP remains in its Apo-form i.e without phosphopantetheine group. ACPS catalyzes the conversion of this apo-form to holo-form by transferring the phosphopantetheine group to these carrier proteins from CoA. Therefore, ACPS indirectly plays a crucial role in the FASII pathway by activating ACP.

β-Ketoacyl-ACP synthase III (FabH): This is the final step of the initiation phase, in which, FabH converts malonyl-ACP into acetoacetyl-ACP in the presence of acetyl-CoA. This reaction generates carbon dioxide and a four-carbon compound acetoacetyl-ACP, which is further used in the chain elongation. Several inhibitor studies have shown that the naturally occurring antibiotic thiolactomycin and its analogs can kill the *Plasmodium* and *Pf*FabH was believed to be its target (Jackowski et al., 1989). But *in-vitro* testing shows that thiolactomycin acts against *Pf*FabB/F and its analogs inhibit *Pf*FabH specifically (Jones et al., 2005; Prigge et al., 2003).

2.4.1.3 Elongation Phase of FASII pathway

β-Ketoacyl-ACP synthase I/II (FabB/F): The first step of the elongation phase is catalyzed by FabB/F enzyme, in which condensation of malonyl-ACP with acyl-ACP results into the formation of β-ketoacyl-ACP and carbon dioxide. The product β-ketoacyl-ACP is extended by two carbon units. The *Pf*FabB/F shares similarity in FabF activity and sequence similarity with both FabF β-ketoacyl-ACP and FabB synthetase (Sharma et al., 2009). It is the second enzyme of the FASII system at which genetic studies have been performed in *P. falciparum*, *P. yoelii* and *P. berghei*. The knockout of FabB/F showed no effect on the blood stage parasites but had a deleterious effect at the liver stage parasites. In *P. falciparum*, loss of FabB/F affects sporozoite development, reflecting similar phenotype to the *Pf*PDH knockout parasites.

β-Ketoacyl-ACP reductase (FabG): The second enzyme of the elongation phase is FabG which catalyzes the formation of β-hydroxyacyl-ACP from β-ketoacyl-ACP using NADPH as an electron donor. The *in-vitro* activity studies of *Pf*FabG showed the preference of NADPH over NADP. Crystal structure has been solved for *Pf*FabG and ACP, and the interacting residues have been also identified using site-directed mutagenesis studies.

β-Hydroxyacyl-ACP dehydratase (FabZ): The Third step of the elongation phase involves the formation of enoyl-ACP from β-hydroxyacyl-ACP by FabZ. Although, *Pf*FabZ can do hydration (reverse) and dehydration (forward) reactions both (Sharma et al., 2003), it prefers the first one when alone but in presence of the other components of the FASII pathway reaction is carried-out in forward (dehydration) direction (Sharma et al., 2007). Functional characterization of the FabZ has been done by knock-out studies in *P. yoelii*. FabZ was found essential at the liver stage parasite as the knockout sporozoites fail to establish blood stage infection *in-vivo*. Crystal structure of *Pf*FabZ showed that the enzyme has two conformation states (Kostrewa et al., 2005; Vaughan et al., 2009).

The NAS compounds (NAS-21, NAS-91) have been co-crystalized with *Pf*FabZ and they successfully inhibited the activity of FabZ *in-vitro* (Ramakrishnan et al., 2013; Swarnamukhi et al., 2006). As *P. falciparum* parasites were unable to incorporate the

acetyl-CoA into fatty acids, the FabZ seemed to be a target of these compounds (Swarnamukhi et al., 2006).

Enoyl-ACP reductase (FabI): The final step of the elongation phase involves the conversion of enoyl-ACP into acyl-ACP by FabI using NADH as a co-factor. In *P. falciparum,* apicoplast localization of FabI was confirmed by GFP tagging approaches (Ramakrishnan et al., 2013) and *in-vitro* studies have shown that it prefers NADH over NADPH (Kapoor et al., 2001). In terms of inhibitor studies, this enzyme is the most studied among all the enzymes of FASII pathway and most of the studies have focused on antibacterial triclosan which inhibits the enoyl-ACP reductase (Yu et al., 2008). The triclosan inhibits acetate and malonyl-CoA incorporation in fatty acids and efficiently kills the *Plasmodium*. These findings suggested that triclosan specifically inhibits the FabI and kills the parasite but again dispensability of FASII pathway at asexual blood stage parasite suggested that this compound have some other targets also. The product of FASII pathway, octanoyl-ACP has two fates; either it can be retained in FASII pathway for further elongation or can go to the lipoic acid synthesis pathway.

2.4.2 The lipoic acid synthesis pathway

The sulfur-containing octanoic acid's derivative lipoic acid is required as a co-factor for the PDH complex of apicoplast in both *Plasmodium* and *Toxoplasma*. Lipoic acid pathway enzymes use S-adenosylmethionine as co-factor and catalyze the conversion of octanoyl-ACP into lipoic acid (Wrenger and Muller, 2004). The canonical lipoic acid synthesis pathway has two enzymes; LipB and LipA but in *Plasmodium*, this pathway is composed of three enzymes (LipB, LipA, LplA2). The first step of this pathway is catalyzed by LipB enzyme. It transfers the octanoyl-ACP to the E2 subunit of the PDH complex and genetic knock-out studies in *Plasmodium* showed that although this enzyme is not essential for the parasite but there is acceleration in the parasite growth suggesting its role in cell cycle regulation (Gunther et al., 2007). In LipB depleted parasites, PDH lipoylation is significantly decreased but not abolished completely (Falkard et al., 2013). Genetic studies of LipB challenge the theory that mitochondria and apicoplast lipoic acid metabolism act in isolation. In LipB deleted parasites there is a decrease in the lipoylation of the PDH

complex and lipoic acid scavenged from the medium is utilized for the lipoylation of mitochondrial enzyme by the parasite (Gunther et al., 2007). Further research is required to explore the lipoic acid synthesis and the role of LipB beyond apicoplast. In LipB deleted parasites, PDH lipoylation in the apicoplast was not completely abolished but decreased significantly. The lipoate protein ligase A2, which is less active than the LipB can compensate its function. In *P. falciparum* and *T. gondii,* two LpLA enzymes are present; LplA1 and LplA2 which are localized to the mitochondria and apicoplast, respectively. The second step of the lipoic acid pathway is generation of lipoate by the addition of the two sulfur atoms into the PDH-bound octanoate by LipA enzyme. The knockout of LipA was not successful so its function is yet to be identified (Gunther et al., 2009). However, most of the enzymes of FASII and lipoic acid synthesis are dispensable but knockout of LipA was not successful indicating an important role of this enzyme in some other pathway as well.

2.4.3 Lipid precursor (Phosphatidic acid) synthesis pathway

Phosphatidic acid serves as a major precursor for most of the phosphoglycerolipids and acylglycerol lipids in the parasite (Athenstaedt and Daum, 1999; Yao and Rock, 2013). The fatty acids synthesized via the FASII pathway can be incorporated into Phosphatidic acid inside the apicoplast. Earlier, it was believed that this pathway is catalyzed by three enzymes in the apicoplast, but recent studies in *P. yoelii* showed that the pathway involves two enzymes which are localized in the apicoplast and the third enzyme is present in the ER. These studies suggested that the phosphatidic acid synthesis pathway is incomplete in *Plasmodium* apicoplast. The two enzymes only synthesize an intermediate lysophosphatidic acid (LPA) from acyl-ACP and DHAP in the apicoplast (Lindner et al., 2014).

Glycerol-3-phosphate dehydrogenase (G3PDH) catalyzes the first step by the generation of glycerol-3-phosphate from DHAP using NADPH as an electron donor. Three G3PDH isoforms are present in *Plasmodium,* two of them are present in mitochondria (Mather et al., 2007; Seeber et al., 2008) and the third one is targeted to the apicoplast (Lindner et al., 2014). The second step of the pathway is catalyzed by **Glycerol-3-phosphate**

acyltransferase (G3PAT). In this step, fatty acid chain from the acyl-ACP is transferred to glycerol-3-phosphate leading to generation of lysophosphatidic acid. Two G3PAT enzymes are present in *Plasmodium* one is in ER (Santiago et al., 2004) and other is in apicoplast (Lindner et al., 2014). Their localizations are confirmed by GFP tagging studies in *P. yoelii*. The absence of the third enzyme, **lysophosphatidic acid acyltransferase,** in apicoplast of the *Plasmodium*, makes the phosphatidic acid synthesis pathway puzzling. This enzyme is present in the ER which indicates that in *Plasmodium*, the LPA was likely to be transported to the ER from apicoplast. Genetic studies have revealed these enzymes are not essential at the asexual stage. Existing studies indicated how FASII fatty acids are utilized by the parasite but require further studies to get clear insights on these pathways.

The synthesized fatty acids of FASII pathway are exported from the apicoplast to the other cellular locations for utilization. Although, this fatty acid export is not well studied in *Plasmodium* but acyl-CoA synthetase (ACS) is thought to be involved (Ralph et al., 2004). Different isoforms of ACS are present in the *P. falciparum* and *T. gondii*. In *P. falciparum*, 13 isoforms are present and two of them (*Pf*ACS8, *Pf*ACS9) have the putative substrate-binding motif and the apicoplast signal sequence (Ralph et al., 2004).

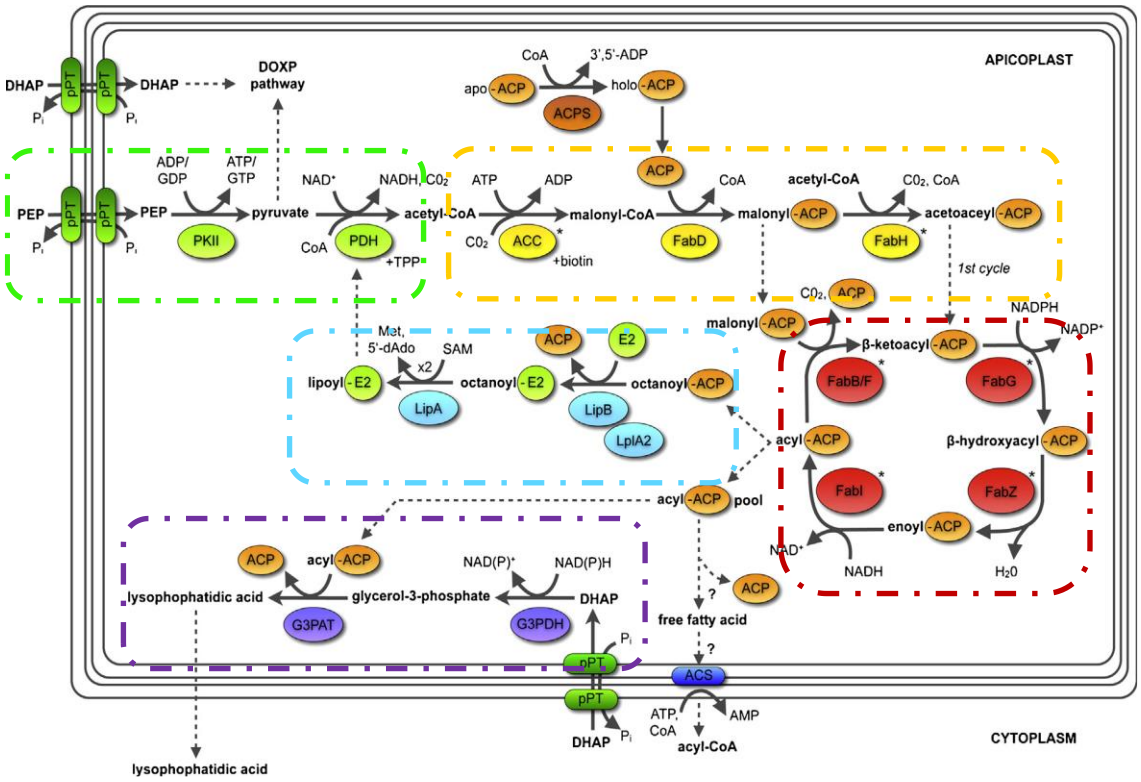

Figure 4: Different pathways of fatty acid metabolism in *Plasmodium* apicoplast: Preparation phase of FASII (Green), Initiation phase of FASII (orange), Elongation phase of FASII (Red), Lipoic acid synthesis pathway (Cyan), Phosphatidic acid synthesis pathway (violet). Source: (Shears et al., 2015)

2.4.4 Phospholipids and their synthesis pathways

Malaria parasite completes its complex life cycle in two different hosts and during this, it undergoes several developmental stages and morphological changes. It requires well-controlled gene expression, regulatory mechanisms, and several metabolic and biochemical changes (Ben Mamoun et al., 2001; Le Roch et al., 2003). Phospholipids have been believed to be structural components of the membranes only, recent studies have shown that their byproducts act as major signal molecules that also control differentiation and development process in *P. falciparum* (Bobenchik et al., 2013; Flammersfeld et al., 2018; Gulati et al., 2015; Pessi et al., 2004; Ramakrishnan et al., 2013; Witola et al., 2008). Lipid metabolism drastically increases as the parasite life cycle progresses. There is a six-fold increase in the phospholipid levels in the infected erythrocytes to fulfill the lipid

requirement (Mitamura and Palacpac, 2003; Pessi and Ben Mamoun, 2006). Three hundred different species of lipids are scavenged by the parasite to facilitate asexual and sexual reproduction, proliferation, and transmission (Gulati et al., 2015). *P. falciparum* membrane composed of phosphatidylcholine (PC), phosphatidylethanolamine (PE) and phosphatidylserine (PS) (75-77,79,83-86). In uninfected erythrocytes, PC, PE, PS share 30-40%, 25-35% and 10-20%, respectively. However, in purified parasites and infected RBCs, they constitute up to 20-55%, 15-40% and 4-15% respectively (Choi et al., 2016; Flammersfeld et al., 2018; Mitamura and Palacpac, 2003; Pessi and Ben Mamoun, 2006; Ramakrishnan et al., 2013).

Phosphatidylcholine (PC): PC is the main structural lipid in the membranes. Hydrolysis of PC lead to the formation of diacylglycerols (DAGs), which acts as a secondary messenger to modulate signaling and can also activate many kinases (Cooke et al., 2017; Mohammadi et al., 2018). There are two pathways for the PC synthesis in *P. falciparum*; 1. CDP-Choline branch of the Kennedy pathway, 2. Serine Decarboxylase-Phosphoethanolamine Methyltransferase (SDPM) Pathway (Flammersfeld et al., 2018; Gibellini and Smith, 2010; Mohammadi et al., 2018; Pessi and Ben Mamoun, 2006). Studies have been shown that 89% of PC is synthesized via the CDP-Choline pathway. CDP-Choline pathway is initiated by the uptake of choline from the host cell via unknown transporters. Once transported, choline kinase (*Pf*CK) performs the phosphorylation of the choline and generates phosphocholine, which is used as a substrate to make CDP-Choline by the choline-phosphate cytidyltransferase enzyme. Further diacylglycerol choline phosphotransferase catalyzes the conversion of CDP-Choline to PC (Gibellini and Smith, 2010).

PC is also synthesized via the SDPM pathway from serine and ethanolamine. Studies have shown that the parasite can survive in the absence of exogenous choline indicating the existence of an alternate pathway for PC synthesis. Decarboxylation of serine, results in the formation of ethanolamine and this ethanolamine act as a precursor for phosphatidylethanolamine. Phosphoethanolamine Methyltransferase (*Pf*PMT) plays a crucial role in the generation of PC from phosphoethanolamine. It catalyzes the methyl transferase activity, three times, and incorporates methyl group from S-

adenosylmethionine to O-phosphoethanolamine. Choline phosphate is produced because of tri-methyl transferase activity of *Pf*PMT and this choline phosphate further goes to the CDP-Choline pathway for PC synthesis. Methionine acquired from hemoglobin degradation gets converted into S-adenosylmethionine which is further utilized by the *Pf*PMT to form choline phosphate. SAM synthetase, also known as methionine adenosyl transferase plays an important role in S-adenosylmethionine synthesis. Presence of *Pf*PMT only in the parasite makes it an attractive drug target for anti-malarial therapy (Bobenchik et al., 2011). *Pf*PMT is inhibited by 4-aminoquinoline and amodiaquine. Studies have shown that amodiaquine is an allosteric inhibitor of *Pf*PMT activity which induces the conformational changes in *Pf*PMT (Emoto et al., 1996).

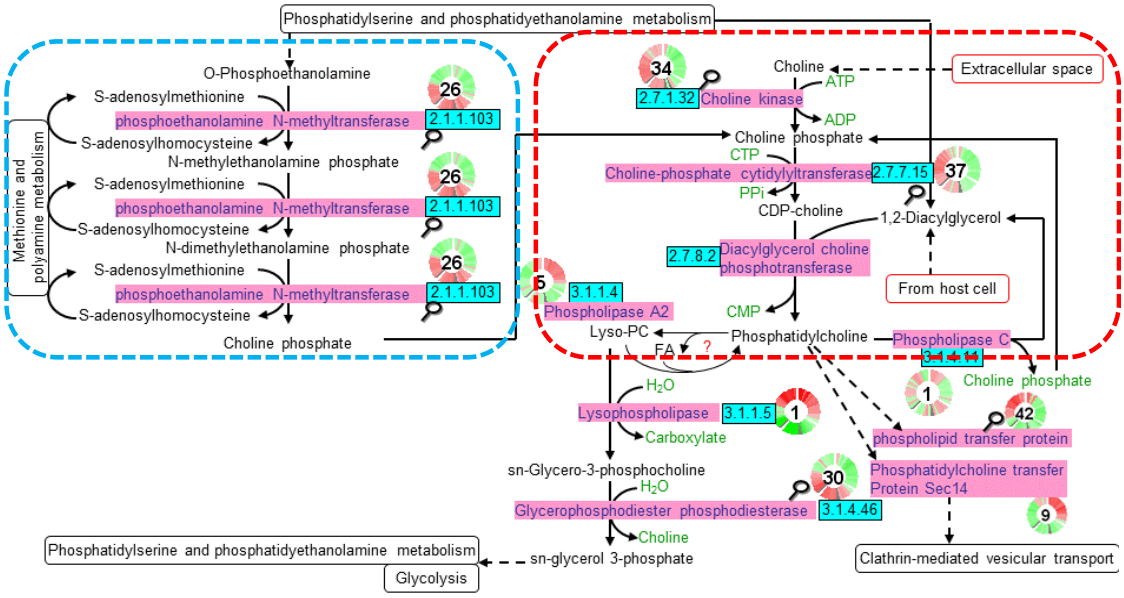

Figure 5: PC synthesis in *P. falciparum* showing two pathways of PC synthesis: Kennedy branch of PC synthesis (Red Box) and the alternate pathway which utilizes PE and PS for PC synthesis (Blue Box). Source: *https://mpmp.huji.ac.il/*

Phosphatidylethanolamine (PE) and Phosphatidylserine (PS): the second most abundant lipid present in the membrane is PE which also plays an important role in membrane fusion and cytokinesis (Emoto et al., 1996). It also serves as a donor of ethanolamine moiety required for post-translation modifications (Vance and Tasseva, 2013). PE metabolism has been implicated in other cellular processes also such as signaling, autophagy and viral

replication. PE can be synthesized either from ethanolamine via the CDP-ethanolamine pathway or via decarboxylation of PS by *Pf*PSD. *Pf*PSD belongs to the D-H-S serine proteases family and possesses auto-endoproteolytic activity (Choi et al., 2015; Eda and Sherman, 2002). Genetic studies have claimed that in absence of the exogenous ethanolamine, *Pf*PSD function is essential for the parasite. However, further studies are required to explore the role of *Pf*PSD in parasite biology.

PS is present in the inner leaflet of the membrane and plays an important role in signaling and apoptosis. In *P. falciparum*, PS plays an important role in cytoadherence (Eda and Sherman, 2002). In *P. falciparum* infected patients' blood, elevated PS microvesicles are thought to play an important role in gametogenesis and intracellular communication (Gulati et al., 2015). The PS is synthesized from PA by enzyme phosphatidate-cytidyltransferase and CDP-DAG- cytidyltransferase. The serine moiety required for PS synthesis is either taken up from the host plasma or obtained from the hemoglobin degradation, the serine gets converted into PS by the phosphatidylserine synthase (*Pf*PSS).

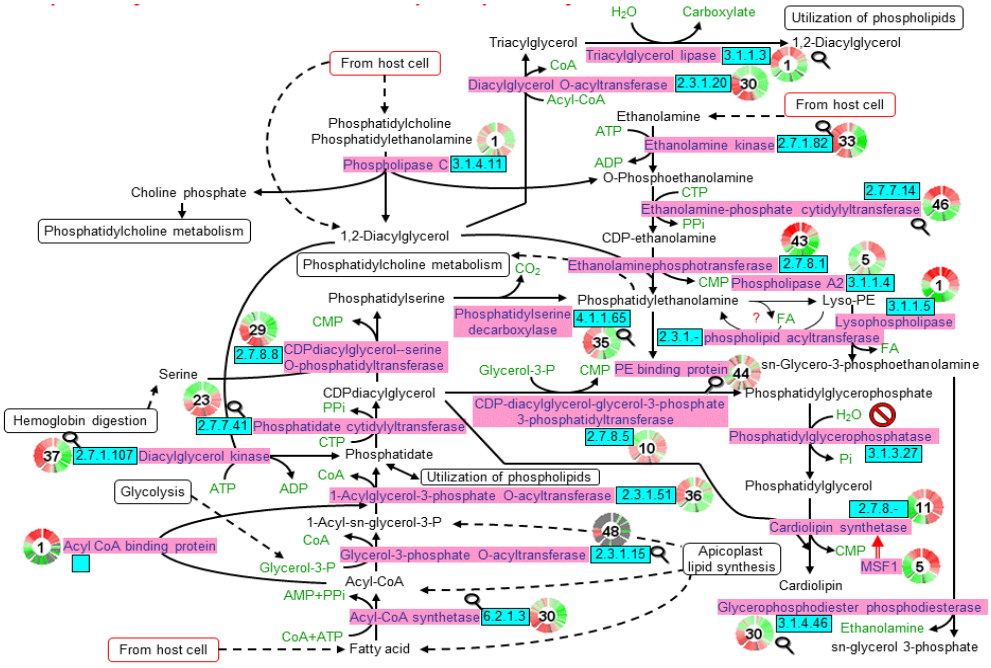

Figure 6: PE and PS synthesis and associated metabolic pathways metabolism in P. falciparum. Source: *https://mpmp.huji.ac.il/*

2.5 Phospholipases and Lysophospholipases

Phospholipases are α/β hydrolase family members mediating various cellular functions, including signaling and membrane synthesis. These are classified into four groups (A, B, C, D) depending on their lipolytic activity. Phospholipase A (PLA) and B (PLB) break the acyl ester bond whereas Phospholipase C (PLC) and D (PLD) target the phosphodiesterase bonds. Therefore, phospholipases are responsible for generation of fatty acids (FAs) and lysophospholipids (LPLs). Lysophospholipases (LysoPLs) are also classified on the bases of their cleavage sites. The fatty acid chain in LPLs is released by LysoPLA.

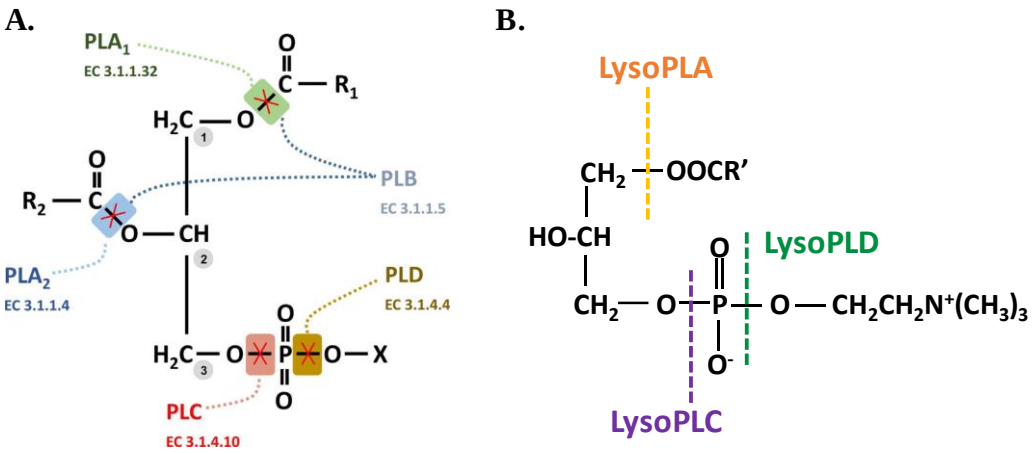

Figure 7: Phospholipid and Lysophospholipid molecules and cleavage sites by different phospholipases: LysoPLA cleaves the acyl ester bond at the sn-1 and LysoPLC hydrolyses the glycerol-oriented and LysoPLD the alcohol- oriented phosphodiester-bond. Numbers indicate stereospecific numbering positions. Crosses indicate cleavage sites. PL, phospholipase; R1/R2, non-polar fatty acid chain; X, EC, enzyme commission number; X denotes the phospholipid head group, e.g. choline, ethanolamine, inositol, or serine.

There are reports claiming that some PLA/ LysoPLA also have lipase activity for non-phospholipids substrates such as acylglycerols and some other enzymes can transfer FAs from PL to an acceptor molecule (cholesterol) via PL;sterol-o-acyltransferase activity (Flores-Diaz et al., 2016). Recently, analysis of *P. falciparum* genome predicted around 22 lipolytic enzymes. In these, 14 proteins have the α/β hydrolase domain, four have a patatin-like domain, one with sphingomyelin phosphodiesterase domain, one with PC; sterol-O-acyltransferase domain and one with a PLA/lipase domain (Flammersfeld et al., 2018). In

P. falciparum 14 putative LPLs were identified, out of these proteins 10 LPLs have high sequence similarity (36-61%) among them. Most of these are 400 amino acid long proteins without having any signal sequences. The characteristic GXSXG motif is conserved among all lysophospholipases, wherein, the active site residue serine (S) is flanked by the glycine. The catalytic triad is composed of serine (S), aspartate (D) and histidine (H) residues. Four of the putative LPLs are 675-921 amino acid long and have a signal peptide. One of the most characterized α/β hydrolase is an esterase; *Pf*PARE (*PF*3D7_0709700) and studies have shown that although this gene is not essential at the asexual blood stage of the parasite but its expression changes in pepstatin-resistant parasites (Istvan et al., 2017). Another *Plasmodium* protein with phospholipase activity, was found to play role in hepatocytic egression (Burda et al., 2015). Conditional knock down of *Pf*PAPTPL1 (Patatin like phospholipase 1) showed that it is dispensable for the asexual blood stage parasite but *Pf*PAPTPL1 depleted parasites have reduced flagellation and egress (Singh et al., 2019). Lipid analysis of *Pf*PNPLA1 depleted parasite observed an increased amount of PC (Flammersfeld et al., 2020).

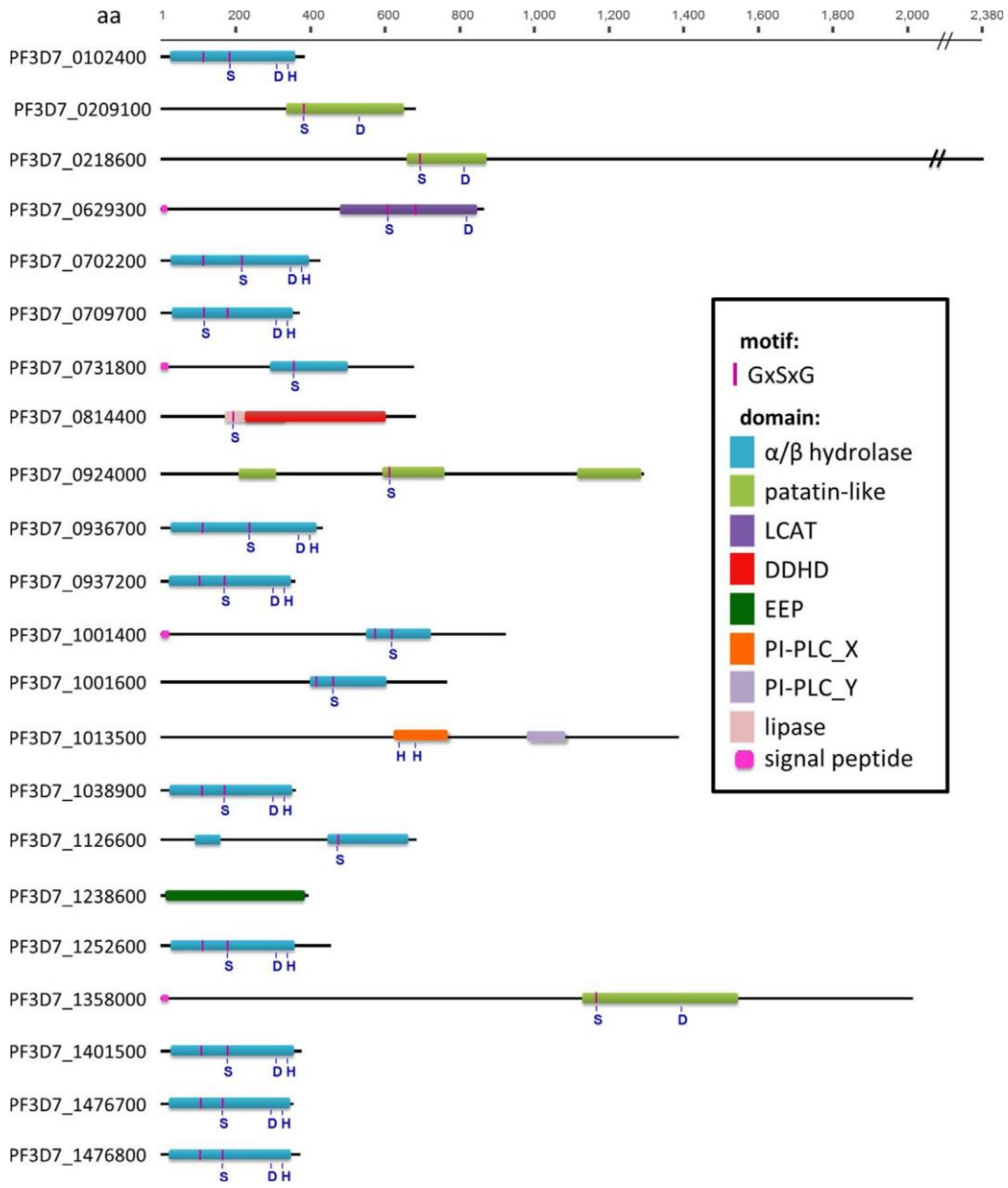

Figure 8: Domain structures of the putative lipolytic enzymes identified in *P. falciparum*: Domains were predicted via the NCBI Conserved Domain Database. Amino acids (aa) depicted belong to the catalytic sites of the protein: D, aspartate; G, glycine; H, histidine; S, serine; X; amino acid. LCAT, Lecithin: cholesterol acyltransferase; EP. Exonuclease-endonuclease phosphatase domain superfamily, GXSXG, motif embedding the putative catalytic serine, PI-PLC, phosphatidylinositol-specific phospholipase C domain. Source: (Flammersfeld et al., 2018)

Chapter 3 Methods

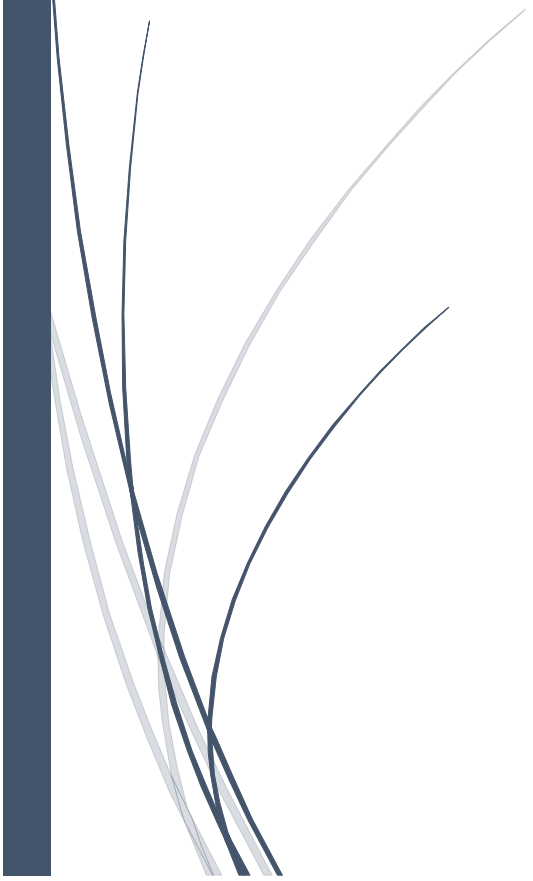

3. Methods:

3.1 General Protocols

3.1.1 PCR amplification and cloning in pJET1.2 cloning vector

Primers with specific restriction sites were designed for PCR amplification of the respective genes using the genomic sequences/coding sequences available in database (www.plasmodb.org). The genes were amplified from genomic DNA or cDNA using Q5 high fidelity polymerase enzyme (NEB) and respective gene specific primers. The PCR product was resolved on a 1% agarose gel containing 0.5 µg/ml of ethidium bromide (EtBr), the expected sized band was excised from the gel and purified using DNA Extraction kit, as per the manufacturer's instructions. The PCR amplified product of each gene was cloned into linear cloning vector pJET1.2. Three µl of each amplicon was used for the ligation reaction. The reaction mixture was incubated for 1 h at room temperature and then transformed in DH5α competent cells. The transformed cells were plated on LB agar plate containing ampicillin antibiotic at 100 µg/ml for the selection of transformed DH5α cells.

Table 1: Different components of reaction mixture for ligation in pJET cloning vector.

S.No.	Components	volume
1.	2X Reaction Buffer	10 µl (1X)
2.	PCR product	3 µl
3.	pJET 1.2 cloning vector	1 µl
4.	T4 DNA ligase	1 µl
5.	Nuclease-Free Water	5 µl

3.1.2 Preparation and transformation of competent cells

DH5α competent cells were prepared using the $CaCl_2$ method. 10 ml LB broth was inoculated with a single DH5α colony and grown overnight at 37°C in a shaker incubator.

Following day, 100 ml LB was inoculated with 1ml overnight grown culture and incubated at 37ºC till the $O.D_{550}$ reaches 0.4-0.6. Cells were chilled on ice for 30 minutes and centrifuged at 6000 rpm for 15 minutes at 4ºC. Pellet was resuspended in one-third volume of filter-sterilized 100 mM $CaCl_2$ and the tubes were kept on ice for another 30 minutes. The cells were centrifuged as before, and the pellet was resuspended in 1ml of chilled 100 mM $CaCl_2$ containing 15% glycerol. This cell suspension was aliquoted in pre-chilled1.5 ml vials (100 µl of cells per vial) and transferred immediately to ice. Then the vials were given a snap chill in liquid nitrogen and stored at -70%.

Transformation of competent cells: The complete ligation mixture was added to 100 µl of competent cells and the vials were kept on ice for 30 minutes. Heat shock was given to the cells at 42ºC for 90 seconds in a water bath and then vials were immediately transferred in ice for 5 minutes. Then, 500 µl of LB broth was added to each vial and incubated in shaker incubator at 37ºC for 45 minutes to allow the cells to revive and express the antibiotic resistance marker of the transformed plasmid. The cells were plated onto LB-agar plates containing 100 µg/ml of ampicillin and incubated at 37ºC overnight. Colonies were selected and checked for the presence of insert by colony PCR and restriction digestion.

3.1.3 Screening of recombinants

Plasmid DNA was isolated using the Miniprep DNA Purification kit following the manufacturer's instructions (Qiagen). A single positive colony was picked up from the plate and was inoculated in 10 ml of LB broth with 100 µg/ml of ampicillin and grown overnight at 37°C. The cells were harvested by centrifugation at 6000 rpm for 15 minutes at room temperature. The bacterial pellet was then re-suspended in 250 µl of cell resuspension solution, followed by addition of 250 µl of cell lysis solution, mixed by inverting the tubes. 350 µl of cell neutralization solution was added and centrifuged at 12000 rpm for 10 minutes at room temperature. The supernatant was added on to a plasmid DNA purification unit and centrifuged at 12000 rpm for 2 minutes at room temperature. The flow-through was discarded and column was washed with 750 µl of column wash solution by centrifugation at 12000 rpm for 1 minute at room temperature. The wash procedure was repeated with 500 µl of the wash solution for 2 minutes. The bound plasmid

DNA was eluted by adding 100 µl of pre-warmed TE buffer to the column and centrifugation at 12000 rpm for 2 minutes at room temperature.

Digestion reactions were set up using 1 µg of the purified plasmid DNA; 1X restriction enzyme digestion buffer; and 5 units of each restriction enzyme, respectively. The reaction mixture was incubated at 37°C for 20 min and resolved on a 1% agarose gel for analysis. The gene sequence of selected clones was also confirmed by DNA sequencing facility at Macrogen Inc, Korea using the pJET 1.2 specific forward and reverse universal primers.

The insert (gene of interest) band on agarose gel was excised and purified using the gel extraction kit (Qiagen) according to the manufacturer's protocol for subcloning of the gene of interest in the expression vector (pET 28a+/ pETm11/ pETM41/ pSSPF2/ pGFP-glmS).

3.1.4 Subcloning into expression vectors

The gene of interest was excised from the cloning vector using the respective pair of restriction enzymes and gel purified. The restriction digested gene was used for ligation in the expression vector with the compatible restriction sites. For efficient ligation, the quantities of insert and vector were calculated using the formula

X ng of insert = (size of insert in bp) X (75 ng linearized plasmid) / (size of plasmid in bp).

The calculated amount of insert was added to the reaction mixture and 1 µl of T4 DNA ligase and 1X ligation buffer was used and the mixture was incubated at 4°C overnight. The ligation mixture was then used for transformation in desired competent cells. The transformants were screened and selected using the restriction digestion.

In pET expression system (Invitrogen, Life Tech., Carlsbad, CA, USA) the protein can express as both N-terminal and C-terminal fusion to a six-histidine residue sequence. The histidine tag allows affinity purification of the expressed protein using Immobilized Metal Affinity Chromatography (IMAC). The purified insert released from the positive pJET clone was purified using the gel-purification protocol. At the same time respective pET28a, pETM-11 vector plasmid was also digested with respective enzymes to get the plasmid in linearized form. To get active protein LPLs genes were sub-cloned into pETM-41 vector in which desired gene sequence was cloned in downstream of the maltose binding

protein sequence. Maltose-binding protein (MBP) is a highly soluble protein that helps the fusion protein in proper folding and there is a six-histidine residue sequence is also present on the C-terminal of the fusion protein.

3.1.5 Recombinant protein expression

Desired fragments of target genes were amplified by using specific primers and cloned in to pETM41 vector between *Nco*I and *Xho*I sites to give pETM41-His6-MBP-*Pf*LPL construct. The recombinant protein *Pf*LPL was expressed as a soluble protein in the cytosol of the *E. coli* BL21(DE3) codon$^+$ cells. For expression, bacterial cells having pETM41-His6-MBP-*Pf*LPL were grown in LB medium supplemented with kanamycin at 37°C. Expression of the fusion protein was induced using 1mM isopropyl β-D-thiogalactoside (IPTG) overnight at 16°C. Next day, cells were harvested and resuspended into lysis buffer (25mM Tris, pH7.4, 500mM NaCl, 10mM Imidazole) and lysed by sonication (Vibra cell sonicator). The supernatant was subjected to a combination of Ni-NTA affinity chromatography followed by amylose affinity chromatography. Eluted fractions were subjected to SDS-PAGE as well as western blot analysis to assess the purity of the purified recombinant protein.

3.1.6 Analysis of protein expression by SDS-PAGE and Western blotting

The SDS-polyacrylamide gel electrophoresis (SDS-PAGE) was performed to analyse the expression of recombinant proteins. The 12% resolving gel was poured within the assembled 1 mm thickness SDS-PAGE assembly and allowed to polymerize at room temperature. After polymerization, 5% stacking gel was poured and allowed to polymerize. Fifty microlitres of SDS-PAGE sample loading buffer was added in each fraction. The samples were then mixed by vortexing, boiled at 100°C for 10 minutes, spun down at 9000 X g for 3 minutes and the supernatant was loaded in the wells and resolved at 90 Volt till the bromophenol blue ran out of the gel. For each set, the SDS-PAGE was run in duplicate, one was stained with Coomassie Brilliant Blue and the other was used for western blot analysis. The gel intended for western blot analysis was fixed in transfer buffer and transferred to nitrocellulose membrane (Millipore Corporation, Billerica MA, USA) or PVFD membrane using semi-dry blotting apparatus (Bio-Rad Lab. Inc., CA, USA)

following manufacturer's instructions. The protein transferred the nitrocellulose membrane was blocked in 5% BSA (prepared in PBS) at 4ºC overnight. The membrane was then washed thrice with 1x PBS and incubated with 1:3000 dilution of the anti-His_6 HRP-conjugated anti-mouse IgG antibody (Pierce Chemical Company, Rockford, IL, USA) in 1X PBS room temperature with shaking, and developed using diaminobenzidine (DAB) and H_2O_2 (substrate-buffer Tablet sets; Sigma-Aldrich, St. Louis, MO, USA).

3.1.7 Complete media preparation for *P. falciparum* culture

RPMI with Albumax-Hypoxanthine: For one litre of complete media; RPMI (Invitrogen), 2.1g of sodium bicarbonate, 50mg of Hypoxanthine and 5g of Albumax was dissolved in 900ml of double-distilled water. Volume was then made up to one litre, 20µg/ml of gentamycin was added, and filter sterilized through 0.22µ PES filter.

RPMI with Human Serum: For one litre of complete media; RPMI and 2g of sodium bicarbonate were dissolved in 900 ml of double-distilled water and100 ml heat -inactivated human serum and 20µg/ml of gentamycin was added, and filter sterilized through 0.22µ PES filter.

3.1.8 Thawing of *P. falciparum* culture frozen stock

Frozen vial of parasite culture was thawed at 37ºC in the circulating water bath for 1min and immediately transferred to a sterile tube. An equal volume of thawing solution was added drop by drop to the tube with gentle mixing of sample. The mixture was centrifuged at 1200rpm for 2min at RT. The supernatant was discarded, and addition of thawing solution was continued till there was no lysis of RBC. Fresh 5ml of complete media with 2% hematocrit was added to the pellet and mixed thoroughly. The parasite culture was transferred to 6 well microtitre plate and kept in a 37ºC incubator (SMS Multitech, India), which was flushed with a gas mixture (90% N_2, 5% CO_2 and 5% O_2).

3.1.9 Sub-culture and dilution of parasite culture

Once the parasite culture reaches 5-10% parasitemia, the culture should be diluted or sub-cultured, before dilution, the culture in the plate was thoroughly mixed to make sure that

no RBC is stuck to the bottom of the plate. Afterward, the culture was diluted by removing an appropriate amount of culture volume and adding the same amount of complete media with 4% hematocrit In case of transgenic lines, WR99210 drug was added at a final concentration of 5nM to the culture before incubation.

3.1.10 Synchronization of *P. falciparum* by sorbitol treatment

The culture was harvested at about 10% parasitemia with a majority at the ring stage by centrifuging at 1600rpm for 5min at RT. To the cell pellet, 5 volume of 5% sorbitol solution was added and mixed gently. This solution was incubated at 37^{o}C for 10min and centrifuged at 1600rpm for 5min. The supernatant was carefully discarded without disturbing the pellet. Culture pellet was washed twice with pre-warmed complete media. The culture was mixed thoroughly and incubated at 37^{o}C for the growth of parasite.

3.1.9 Isolation of purified parasite from infected blood by saponin lysis

The culture for saponin lysis was harvested by centrifuging at 1600rpm for 5min at RT. To the pellet, 1.5 volumes of 0.15% saponin were added and mixed gently. The solution was incubated in ice for 10min and centrifuged at 2000rpm for 30min. The supernatant was discarded without disturbing the pellet. The pellet was washed with ice-cold 1×PBS till the red colour of the supernatant disappeared. Parasite pellet was stored at -70^{o}C till further use.

3.1.12 Preparation of frozen stocks of parasite culture

To prepare the stocks, parasite culture at ring stage with ~5%, parasitemia was harvested by centrifuging at 1600rpm for 5min. The cell pellet was re-suspended in 1.5 volumes of a freezing mixture, dispensed in freezing vial (1ml per vial) and stored immediately in liquid nitrogen.

3.1.13 Transfection of *P. falciparum*

About 100µg of plasmid DNA (in 30µl TE) was thoroughly mixed with 370µl of transfection cytomix. Infected RBCs at ring stage (3-5%) were gently suspended with the plasmid DNA-cytomix solution. The mixture was transferred into a 2mm electroporation

cuvette and DNA was electroporated at 310V, 950µF and 200Ω. The time constant should be between 0.7 to 0.9ms. The cells were immediately transferred into the complete medium and 50µl fresh RBCs were added. WR99210 drug was added after 6hrs of transfection for selection.

3.2 Protocols for molecular and functional characterization of *Pf*LPL3

3.2.1 Generation of *Pf*LPL3-GFP-glmS parasite line

To generate *Pf*LPL3-*glmS*-GFP construct, C-terminal fragment (702base pair) of *pfLPL3* gene was amplified using specific primers 1222A & 1223A. The amplified C-terminal fragment was cloned into *glmS*-GFP vector in frame to the N-terminus of GFP in the *Spe*I and *Kpn*I restriction enzymes sites. Parasite cultures were synchronized by repeated sorbitol treatment and 100 µg of purified plasmid DNA (Plasmid Midi Kit, Qiagen, Valencia, CA) was transfected in *P. falciparum* by electroporation (310 V, 950 µF) (Crabb et al., 2004). Transfected parasites were selected over 2.5 µg/ml blasticidin (Calbiochem) and subsequently subjected to on and off cycling of blasticidin drug to promote integration of the plasmid in the main genome. Integration was confirmed by PCR using 1270A and 1234A as well as by western blot analysis using anti-GFP antibody.

3.2.2 Conditional knock-down analysis and in-vitro growth assays:

To assess the effect of knock-down of *PfLPL3* on parasite growth and development, *Pf*LPL3-*glmS*-GFP transgenic parasites were tightly synchronized with 5% sorbitol and grown in presence of different concentration (0mM, 1.25mM, 2.5mM, and 10mM) of glucosamine (Sigma-Aldrich). For microscopic analysis and morphological analysis of the parasites, Giemsa smears were prepared at every 8hr interval from both glucosamine treated and control parasites. Parasite growth was assessed at 48 and 96 hours after the addition of glucosamine by flow cytometry using BD FACS Calibur. For flow cytometry, EtBr stained uninfected erythrocytes were used as background control. Cells were incubated with EtBr for 30 minutes at 37 °C in dark followed by two washing with 1x PBS and subjected to FACS analysis using a BD FACS Calibur system (Beckton

Dickinson) A total of 100000 events were acquired the data was analysed by using the software.

3.2.3 Membrane association assay and Western blotting:

Trophozoite stage parasites were isolated from infected RBCs by saponin lysis procedure as detailed earlier. Parasite pellet was suspended with an equal volume of RIPA buffer for 30 minutes on ice for lysis and centrifuged. Laemmli buffer was added to the supernatant and proteins were separated in 12% SDS-PAGE. Next, fractionated proteins were transferred to PVDF membrane (Millipore) and incubated with blocking buffer (4 % skim milk in 1X PBS). The antibodies (monoclonal anti-GFP mice 1:5000 (Roche), rabbit anti-GFP 1:10000, rabbit anti-BiP 1:15000 and monoclonal anti-spectrin 1:1000, were diluted in 0.1% (W/V) Tween20- PBS with 2% (w/v) skim milk and incubated for desired times. Blots were washed 5 times with 1X PBS and probed with HRP conjugated secondary antibody (1:100000). Later blots were washed 5 times with 1X PBS and visualized using a thermo-scientific ECL kit. To assess the effect of glucosamine on the downregulation of *Pf*LPL3 at protein level, *Pf*LPL3-GFP-glmS ring stage parasites were treated with various concentration of glucosamine (1.25mM, 2.5mM, 5mM, 10mM), harvested at schizonts stage and subjected to the western blotting.

To assess the membrane association of *Pf*LPL3, percoll purified infected RBCs were incubated overnight at -80°C with 200 µl of 7.5mM Tris-Cl pH 8 for hypotonic lysis. After the centrifugation remaining pellet was washed twice with 7.5mM Tris-Cl pH 8 and incubated for 1 hour in four different buffers (200 µl 100 mM Sod. carbonate, 200 µl 6 M Urea in 7.5mM Tris-HCl pH 8.0, 200 µl of 1 % Triton-X100 and 200 µl of 2 % SDS) and centrifuged. Next, samples for western blotting were prepared from both soluble and pellet fraction of these buffers.

3.2.4 Immuno-fluorescence assay (IFA) and fluorescent microscopy

*Pf*LPL3-GFP-glmS parasites were fixed in 4 % paraformaldehyde and permeabilized with 0.1 % TritonX-100. Permeabilized cells were blocked with 10%FBS and then, incubated with rabbit polyclonal anti-GFP 1:500, mice polyclonal anti-SERA 5 1:500, for 2 hours

and subsequently with Alexa Flour-488 or 594 secondary antibodies. Immuno-stained parasites were washed three times with 1x PBS. Parasite nucleus was stained with a final concentration of 5 µg/ml DAPI. The membrane structures in parasitized erythrocytes were labelled with BODIPY TR-ceramide (Invitrogen) at a final concentration of 1µM. Images were captured by Nikon A1 confocal laser scanning microscope and analysed by Nikon-nis element software (version 4.1). The 3D images were constructed by using series of Z-stack images using IMARIS 7.0 (Bitplane Scientific) software.

3.2.5 Lipid extraction from *Plasmodium falciparum* and liquid chromatography-mass spectrometry analysis

Total lipids were extracted from treated (1.25mM glucosamine) and control parasites. An equal number of parasites (4×10^8 cell equivalents) were harvested from infected RBCs by using 0.15% saponin treatment. Total lipid was spiked with 20 nmol C21:0 phosphatidylcholine and extracted by chloroform:methanol, 1:2(v/v) and chloroform:methanol, 2:1 (v/v). The pooled organic phase was subjected to biphasic separation by adding 0.1% KCl and was then dried under N_2 gas flux prior to being dissolved in 1-butanol. For the total fatty acid analysis, an aliquot of the lipid extract was derivatized on-line using MethPrep II (Alltech) and the resulting FA methyl esters were analyzed by GC-MS as previously described. For the quantification of each lipid, total lipid was separated by 2D HPTLC using chloroform/methanol/28% NH_4OH, 60:35:8 (v/v/v) as the 1st dimension solvent system and chloroform/acetone/methanol/acetic acid/water, 50:20:10:13:5 (v/v/v/v/v) as the 2nd dimension solvent system. Each lipid spot was extracted for quantification of fatty acids by gas chromatography-mass spectrometry (Agilent 5977A-7890B) after methanolysis. Fatty acid methyl esters were identified by their mass spectrum and retention time and quantified by Mass Hunter Quantification Software (Agilent) and the calibration curve generated with fatty acid methyl esters standards mix (Sigma CRM47885). Then each lipid content was normalized according to the parasite cell number and a C21:0 internal standard (Avanti Polar lipids). All analyses were performed in triplicate or more (n=3). * P values of ≤ 0.05 from statistical analyses (Student's t-test) obtained from GraphPad software analysis were considered statistically significant.

3.2.6 Cloning, expression, and purification of recombinant *Pf*LPL3 protein

Hydrolase domain of *Pf*LPL3 was amplified by using specific primers 1270A & 1271A and cloned into pETM41 vector between *NcoI* and *XhoI* sites to give pETM41-His6-MBP-*Pf*LPL3 construct. The recombinant protein *Pf*LPL3 was expressed as a soluble protein in the cytosol of the *E. coli* BL21(DE3) cells and purified as described earlier in the general protocols section.

3.2.7 Lysophospholipase (LPL) activity assay using lysoPC as substrate and enzyme kinetics

In-vitro activity assay carried out for assessing the lysophospholipase like activity of the recombinant *Pf*LPL3 was using lysophosphatidylcholine (LPC) substrate. Reaction mixture contained 16:0 lysophosphatidylcholine (LysoPC) as substrate, 20µg (285pmol) of recombinant protein, 0.1 unit glycerophosphodiestrase (sigma), 0.2 U/ml choline oxidase (sigma # 26978), 2U/ml horseradish peroxidase (sigma#P8125), 100µM AmplexRed (Invitrogen) and reaction buffer (50mM Tris pH8, 5mM $Cacl_2$). The *Pf*LPL3 cleaves the acyl chain from lysoPC resulting the generation of glycerophosphocholine on which glycerophosphodiestrase acts and cleaves the choline moiety. This choline was oxidized by choline oxidase to betaine and H_2O_2. Finally, H_2O_2 in presence of horseradish peroxidase reacts with Amplex Red reagent in 1:1 stoichiometry to generate the highly fluorescent product resorufin, which has absorption and fluorescence emission maxima of approximately 571 nM and 585 nM respectively. Assay was performed in 96 wells black plate (200 µL total volume) using spectramax M2 microplate reader. The LPL activity was monitored by measuring resorufin fluorescence (530 ex/590 em) for 6 hrs. The assay was performed by varying the amount of protein and substrate to get optimum LPL activity. For calculating the kinetic parameter *K*m, varied concentration of the LPC substrates at constant enzyme concentration (20µg) was set up in a reaction plate in duplicates. Rate of hydrolysis was recorded for 6hrs at every 20minutes interval. The kinetic constant *K*m was determined by fitting the Michalies-Menten curve using the Graph Pad Prism V5.0 software package.

3.2.8 Standardization of a robust assay for inhibitor screening and screening of compound library in lysophospholipase (LPL) activity assay

To identify specific inhibitors of *Pf*LPL3, an *in-vitro* 96 well lysophospholipase activity assay was designed. We conducted HML test of the assay for a period of two days in accordance with a statistical test to calculate the Z-value. The HML assay employed three different reaction wells: the **H**igh activity well i.e. lpl activity well with 20µg protein; **M**edium activity well i.e. in the presence half protein, (10µg protein); and the **L**ow activity well that is the substrate control well without the protein; this set of three wells (HML) was repeated throughout the 96-well plate. The assay was repeated for two consecutive days. The Z-value was calculated based on the change in fluorescence after 6hrs. To assess the *Pf*LPL3 inhibition by different anti-malarial compounds, the recombinant enzyme (20µg) was incubated with different concentrations of each of the compound or DMSO alone in 100µl of assay buffer for 60min at 37ºC; then the reactions were initiated by addition of the reaction mixture to a final volume of 200µl and the substrate hydrolysis was monitored as above. To assess the effect of *Pf*LPL3 inhibitors of the parasite, 1 % ring-stage parasites at 4% hematocrit were incubated with varying concentrations of MMV compounds (5 to 0.2µM) and parasite growth was estimated in next cycle by flow cytometry. DMSO was used as a control. The *K*m, IC_{50} and EC_{50}values were calculated from curve fittings by Graph Pad Prism V5.0 software.

3.2.9 *In-silico* structural analysis of protein

3D structure of *Pf*LPL3 was predicted by using I-TASSER. The model was then simulated using molecular dynamics in Gromacs version 8 and stability of the simulated protein was confirmed by considering the parameters of the RMSD plot and Ramachandran plot. F-pocket prediction tool was used for finding the ligand-binding pocket of *Pf*LPL3. The model was then docked with selected inhibitors keeping the binding pocket and catalytic residues as the center for the grid generation and default docking parameters.

3.3 Protocols for molecular and functional characterization of *Pf*LPL4

3.3.1 Generation of *Pf*LPL4-GFP-DD parasite line

To generate *Pf*LPL4-GFP-DD construct, C-terminal fragment (702base pair) of *pfLPL4* gene was amplified using specific primers 1189A & 1063A and cloned into pARL^{a-}GFP-DD vector. The C-terminal fragment was cloned in-frame to the N-terminus of GFP in the *Kpn*I and *Avr*II restriction enzyme sites. Parasite cultures were synchronized and transfected with 100 µg of purified plasmid DNA as described earlier. Transfected parasites were selected over WR99210 drug in presence of Shld1 (1µM) and subsequently subjected to on and off cycling of WR99210 drug to promote integration of the plasmid in the main genome. Integration was confirmed by western blot analysis by using an anti-GFP antibody.

3.3.2 Conditional knock-down analysis and in-vitro growth assays

Parasite growth inhibition assays were carried out in 24 well plates (nunc) using synchronized parasite cultures at the ring stage. Each assay was performed in triplicate. Each well was containing 4% hematocrit and 1ml of complete media supplemented with 1µM Shld1 and the parasitemia was adjusted to ≤0.5%. A parallel set was maintained for each parasite line with solvent only. Smears were made from each well at different time points, stained with Giemsa, and the numbers of ring-stage parasites per 10000 RBCs were determined and percentage ring stage parasitemia was calculated manually to assess the parasite growth. Parasite growth was assessed at 48 and 96 hours after the addition of glucosamine by flow cytometry using BD FACS calibur. For flow cytometry, EtBr stained uninfected erythrocytes were used as background control. Cells were incubated with EtBr for 30 minutes at 37 °C in dark followed by two washing with 1X PBS and subjected to FACS analysis using a BD FACS Calibur system (Beckton Dickinson). A total of 100000 events were acquired and the data were analysed by using the Cell-Quest pro software.

3.3.3 Cloning, expression, purification, and LPL activity assay of recombinant *Pf*LPL4 protein

A fragment of *pfLPL4* gene corresponding to hydrolase domain region was amplified by using specific primers and cloned into pETM41 vector between *NcoI* and *XhoI* sites to give pETM41-His6-MBP-*Pf*LPL4 construct. The recombinant protein *Pf*LPL4 was expressed as a soluble protein in the cytosol of the *E. coli* BL21(DE3) cells and purified as described earlier. LPL specific activity assay was carried out and the kinetic constant *K*m, was determined by fitting the Michalies-Menten curve using the Graph Pad Prism V5.0 software package as described earlier in section 3.2.7.

3.4 Protocols for molecular and functional characterization of *Pf*LPL20

3.4.1 Generation of *Pf*LPL20-pSSPF2-GFP and *Pf*LPL20-GFP-glmS parasite lines

To generate an overexpression line, full length *PfLPL20* gene was amplified using primers 1294A, 1295A and cloned into pSSPF2-GFP vector. Parasite cultures were synchronized by repeated sorbitol treatment and 100 μg of purified plasmid DNA (Plasmid Midi Kit, Qiagen, Valencia, CA) was transfected in *P. falciparum* by electroporation (310 V, 950 μF. Transfected parasites were selected over 2.5 μg/ml blasticidin (Calbiochem). To generate *Pf*LPL20-glmS-GFP construct, C-terminal fragment (750base pair) of *PfLPL20* gene was amplified using specific primers 1224A and 1225A and cloned into GFP- *glm*S vector (Prommana et al., 2013). The C-terminal fragment was cloned in-frame to the N-terminus of GFP in the *Spe*I and *Kpn*I restriction enzymes sites. Transfected parasites were selected over 2.5 μg/ml blasticidin (Calbiochem) and subsequently subjected to on and off cycling of blasticidin drug to promote integration of the plasmid in the main genome. Integration was confirmed by PCR using 2200F and 1234A as well as by western blot analysis using anti-GFP antibody. Individual parasite clones were isolated by serial dilution method, and integration was also confirmed in the clonal parasite population.

3.4.2 Conditional knock-down analysis and in-vitro growth assays

To assess the effect of knock-down of *Pf*LPL20 on parasite, *Pf*LPL20-GFP-*glmS* transgenic parasites were tightly synchronized with 5% sorbitol and grown with media containing glucosamine 2.5mM (Sigma-Aldrich) or solvent alone. For microscopic analysis of morphology of the parasites, Giemsa stained smears were prepared at every 8hr interval from both glucosamine treated and control parasites. Parasite growth was assessed after 48 and 96 hours by flow cytometry using BD FACS Calibur (Beckton Dickinson) as described previously. To assess the effect of glucosamine on downregulation of *Pf*LPL20 at protein level, *Pf*LPL20-GFP-glmS ring-stage parasites were treated with 2.5 mM glucosamine, harvested at the schizont stage, and subjected to the western blotting.

3.4.3 Immuno-fluorescence assay (IFA) and fluorescent microscopy Infected RBCs were fixed in 4% paraformaldehyde and 0.05 % glutaraldehyde. After permeabilization with 0.1 % TritonX-100. Permeabilized cells were blocked with 10% FBS and then, incubated with rabbit polyclonal anti-GFP (1:500) for 2 hours and subsequently labelled with Alexa Flour-488 labelled secondary antibodies. Labeled parasites were washed three times with 1×PBS. Parasite nucleus was stained with DAPI at a final concentration of 5 µg/ml. To label the neutral lipid storage structures, infected erythrocytes were stained with Nile Red (Molecular Probes) using a modified method of (Palacpac et al., 2004). Briefly, Nile Red was added to a final concentration of 1 µg/ml into the parasite culture (5-10% parasitemia), the culture was incubated on ice for 30 min and subsequently washed with 1×PBS before analysis by confocal microscopy. Images were captured by Nikon A1 confocal laser scanning microscope and analysed by Nikon-NIS element software (version 4.1). The 3D images were constructed by using series of Z-stack images using IMARIS 7.0 (Bitplane Scientific) software.

3.4.4 Quantitative real-time PCR

For transcriptional analyses of different genes, total RNA was extracted using the TRIzol method from both *Pf*LPL20-iKD and control parasite cultures; reverse transcription reaction was carried out using the iScript cDNA Synthesis Kit (Bio-Rad), following

manufacturer's recommendations. Real-time amplification reactions were performed in triplicate on the StepOnePlus™ Real-Time PCR System (Applied Biosystems, Foster City, CA, USA) using an SYBR Green master-mix from Biorad (CA, USA). Each reaction comprised an equal amount of cDNA, 100 ng of both the gene-specific primers for *Pf*LPL20, *Pf*PMT (phosphoethanolamine-methyltransferase), *Pf*SAMS (S-adenosylmethioninesynthetase) and *Pf*EK (ethanolamine kinase) (Table 2), and 1× SYBR Green PCR mix. The threshold cycles (CTs) generated by the qPCR system were used to calculate fold change for relative quantitative analysis as described earlier.

3.4.5 LC-MS analysis to estimate cytosolic choline and phosphocholine levels

Parasites were isolated from Infected red blood cells (5×10^7 cell equivalents) from both *Pf*LPL20-iKD and control by using saponin lysis. Their total lipids were extracted by chloroform: methanol, 1:2(v/v) and chloroform: methanol, 2:1 (v/v) as previously described (Botte et al., 2013). The standard compounds (both choline and phosphocholine) were purchased from Sigma-Aldrich in form of choline chloride and phosphorylcholine chloride calcium salt tetrahydrate respectively, which were dissolved in HPLC grade solvents. Samples were analyzed by a 3200-QTRAP LC-MS system for estimation as described previously (Mimmi et al., 2013).

3.4.6 Cloning, expression, purification, and LPL activity assay of recombinant *Pf*LPL20 protein

Full-length *pfLPL20* was amplified by using specific primers 2200F and 2200R and cloned into pETM41 vector between *Nco*I and *Xho*I sites to give pETM41-His6-MBP-*Pf*LPL20 construct. The recombinant protein *Pf*LPL20 was expressed and purified as described earlier in section 3.1.5. Eluted fractions were subjected to SDS-PAGE as well as western blot analysis to assess the purity of the purified recombinant protein. LPL specific activity assay was carried out and the kinetic constant *K*m, was determined by fitting the Michalies-Menten curve using the Graph Pad Prism V5.0 software package as described earlier in section 3.2.7.

3.4.7 Identification of *Pf*LPL20 interacting partners

Affinity Pull-down of GFP-fusion protein complex: Schizont stage lysate of *Pf*LPL20-pSSPF2 and *Pf*LPL20-GFP-*glmS* parasites was obtained as described above and immunoprecipitation was done using GFP-Trap®-A Kit (Chromotek) following the manufacturer's instructions. Briefly, GFP-Trap®-A beads were equilibrated with dilution buffer and allowed to bind to proteins in the parasite lysate by tumbling the tube end-over-end for 3 h at 4ºC. Samples were then centrifuged at 1600 rpm for 1 min and the beads were washed twice with dilution buffer. Bound proteins were eluted in 50 µl elution buffer, trypsin digested peptides were analysed by mass spectrometry following in-solution digestion.

Tryptic digestion and Mass spectroscopy:

In-Solution Digestion: Eluted proteins were diluted in 50 mM ammonium bicarbonate, and subsequently reduced for disulphide bonds with 10 mM DTT for 1 h followed by sulfhydryl alkylation using iodoacetamide (IAA) for 1 h at RT. Trypsin was added to the samples at a ratio of 1:50 (w/w) of trypsin: protein, and incubated overnight at 37°C. Digestion reaction was stopped by acidification with 0.1% trifluoroacetic acid, samples were cleared by centrifuging at 10000 rpm for 10 min and subjected to LC-MS/MS.

Liquid chromatography -tandem mass spectrometry: The peptides were subjected to mass spectrometry using Orbitrap VelosPro mass spectrometer coupled with nano-LC 1000 (Thermofisher Scientific Inc, USA). The acquired spectra were analysed using the SEQUEST search engine algorithm in Proteome Discoverer version 1.4 software with a precursor tolerance of 20 ppm and tolerance of 0.6 Da for MS/MS against *P. falciparum* database downloaded from *PlasmoDB*. Five missed cleavages were allowed. The resultant identified peptides were validated using Percolator at less than 5% FDR with high confidence.

Table 2: List of primers used in the study

Name	Sequence	Gene/gene fragment	Construct/ application
1270A	GGATCCACCATGGAAGTATCATAATATTAATA CATGGGTTAGC	*LPL3*	Recombinant protein expression
1271A	CCTAGGTCCTTTTTCGATTGTTATAACATGAC		
1222A	ACTAGTAGTATTTTAGAATCTGAAACG		*Pf*LPL3-GFP-*glmS* Construct
1223A	GGTACCTTTCTTTTCTTTTTCTTTTTGC		
1189A	TATAAATTTAAAGTTTTAGGTAGGAC	*PfLPL4*	*Pf*LPL4-GFP-DD Construct
1063A	GCTAAATATATTATTAAGCCAATCAAC		
1224A	ACTAGTAATGGTGTATCAGAATGTGATAC	*pfLPL20*	*Pf*LPL20-GFP-*glmS* Construct
1225A	GGTACCTTCAATATATTCTTCTACTTTTGTGAC		
1294A	AGATCTATTATAAATATCATGGTATCTAATG		pSSPF2-LPL20-GFP Construct
1295A	TTCAATATATTCTTCTACTTTTGCCTAGG		
2200F	ATGGTATCTAATGAATTAAATTGTGAACCG		Recombinant protein expression
2200R	TTCAATATATTCTTCTACTTTTGTGACATC		
1234A	ACTCCAGTGAAAAGTTCTTCTCCT	*Reverse primer on 5' of GFP*	To assess the integration of GFP-*glmS* plasmid in main genome
1371A	GCTGATATTCTTACTGCTTGC	*pfPMT*	Quantitative Real-Time PCR
1372A	ACCAGCCATCATCAAGACTA		
1373A	TGCATCAAAAGTCGATCGTT	*pfSAMS*	
1374A	TATCCTGTGCTTACGGTACC		
1375A	AAATTCACCCGTGGTTCTTT	*pfEK*	
1376A	TGCTCTTTCCATTGGACATG		
1406A	AATTTGTGGGTAATCATTTTCCG	*pfLPL20*	
1407A	AATATCTGAAAAGCAAACTGACC		

Chapter 4 Results

4. Results

4.1 Identification and biochemical characterization of lysophospholipases in *Plasmodium falciparum*

Lipid metabolism is one of the most crucial pathways of the *Plasmodium falciparum* life cycle and lysophospholipases plays an important role in lipid metabolism. We identified and characterized lysophospholipases in *P. falciparum.* In this section, results of bioinformatics study to identified putative lysophospholipases (LPLs) in *Plasmodium* genome, and biochemical characterization/ enzymatic activities of selected LPLs are explained.

4.1.1 Identification and sequence analysis of *P. falciparum* lysophospholipases (LPLs)

In enzymology, Lysophospholipase comes under the Enzyme Commission number 3.1.1.5, which catalyzes hydrolysis of lysophospholipids. To identify LPLs in *P. falciparum* genome, we searched the *PlasmoDB* database *(http://plasmodb.org/plasmo; Aurrecoechea et al.,* 2009) using EC number 3.1.1.5 and identified a total of 14 proteins which have α/β hydrolase domain (Table 3). This list includes six putative lysophospholipases, 4 putative esterases, 2 exported lipases, 1 putative patatin-like phospholipase and 1 putative alpha/beta hydrolase enzyme. Ten of these proteins were about 353-453 amino acids long and have high degree of homology (36-61%) with each other; none of these proteins contain any signal sequences or any other functional domain. Their hydrolase domain harbors the lysophospholipase characteristic motif GXSXG, wherein the catalytic active site serine (S) is flanked by glycine amino acid residues, other two residues of the catalytic triad are aspartic acid (D) and the histidine (H). The remaining four members of this lysophospholipase l-like protein family are larger proteins (675-2380 amino acid long) having substantial protein sequence stretch outside the α/β hydrolase domain. Multiple sequence alignment of all these LPLs shows that the catalytic triad of the active site (Serine, Histidine, Aspartic acid) and G-X-S-X-G motifs are conserved in all LPLs (Figure 9). We selected PF3D7_1476800, PF3D7_0702200, and PF3D7_0731800 lysophospholipases for further study, which are named as LPL3, LPL20, and LPL4, respectively.

Table 3: List of fourteen proteins having alpha/beta hydrolase domain present in *P. falciparum* genome**.**

	Gene ID	Product Description	Protein Length
1	PF3D7_0102400.1	lysophospholipase, putative, pseudogene	383
2	PF3D7_0218600	patatin-like phospholipase, putative	2380
3	PF3D7_0702200	lysophospholipase, putative	424
4	PF3D7_0709700	prodrug activation and resistance esterase	368
5	PF3D7_0731800	alpha/beta hydrolase, putative	675
6	PF3D7_0936700	lysophospholipase, putative	432
7	PF3D7_0937200	lysophospholipase, putative	357
8	PF3D7_1001400	exported lipase 1	921
9	PF3D7_1001600	exported lipase 2	763
10	PF3D7_1038900	esterase, putative	359
11	PF3D7_1252600	esterase, putative	453
12	PF3D7_1401500	esterase, putative	373
13	PF3D7_1476700	lysophospholipase, putative	353
14	PF3D7_1476800	lysophospholipase, putative	371

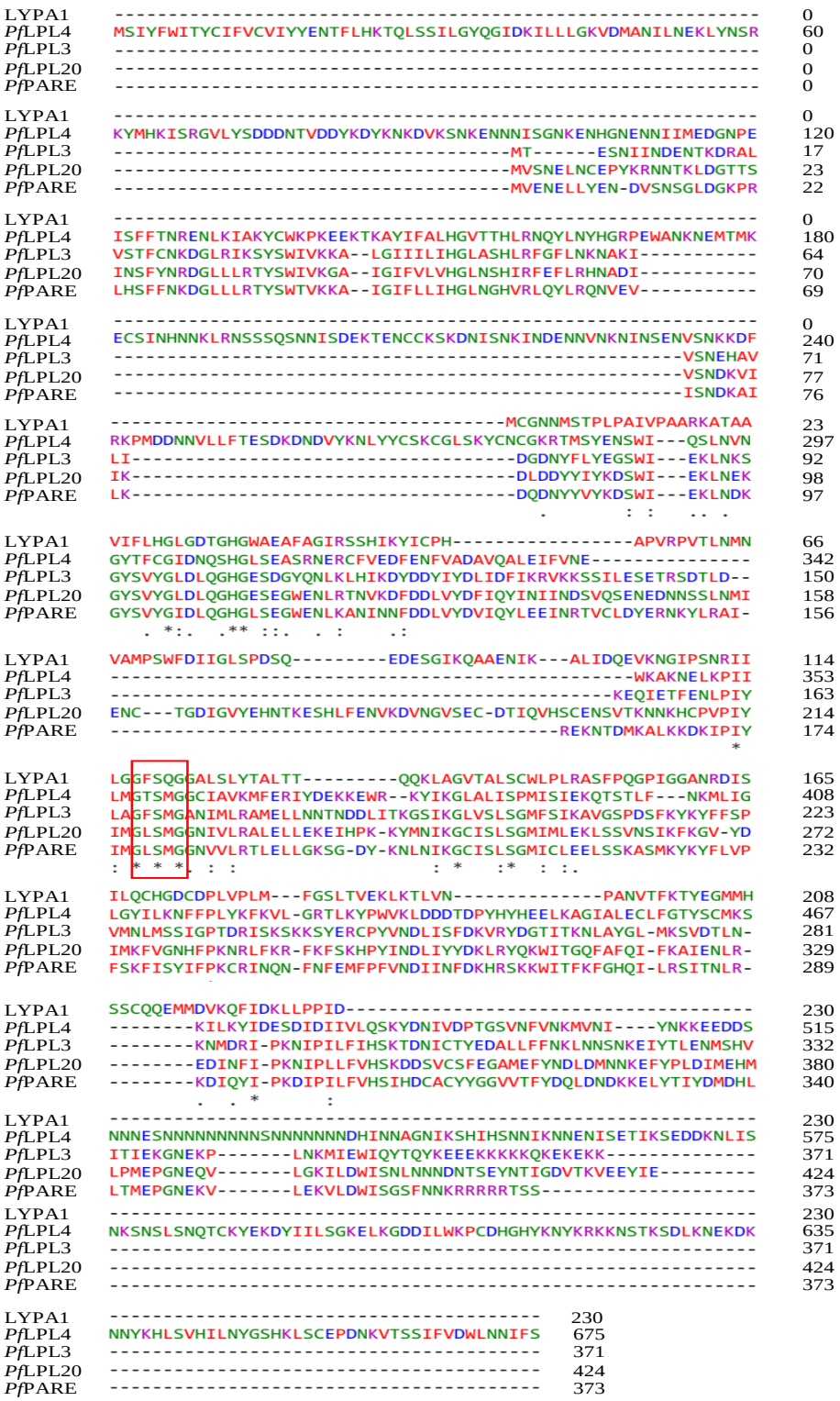

Figure 9: Multiple Sequence Alignment of *Pf*LPLs: Multiple sequence alignment of selective *Pf*LPLs showing the characteristic motif (red box) conserved among all LPLs.

4.1.2 Cloning, expression, purification, and enzymatic activity of *Pf*LPL3 (PF3D7_1476800)

For the biochemical characterization, we expressed and purified the recombinant *Pf*LPL3 using *E. coli* expression system. The gene fragment corresponding to hydrolase domain of *Pf*LPL3 was amplified using specific primers 1270A and 1271A (Figure 10A) and cloned in to pETM41 vector between *Nco*I and *Xho*I restriction sites to give pETM41-His6-MBP-*Pf*LPL3 construct (Figure 10B). The recombinant protein was expressed using *E. coli* expression system (Figure 10C) and purified by using a combination of affinity chromatography techniques. Eluted fractions were subjected to SDS-PAGE and western blot analysis to check the purity of the recombinant protein. The purified recombinant protein migrated on SDS-PAGE at the expected size of ~70kDa (Figure 10D).

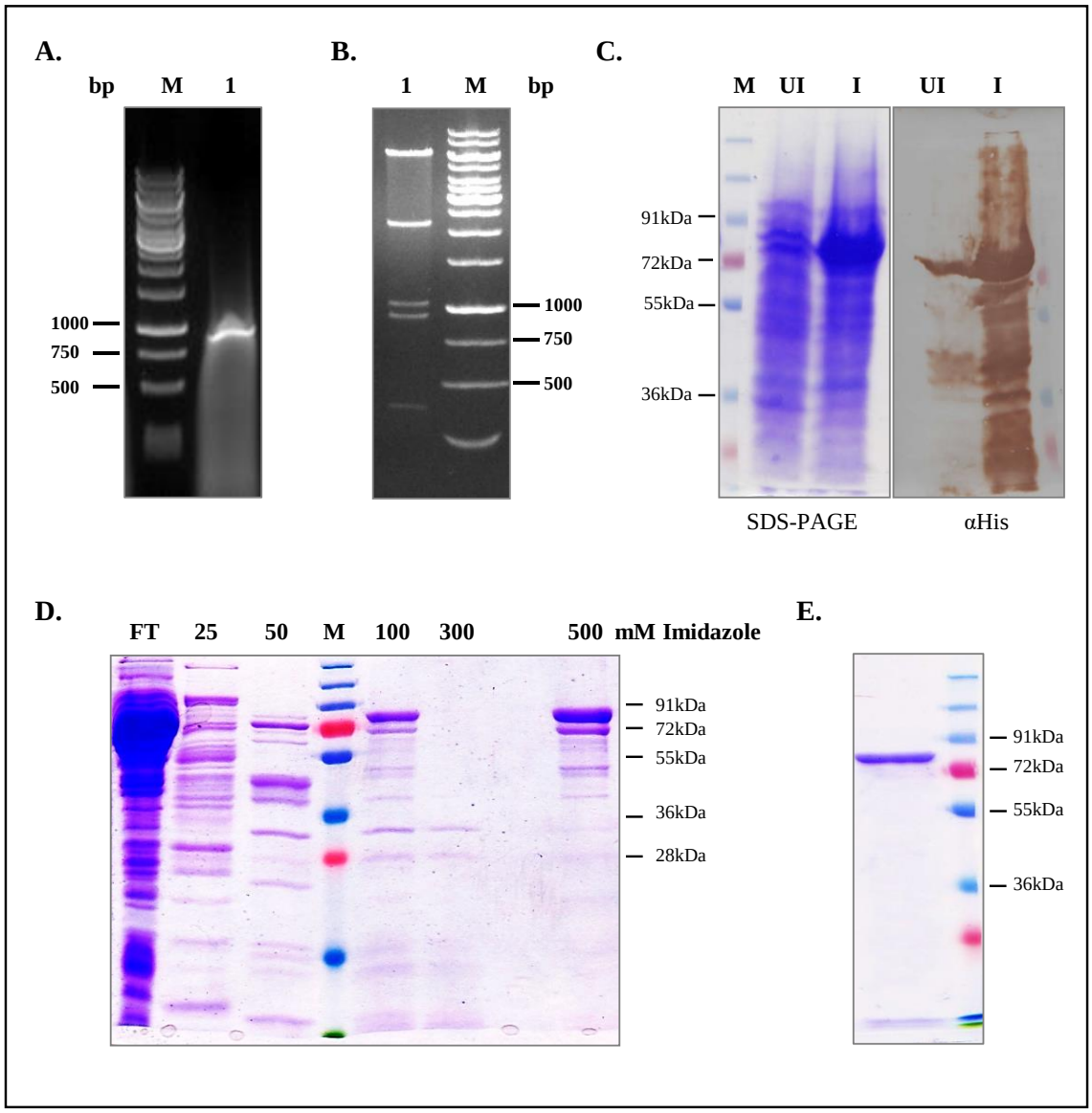

Figure 10: Expression and purification of LPL domain of *Pf*LPL3 in *E. coli*: (A) Agarose gel showing the PCR amplified 890 base pair long gene fragment corresponding to hydrolase domain of *Pf*LPL3. (B) Agarose gel showing the restriction digestion with *Nco*I and *Xho*I enzymes of *Pf*LPL 3 hydrolase domain cloned in pETM41 vector. (C) SDS-PAGE and western blot showing induction of recombinant protein with 1mM IPTG. UI: Uninduced, I; Induced. (D) SDS-PAGE showing the purification profile of the recombinant protein by using affinity (Ni^{2+}-NTA) chromatography. Protein fractions were eluted in presence of the increasing concentration of imidazole. (E) SDS-PAGE of recombinant *Pf*LPL3 further purified using MBP affinity chromatography. Purified protein migrated at the expected size of ~70kDa. FT and M denotes the flow through fraction and known molecular weight marker, respectively.

To characterize the enzymatic activity of *Pf*LPL3, we utilized standardized a fluorescence based lysophosphatidylcholine (LPC) substrate. The assay was standardized in a 96 well plate format so that it can be subsequently used for screening of compound library. In this assay the LPL cleaves the acyl chain from lysophosphatidylcholine (LPC) resulting into generation of glycerophosphocholine, which is a substrate for the glycerophosphodiestrase and upon cleavage leads to free choline moiety. This choline is then oxidized by choline oxidase to betaine and H_2O_2. Finally, the released H_2O_2 in presence of horseradish peroxidase, reacts with Amplex Red reagent in 1:1 stoichiometry to generate a highly fluorescent product resorufin; generation of resorufin was monitored by measuring fluorescence intensities (530 ex/ 590 em) (Figure 11A). The purified recombinant protein was used in activity assay of lysophospholipase using LPC substrate (Figure 11B). The recombinant *Pf*LPL3 showed concentration dependent activity in the assay, confirming it to be a lysophospholipase. The recombinant MBP (maltose binding protein) purified in same way was used as a control, which did not show any enzymatic activity in the assay. The *K*m value for the *Pf*LPL3 were found to be 40µM (Figure 11C).

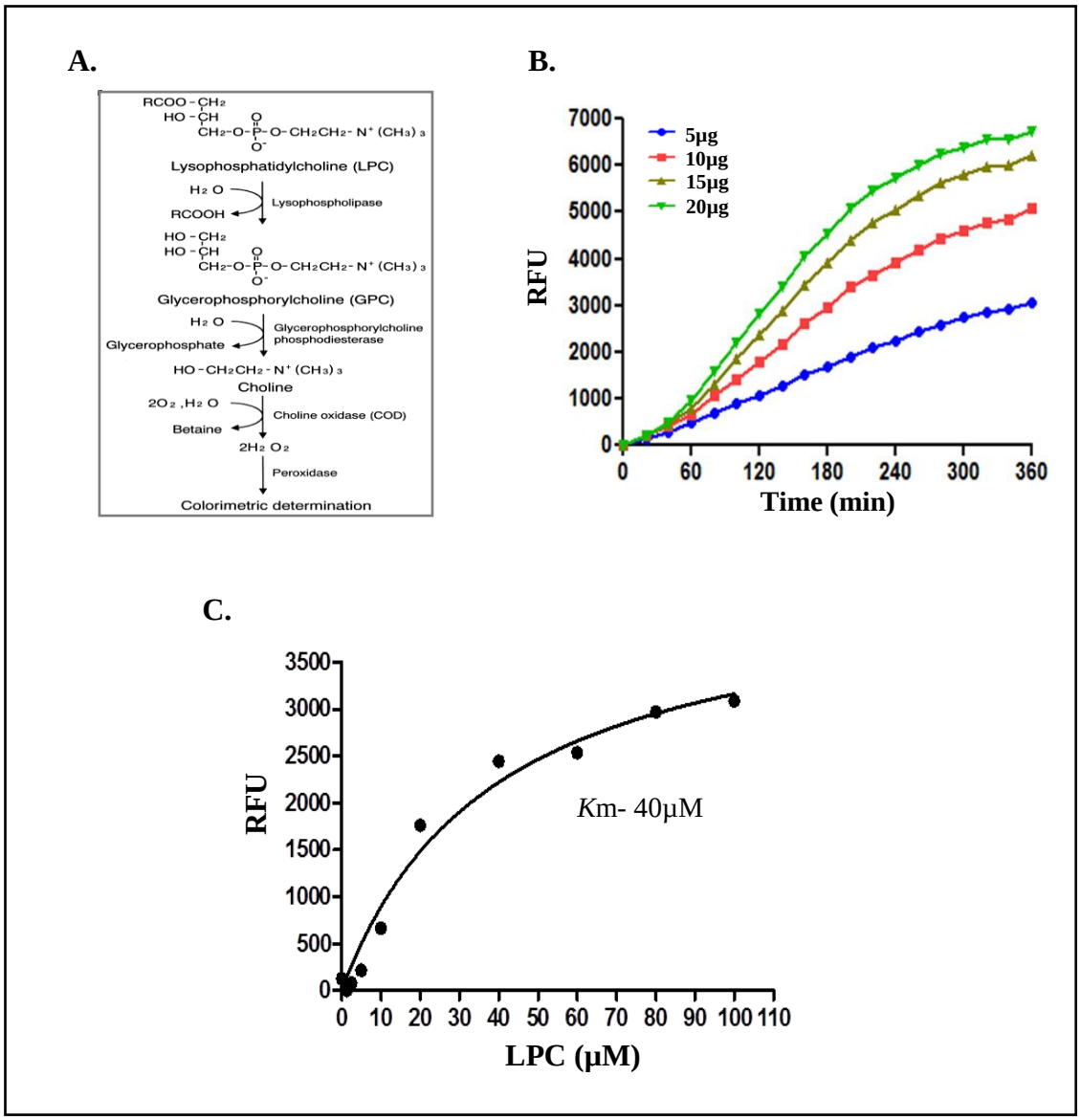

Figure 11: Standardization of lysophospholipase specific activity of the recombinant *Pf*LPL3: (A) Representative diagram of reaction and components involved in the LPL activity assay. LPC was used as a substrate and fluorescence of resorufin end product was measured. (B) Graphical representation of LPL activity of *Pf*LPL3 in presence of varying amount of protein. (C) Line graph of Michelis-Menten fit for *Pf*LPL3 enzymatic activity in presence of 20µg (85pmoles) recombinant protein. *K*m value of *Pf*LPL3 was found to be 40µM.

4.1.3 Cloning, expression, purification, and enzymatic activity of *Pf*LPL20 (PF3D7_0702200)

To express and purify recombinant *Pf*LPL20 protein, the full length (1250 base-pair) *PfLPL20* gene was PCR amplified using gene specific primers 2220F and 2200R (Figure 12A) and cloned in to pETM41 vector between *Nco*I and *Xho*I restriction sites to give pETM41-His6-MBP-PfLPL20 construct (Figure 12B). The recombinant protein was expressed using *E. coli* expression system and purified by using a combination of affinity chromatography techniques. Eluted fractions were subjected to SDS PAGE analysis to check the purity of the recombinant protein. The purified recombinant-*Pf*LPL20 migrated slightly above the expected size of ~84kDa on SDS-PAGE (Figure 12D). The purified recombinant *Pf*LPL20 was used to assess its LPL activity as described earlier and showed concentration dependent activity in the assay (Figure13B), confirming it to be a lysophospholipase. The *K*m value for the *Pf*LPL20 was found to be 33.41 µM (Figure 13C).

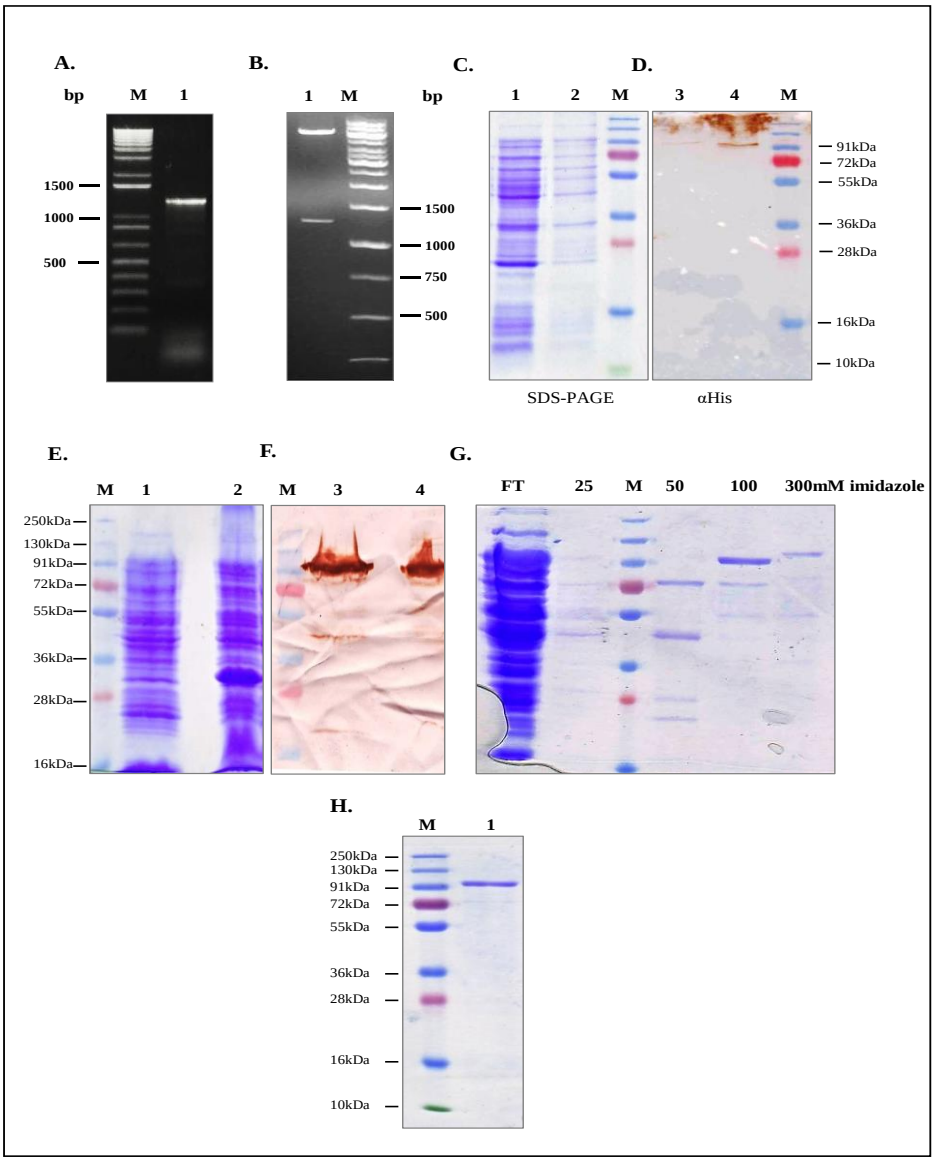

Figure 12: Expression and purification of*Pf*LPL20 in *E. coli*: (A) Agarose gel showing PCR amplified 1250 base pair *PfLPL20* gene. (B) Agarose gel showing the restriction digestion with *NcoI* and *XhoI* enzymes of *Pf*LPL20 cloned in pETM41 vector. (C) SDS-PAGE and (D) western blot showing induction of recombinant protein with 1mM IPTG. Lane 1,3: Uninduced, Lane 2,4; Induced. (E) SDS-PAGE and (F) western blot showing that recombinant is present in both soluble fraction as well as in inclusion bodies (insoluble fraction) Lane 1&3; insoluble fraction, Lane 2 & 4 soluble fraction. (G) SDS-PAGE showing the purification profile of the recombinant protein using affinity (Ni^{2+}-NTA) chromatography. Protein fractions were eluted in the presence of increasing concentrations of imidazole (25mM-300mM) written on the top of each lane, respectively. Purified protein migrated at the expected size of ~94 kDa. (H) SDS-PAGE of recombinant *Pf*LPL20 further purified using MBP affinity chromatography. FT and M denotes the flow through fraction and known molecular weight marker, respectively.

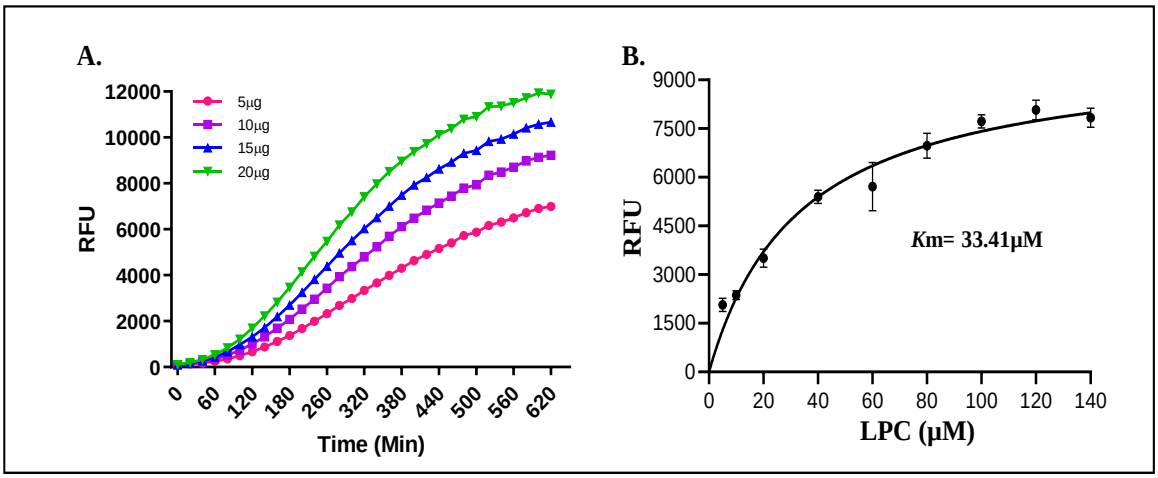

Figure 13: Standardization of lysophospholipase specific activity of the purified recombinant *Pf*LPL20: (A) Graphical representation of LPL activity of *Pf*LPL20 in presence of varying amount of protein. (B) Line graph of Michelis-Menten fit for *Pf*LPL20 enzymatic activity in presence of 20µg (85pmoles) of recombinant protein. *K*m value of *Pf*LPL20 was found to be 33.41µM.

4.1.4 Cloning, expression, purification, and enzymatic activity of *Pf*LPL4 (PF3D7_0731800)

*Pf*LPL4 is 675 amino acid long, protein having hydrolase domain (280 amino acid – 510 amino acid). To ascertain and characterize the enzymatic activity of *Pf*LPL4, recombinant protein corresponding to hydrolase domain was expressed and purified using *E. coli* expression system. The gene fragment corresponding to hydrolase domain of *Pf*LPL4 (710 base pair) was PCR amplified using gene specific primers (Figure 14A) and cloned in to pETM41 vector between *Nco*I and *Xho*I restriction sites (Figure 14B). The recombinant protein was purified by using a combination of affinity chromatography techniques as described earlier and checked for purity. As shown in figure 14, the purified recombinant protein was migrated at the expected size of ~68 kDa. The purified recombinant protein was further assessed for its ability to hydrolyze LPC using fluorescent based assay as described previously. The recombinant protein was purified with more than 90% purity (Figure 15A and B). The *K*m value for *Pf*LPL4 was found to be 42µM (Figure 15C).

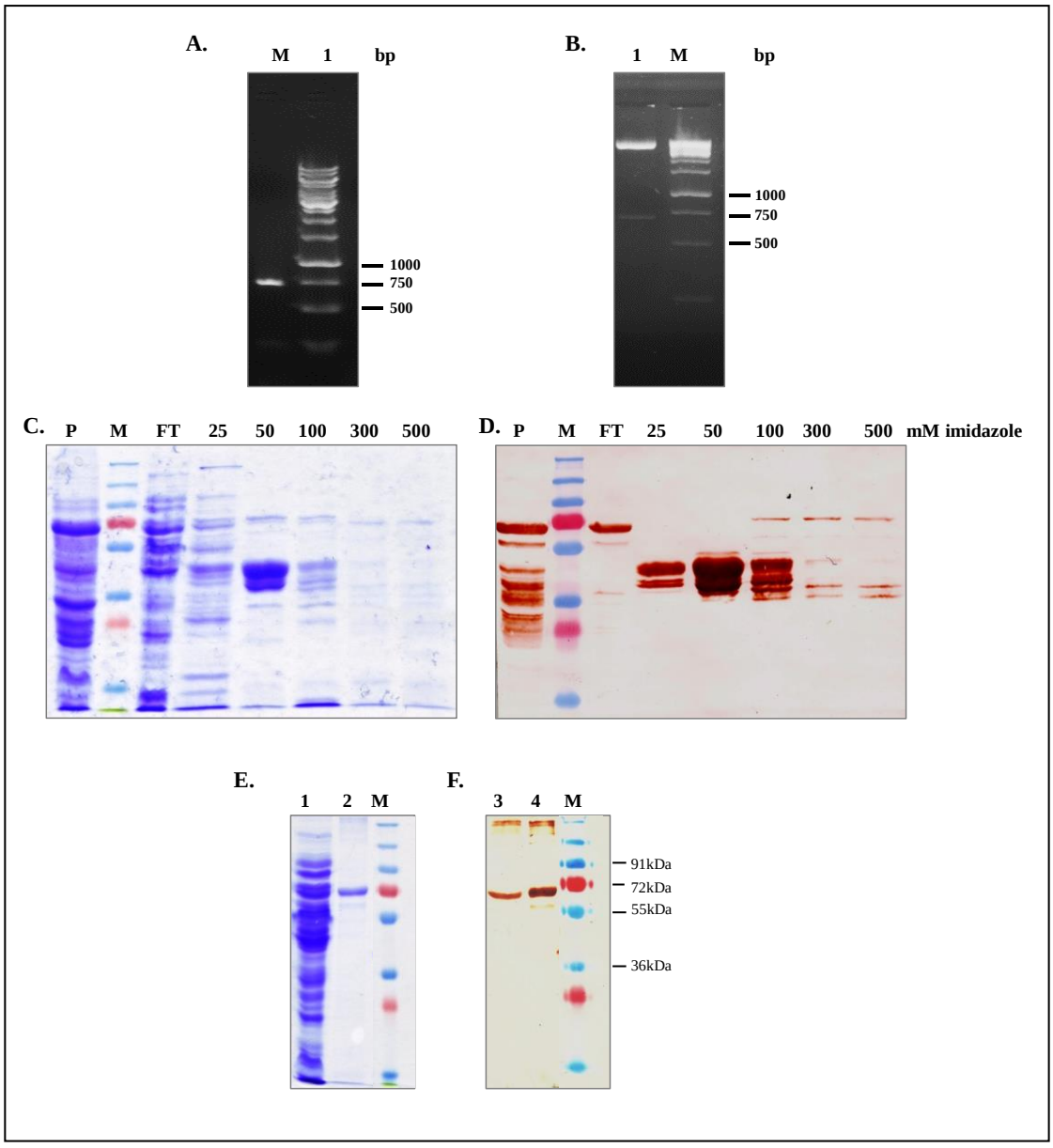

Figure 14: Expression and purification of LPL domain of *Pf*LPL4 in *E. coli*: (A) Agarose gel showing the PCR amplified 710 base pair long gene fragment corresponding to hydrolase domain of *Pf*LPL4. (B) Agarose gel showing the restriction digestion with *NcoI* and *XhoI* enzymes of *Pf*LPL 4 hydrolase domain cloned in pETM41 vector. (C) SDS-PAGE and (D) western blot showing the purification profile of the recombinant protein Ni^{2+}-NTA using affinity chromatography. Protein fractions were eluted in presence of the increasing concentrations of imidazole (25mM-300mM) written on the top of each lane, respectively. Purified protein migrated at the expected size of 68 kDa. (E) SDS-PAGE and (F) western blot of recombinant *Pf*LPL4 further purified using MBP affinity chromatography. Lane 1,3 Flow-through and Lane 2, 4 purified protein.

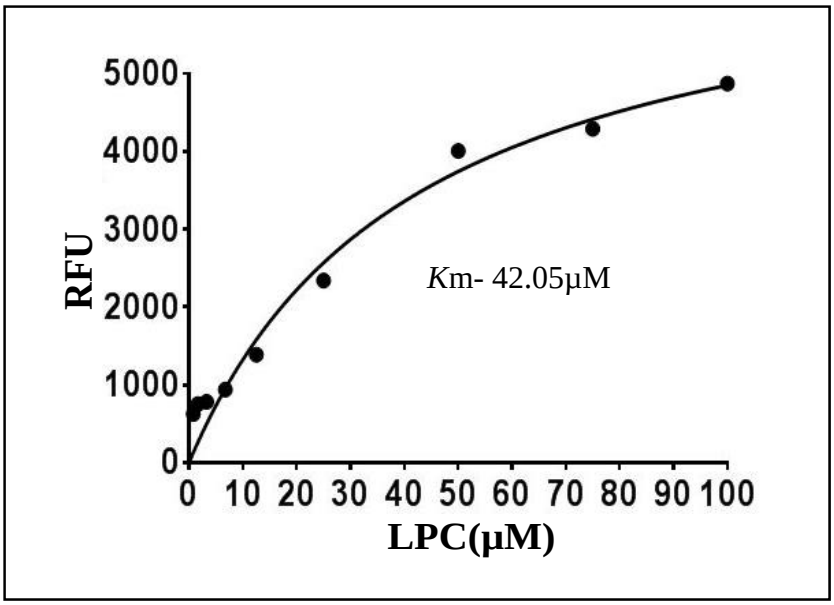

Figure 15: Standardization of lysophospholipase specific activity of the purified recombinant *Pf*LPL4: Graphical representation of Michelis-Menten fit for LPL activity in presence of the 20µg (85pmoles) of recombinant protein. *K*m value of *Pf*LPL4 was found to be 42µM.

4.2 Functional significance of lysophospholipases and their role in lipid homeostasis in the parasite

In this section, we tried to elucidate the functional role of selected lysophospholipases in parasite growth and survival. We used various strategies including reverse genetic approaches, GFP tagging for localization studies as well as metabolic studies to explore the role of these lysophospholipases in maintaining the lipid homeostasis in the parasite.

4.2.1 Functional characterization of *Pf*LPL3

4.2.1.1 Endogenous tagging of *Pf*LPL3 gene and its localization in transgenic parasites

We tagged the endogenous *Pf*LPL3 for localization studies as well as to study its functional essentiality by conditional knock-down strategy. We used GFP-*glmS* ribozyme system (Prommana et al., 2013) for C-terminal tagging of the native *PfLPL3* gene by single cross-over, so that the fusion protein gets expressed under the control of native promoter (Figure 16). The *glmS* ribozyme is an inducible knockdown reverse genetic approach in which, *glmS* ribozyme is fused downstream of the target mRNA. In presence of glucosamine (GlcN), ribozyme gets activated and cleaves itself. The mRNA self-cleaving results in degradation of mRNA and ultimately knock-down of the targeted protein expression.

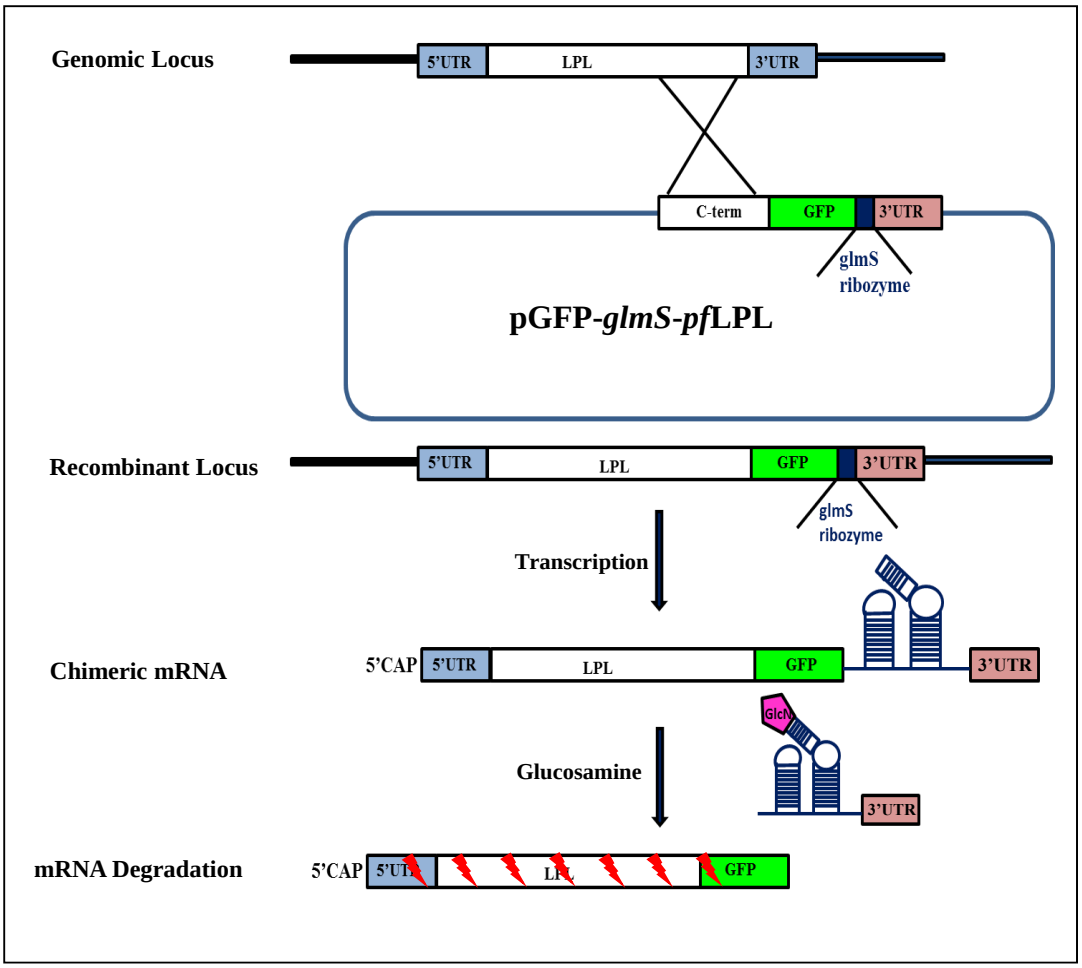

Figure 16: Schematic of GFP-*glmS* tagging of *PfLPL3* gene and gene knock-down approach: A schematic representation of single crossover homologous recombination showing the integration of the LPL3-GFP-*glmS* plasmid at the C-terminus of the endogenous *PfLPL* gene. The ribozyme inserted before the 3'UTR was expressed as chimeric mRNA and its activation in presence of glucosamine results in self-cleaving, which ultimately leads to the degradation of the chimeric mRNA and knock-down of the protein expression.

For endogenous tagging, C-terminal fragment of *PfLPL3* gene was PCR amplified using gene specific primers (1222A and 1223A) and cloned in pGFP-*glmS* vector (Figure 17B&C). All fragments of the final plasmid construct were confirmed using several combinations of the restriction enzymes for correct arrangement of various expression cassettes (Figure 17D). This plasmid construct was used for homologous recombination-based integration in of GFP-*glmS* gene of interest. *P. falciparum* 3D7 parasites were transfected with plasmid construct and transfected parasites were selected on blasticidin

drug. To select parasites having integrated copy of plasmid, drug selected transgenic parasite was subjected to on/off drug cycling. Transgenic integrated parasite line, *Pf*LPL3-GFP-*glmS*, was obtained after several rounds of drug-selection cycles; C-terminal integration was confirmed in selected clonal population using PCR based analyses (Figure 18B). Expression of fusion protein of ~70kDa was detected by western blot analysis using anti-GFP antibody specifically in transgenic parasite line (Figure 18C); this band was not detected in wild type 3D7 parasites.

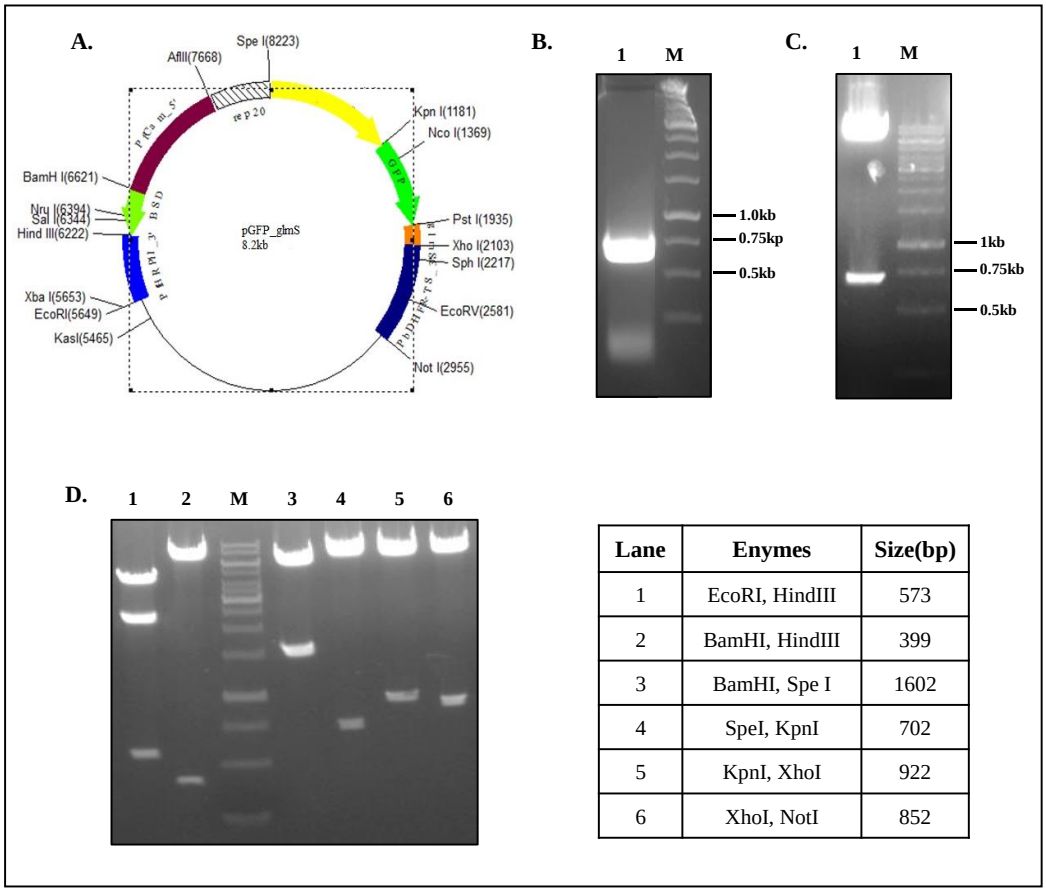

Lane	Enymes	Size(bp)
1	EcoRI, HindIII	573
2	BamHI, HindIII	399
3	BamHI, Spe I	1602
4	SpeI, KpnI	702
5	KpnI, XhoI	922
6	XhoI, NotI	852

Figure 17: Cloning of *Pf*LPL3 in GFP-*glmS* vector and restriction digestion analysis of *Pf*LPL3-GFP-*glmS*: (A) Schematic of the pGFP-*glmS* vector showing different vector cassettes and restriction sites. (B) Agarose gel showing PCR amplified C-terminal of the *pflpl3* gene. (C) Agarose gel showing restriction digestion of *Pf*LPL3-GFP-*glmS* plasmid construct with SpeI & KpnI enzymes, showing exicision of cloned fragment. (D) Agarose gel electrophoresis of the *Pf*LPL3-GFP-*glmS* plasmid construct with different sets of restriction enzymes to analyse the vector cassette. Table showing different combination of restriction enzymes used to check different expression cassette along with respective size of excised fragments.

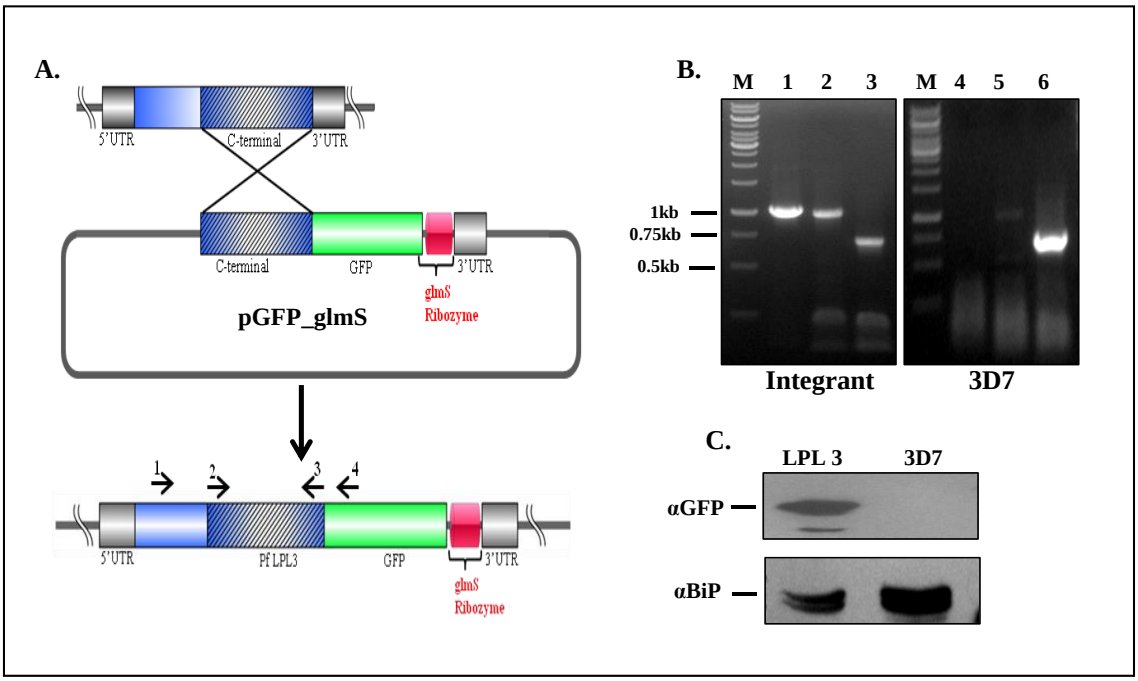

Figure 18: Confirmation of genomic integration of GFP-*glmS* at *PfLPL3* locus: (A) Schematic diagram showing the predicted C-terminal homologous recombination between the *Pf*LPL3 locus and *Pf*LPL3-GFP-*glmS* construct along with the primers position to check the integration. (B) Agarose gel showing PCR based analysis of the selected parasites after 2 drug cycles and parent 3D7 parasite lines. Lane 1 and 4; amplicon using primer number 1270A and 1234A detected only in the integrants, Lane 2 and 4; PCR amplicon using primer number 1223A and 1234A detected in integrants and episomal parasites, Lane 3 and 6 ; PCR amplificon using primer number 1222A and 1223A detected in all the episomal, integrants as well as the parent line. (C) Western blot analysis of transgenic parasite lysate probed with anti-GFP antibody. The fusion protein band was detected only in the transgenic parasites and not in the 3D7 parent parasite line. Blot ran in parallel and probed with anti-BiP was used as loading control.

4.2.1.2 Localization of *Pf*LPL3 in the parasite

The endogenously tagged *Pf*LPL3-GFP-*glmS* parasites were used for localization studies as well as to study functional essentiality by conditional knock-down strategy. The *Pf*LPL3-GFP-*glmS* transgenic parasites were studied for localization of the *Pf*LPL3-GFP fusion protein by fluorescence/confocal microscopy. The chimeric protein was found to be expressed in all stages of asexual life cycle of the parasite (Figure 19). In early development stages, the ring and mid trophozoite stages, GFP fluorescence was mainly observed in the cytosol; as the parasites mature into late-trophozoite and schizonts stages, the GFP

labelling was observed at the parasite periphery in the parasitophorous vacuole (PV) region. It was intriguing to observe *Pf*LPL3 was also present in the in the tubulovesicular networks (TVN) during the late trophozoite stages (Figure 19).

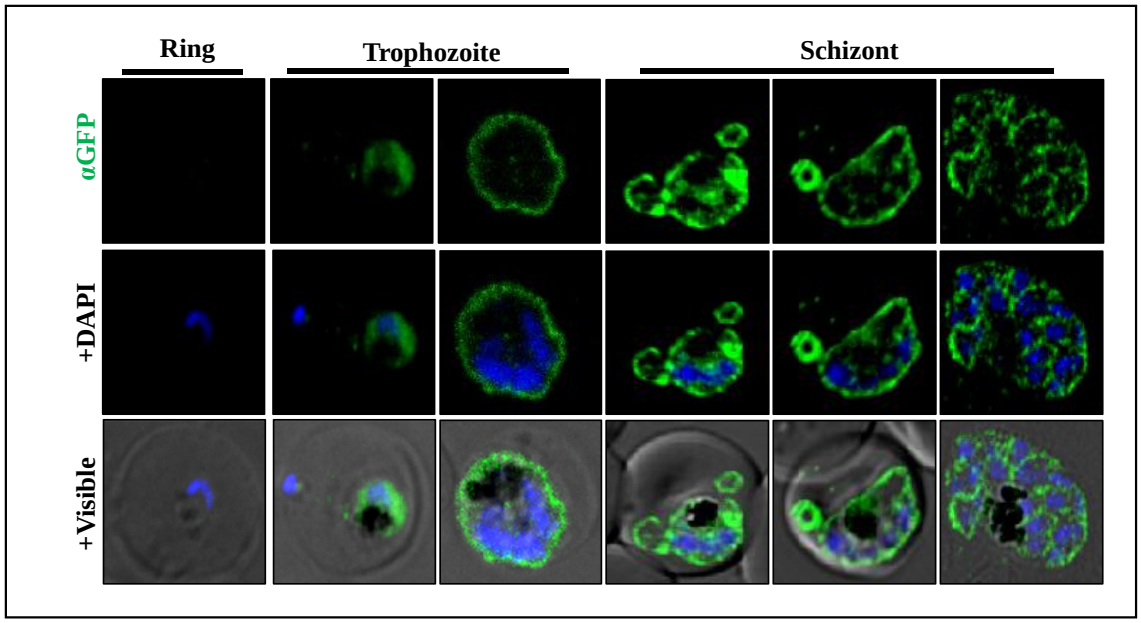

Figure 19: Localization of *Pf*LPL3-GFP fusion protein in transgenic parasites: Fluorescent microscopic images of live transgenic parasites at ring, trophozoite, and schizont stages. The parasite nuclei were stained with DAPI and parasites were visualized by confocal laser scanning microscope. In young parasites, the fusion protein was observed in the cytosol of the parasite but as the parasite matures, the fluorescence was observed towards the periphery of the parasite.

4.2.1.3 *Pf*LPL3 associates with PV and PVM of the parasite

To further investigate these localization patterns, we carried out molecular staining and immuno-staining studies using transgenic parasites. The GFP tagged parasites were co-stained with the lipid membrane probe BODIPY-TR ceramide. The BODIPY probe labelled parasite periphery, which include plasma membrane and parasitophorous vacuole membrane; in addition, the tubulovesicular extension of the parasitophorous vacuolar membrane were observed in the erythrocyte cytosol for some of the parasites. The *Pf*LPL3-GFP labelling showed overlap with BODIPY-TR ceramide, in the parasitophorous vacuole region as well as in the TVN (Figure 20A). A 3D reconstruction of trophozoite stage parasite images clearly show presence of GFP staining around the parasite periphery and

in the TVN (Figure 20A). To understand if the *Pf*LPL3 is localized in the parasitophorous vacuole region, we co-stained the transgenic parasites with one of the PV resident proteins, SERA5 (Stallmach et al., 2015); As shown in figure 20B, SERA5 staining overlapped with *Pf*LPL3-GFP around the parasite boundary in infected RBC which confirmed the localization of *Pf*LPL3-GFP protein in the PV.

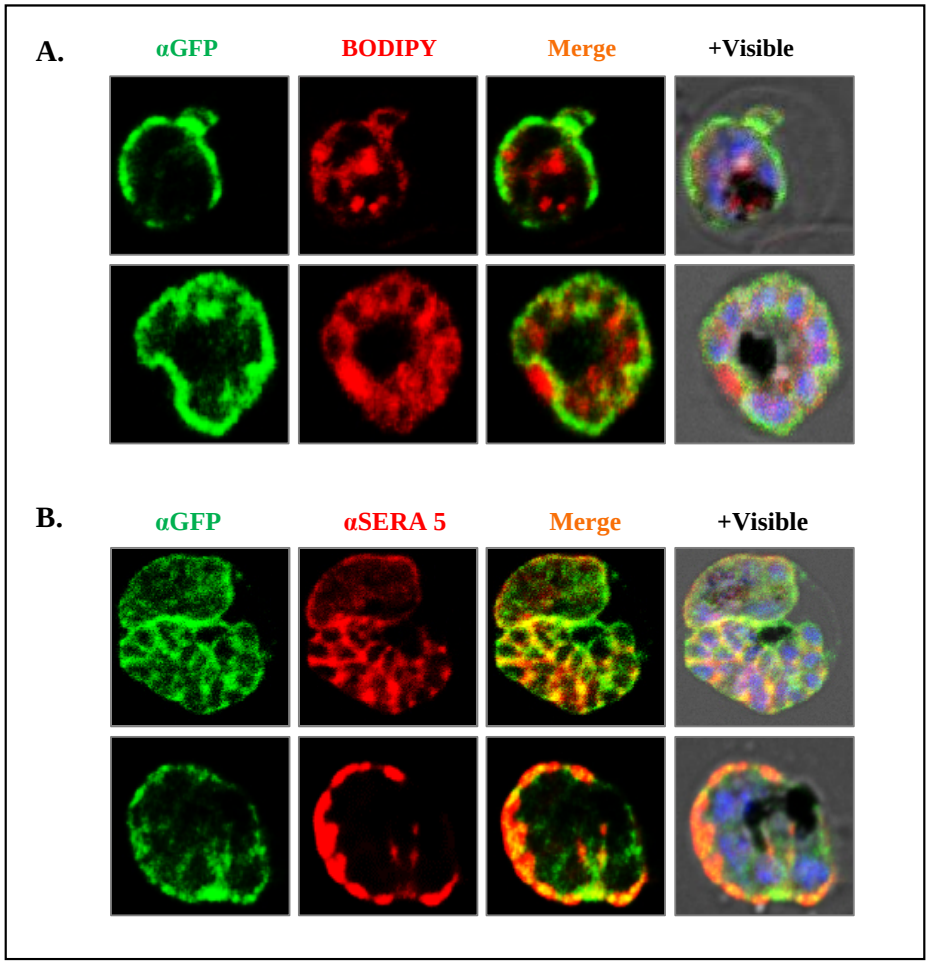

Figure 20. Co-localization study of *Pf*LPL3 with the PV and PVM markers: (A) Fluorescent microscopic images of transgenic parasites stained with membrane probe BODIPY™ TR ceramide, showing GFP fusion protein at the parasite periphery in late parasite stages. Parasite nuclei were stained with DAPI and images were acquired by confocal laser scanning microscope. (B) Fluorescent microscopic images of transgenic parasites immuno-stained with anti-SERA5 antibody showing colocalization of *Pf*LPL3 with SERA5.

To further dissect the localization of *Pf*LPL3 in the transgenic parasites, we fractionated infected RBCs by saponin lysis, and as shown in figure 21A, SERA5 signal

was detected in supernatant fraction while BiP was detected in pellet fraction. We detected fusion protein band in both supernatant and pellet fraction in western blot analysis, which confirmed the presence of *Pf*LPL3 in the PV as well as in parasite cytosol.

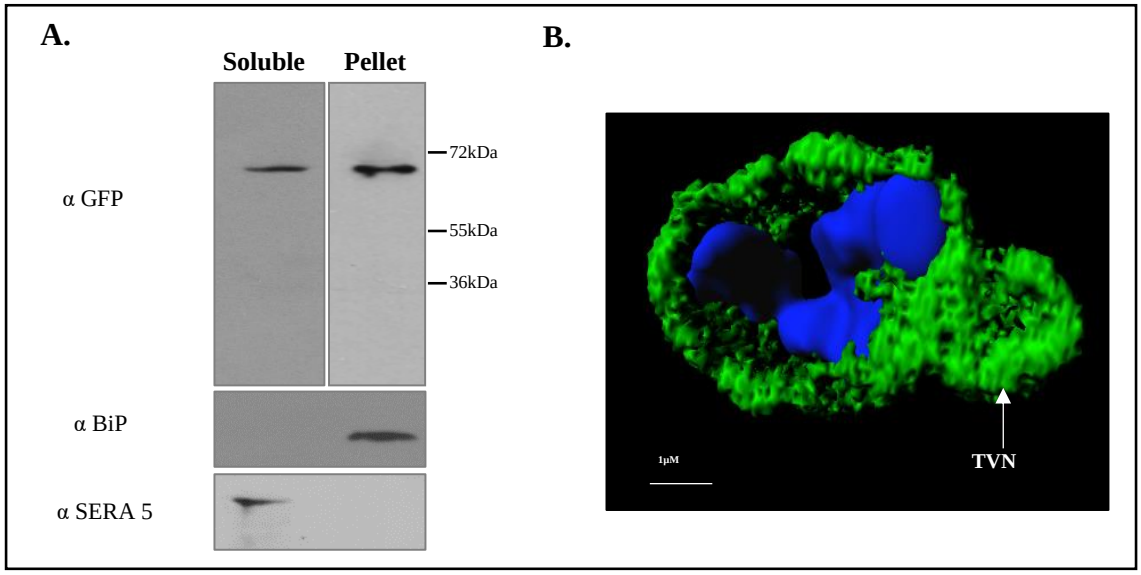

Figure 21: *Pf*LPL3-GFP fusion protein is localized in the parasite cytosol and parasitophorous vacuole region: (A) Western blot of soluble and pellet fraction after saponin lysis of infected RBC showing that the *Pf*LPL3-GFP fusion protein was present in the parasite cytosol as well as in the PV. BiP and SERA5 were used as a negative and positive controls, respectively. (B) 3D- image generated by a series of Z-stack images of the transgenic parasites shows that the fusion protein (green) was present in the PV as well as in the tubulovesicular network (TVN) of the PV. DAPI (blue) was used to stain parasite nucleus.

Further, to assess possible membrane association of *Pf*LPL3, we carried-out the sequential membrane solubilization assay (Nilsson et al., 2012). The cell lysate of transgenic parasites was divided in four aliquots and solubilized with different solubilization buffers, subsequently soluble and pellet fractions were analyzed by western blotting. It has been shown that the cytosolic proteins are solubilized in the Tris-Cl buffer and the Tris-Cl pellet fraction contains membrane associated and transmembrane proteins, the membrane associated proteins can be extracted in 6M urea and sodium carbonate buffer, whereas trans-membrane/membrane bound proteins were solubilized in

SDS+TritonX-100 buffer. The *Pf*LPL3-GFP was detected in the pellet fraction of Tris-Cl buffer and urea buffer; it was also found to be in soluble fractions after extraction with sodium-carbonate buffer as well as with buffers containing Triton-X100 or SDS (Figure 22)**.** The urea and sodium carbonate buffers solubilize the membrane associated proteins: urea buffer disrupts the protein-protein interactions whereas sodium carbonate breaks lipid-protein interactions. The presence of fusion protein in urea pellet and sodium carbonate soluble fraction indicate *Pf*LPL3 membrane association via lipid-protein interactions.

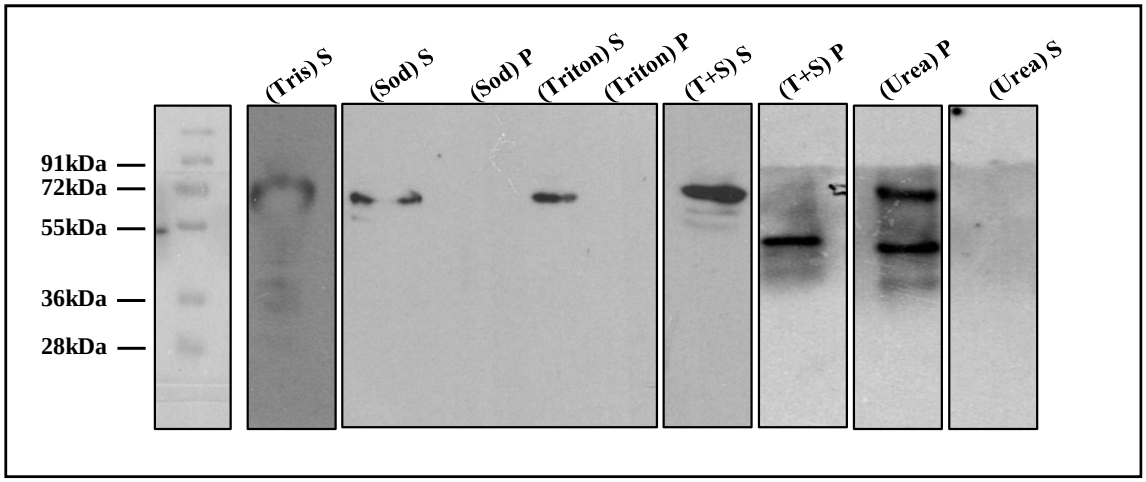

Figure 22: *Pf*LPL3 associates with PVM via lipid-protein interactions: *Pf*LPL3 can be extracted by sodium carbonate, tritonX-100 and tritonX-100+ SDS but not by the urea buffer. Parasitized RBCs at schizont stage was lysed hypotonically by Tris-cl. The pellet fraction was further divided in to four aliquots and were separately dissolved in alkaline sodium carbonate, triton alone, Triton+SDS and urea buffers. Extracts were subjected to SDS-PAGE and western blot analysis.

4.2.1.4 Selective degradation of *Pf*LPL3 inhibits parasite growth

To understand the functional significance of *Pf*LPL3 and its possible involvement in lipid metabolism, we utilized the *Pf*LPL3-GFP-*glmS* parasite line for inducible knock-down of *Pf*LPL3 expression using *glmS* ribozyme. In presence of glucosamine (GlcN), the *glmS*-ribozyme cleaves itself, which in turn leads to degradation of the associated mRNA. Selective down-regulation of *Pf*LPL3 protein was assessed in transgenic parasite grown with different concentrations of GlcN (1.25mM, 2.5mM, 5mM and 10mM). As shown in

figure 23B, *Pf*LPL3 levels showed concentration dependent reduction (60-90%) in GlcN treated sets. To avoid any GlcN mediated toxicity, all further experiments were carried out using 1.25mM concentration of glucosamine. To study the effect of inducible knock-down (iKD) of *Pf*LPL3 on parasite growth, synchronized ring stage parasite was grown in presence of GlcN. The total parasitemia was estimated at different time points (24h, 36h, 48h) and compared with control set (-GlcN); the *Pf*LPL3-iKD set showed ~70% inhibition in the parasite growth (Figure 23C). There was no deleterious effect of 1.25mM glucosamine on the growth of the wild type 3D7 parasite line.

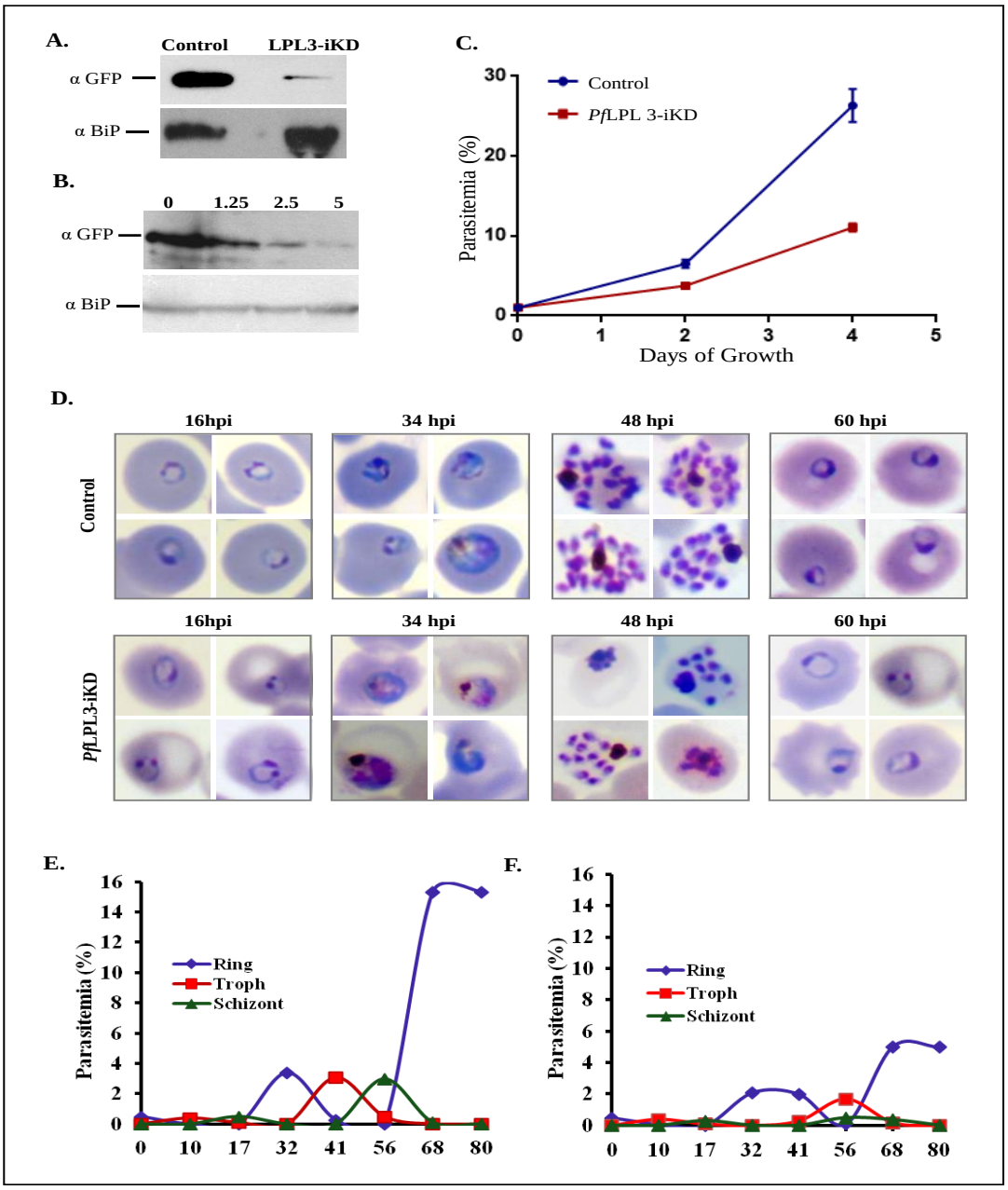

Figure 23: Inducible knock-down of *Pf*LPL3 hampers parasite growth and survival: (A) Western blot analysis showing reduction in the fusion protein in presence of 10mM glucosamine. (B) Western blot showing reduction in the fusion protein expression gradually as the glucosamine concentration is increased. BiP was used as loading control. (C) Graph showing percentage parasitemia in *Pf*LPL3-GFP-*glm*S transgenic cultures grown in presence or absence of 2.5 mM glucosamine (control and iKD), as estimated by new ring stage parasites after 2 and 4 days. (D) Giemsa stained images of parasites showing effect on parasite morphology at different time points (0-48h) for control and *Pf*LPL3-iKD sets. (E) Growth profile of the *Pf*LPL3-GFP-glmS parasites in absence of glucosamine and in presence of the 2.5 mM glucosamine (F).

4.2.1.5 *Pf*LPL3 plays a crucial role in parasite development and schizogony

To study the effect of selective degradation of *Pf*LPL3 on parasite development during asexual cycle, morphology of the parasites in *Pf*LPL3-iKD set and control set was analyzed at different time points during the growth cycle. In the control set, during each intra-erythrocytic cycle, the parasites developed from ring to trophozoites to mature schizonts, subsequently merozoites released from these schizonts invaded new erythrocytes, which effectively increased the total parasitemia about 5-6 times (Figure 23 C). In the *Pf*LPL3-iKD set, the parasite development from ring to trophozoites was delayed for 10-12h as shown in developmental stage profile (Figure 23 D, E and F). In addition, all the trophozoites were not able to developed into schizonts, and there was ~50% reduction in number of schizonts as compared to control; indeed, at 48 hpi, a large number of stressed parasites were observed in treated set as compared to the control set (Figure 23D), which caused ~50% reduction in number of schizonts in the *Pf*LPL3-iKD set as compared to control.

Since lipid metabolism is regulated by lipases may affects the membrane biogenesis in developing parasites. We also assessed the effect of *Pf*LPL3-iKD on division and segregation of merozoites during schizont development. Indeed, the *Pf*LPL3-iKD also affected the replicative fitness of the schizonts. During Schizogony, *P. falciparum* undergoes multiple rounds of nuclear divisions resulting in 16-32 merozoites. In the control set, the schizonts were found to contain 16-32 merozoites with the majority of parasite having 16 merozoites per schizont; however, in the treated parasite set (*Pf*LPL3-iKD), mean number of merozoites per schizonts was significantly reduced (Figure 24A and B). This decrease in replicative fitness of schizonts resulted in ~25% decrease in total number of merozoites (Figure 24C). Overall, we show that *Pf*LPL3-iKD inhibited development as well as replicative fitness of schizont stages, which resulted in >70% parasite growth inhibition.

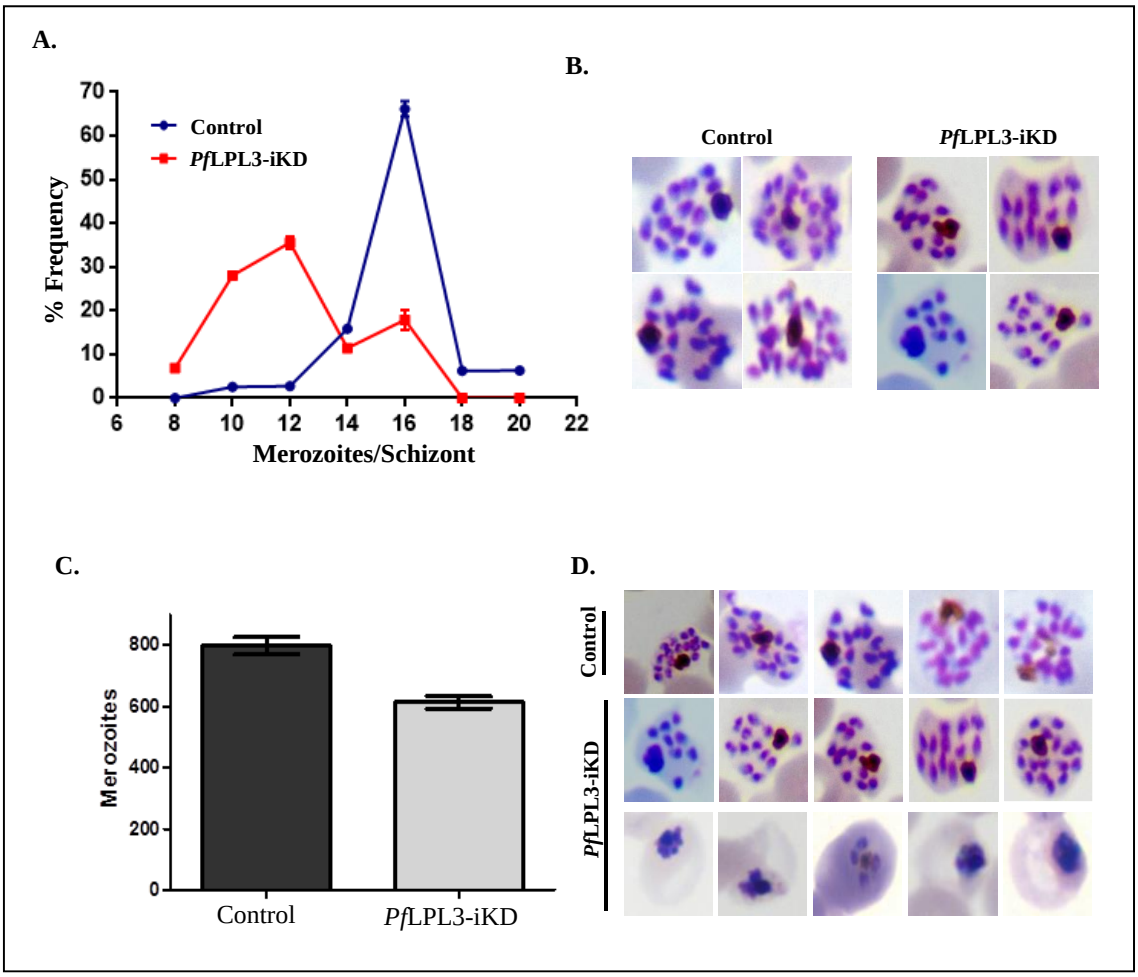

Figure 24: *Pf*LPL3 plays a crucial role in schizogony of the parasite: (A) Frequency distribution of number of merozoites per schizont in the control and *Pf*LPL3-iKD parasite cultures. (B) Representative giemsa smears showing the lesser number of merozoites in the *Pf*LPL3-KD parasites in comparison to the wild type parasites. (C) Graph showing reduction in the total number of merozoites in *Pf*LPL3-iKD parasite line in comparison to the control. (*n*=50). (D) Giemsa smears of the control and the *Pf*LPL3 knock-down parasites showing that the glucosamine treated parasites have stressed schizonts and less number of merozoites per schizont.

4.2.1.6 Knock-down of *Pf*LPL3 does not alter merozoite membrane composition

Since *Pf*LPL3 was found to be localized in PV region, we assessed any effect of its knockdown on development of merozoite plasma membrane using merozoite surface protein marker. Merozoite surface protein 1 (MSP1) is a GPI anchored protein present on the merozoite membrane synthesis. We found that there was no difference in the staining of the MSP1 in *Pf*LPL3-iKD parasite set as compared to the control (Figure 25). It shows

that *Pf*LPL3-iKD parasites, which could develop into schizont stage with less number of merozoites, still have normal plasma membrane composition.

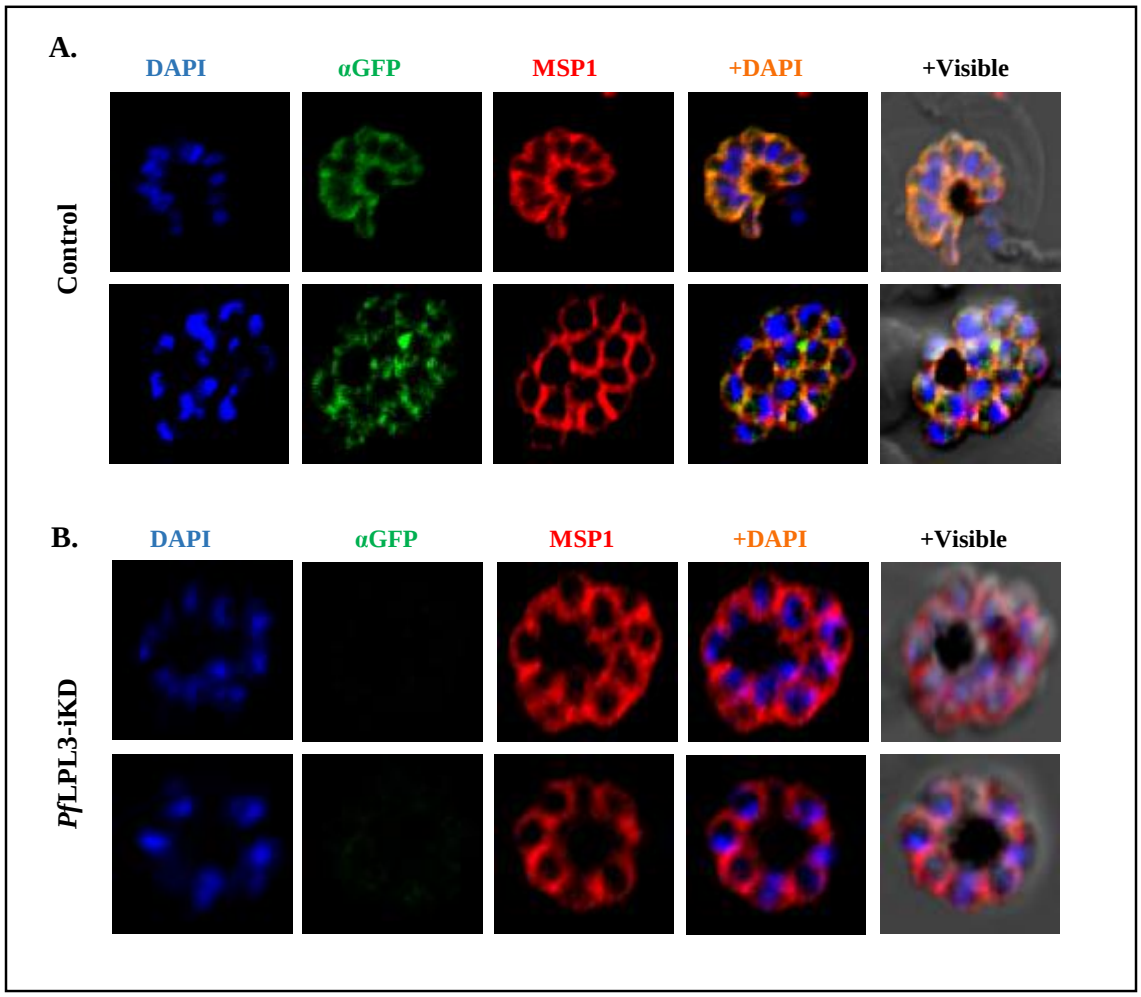

Figure 25: Effect of *Pf*LPL3 knock down on merozoite membrane: Fluorescent images of the control and the *Pf*LPL3 knock-down parasites immune-stained with anti-MSP1 antibody, showing intact plasma membrane in the merozoites of *Pf*LPL3 knock-down parasites. Parasite nuclei were stained with DAPI and images were acquired by confocal laser scanning microscope.

4.2.1.7 Selective degradation of *Pf*LPL3 disrupts lipid homeostasis and neutral lipid ratios

To assess the role of *Pf*LPL3 in lipid homeostasis, we conducted mass spectrometry-based lipidomic analyses on total lipids extracted from *Pf*LPL3-iKD set of parasites. A comparison of lipid profiles of *Pf*LPL3-iKD and control set revealed that the composition of different phospholipids (Figure 26A) as well as that of fatty acids (Figure 26B) was not altered after reduction in *Pf*LPL3-iKD set. However, there was significant decrease in the total fatty acid amount (Figure 26C) and a minor decrease in the phospholipid content of the parasite (Figure 26D). Lysophospholipases are known to cleave the fatty acid chain from the lysophospholipids which ultimately leads to the generation of neutral lipids, Diacylglycerol and Triacylglycerol (DAG and TAG) in the parasite. Comparative analysis of these major neutral lipid concentrations, which make the bulk of lipid bodies composition, showed reduction in the total quantitative levels of neutral lipid (Figure 26E). Further, detailed analysis of neutral lipids showed that TAG to DAG ratio was significantly decreased in *Pf*LPL3-iKD set of parasites (Figure 26F).

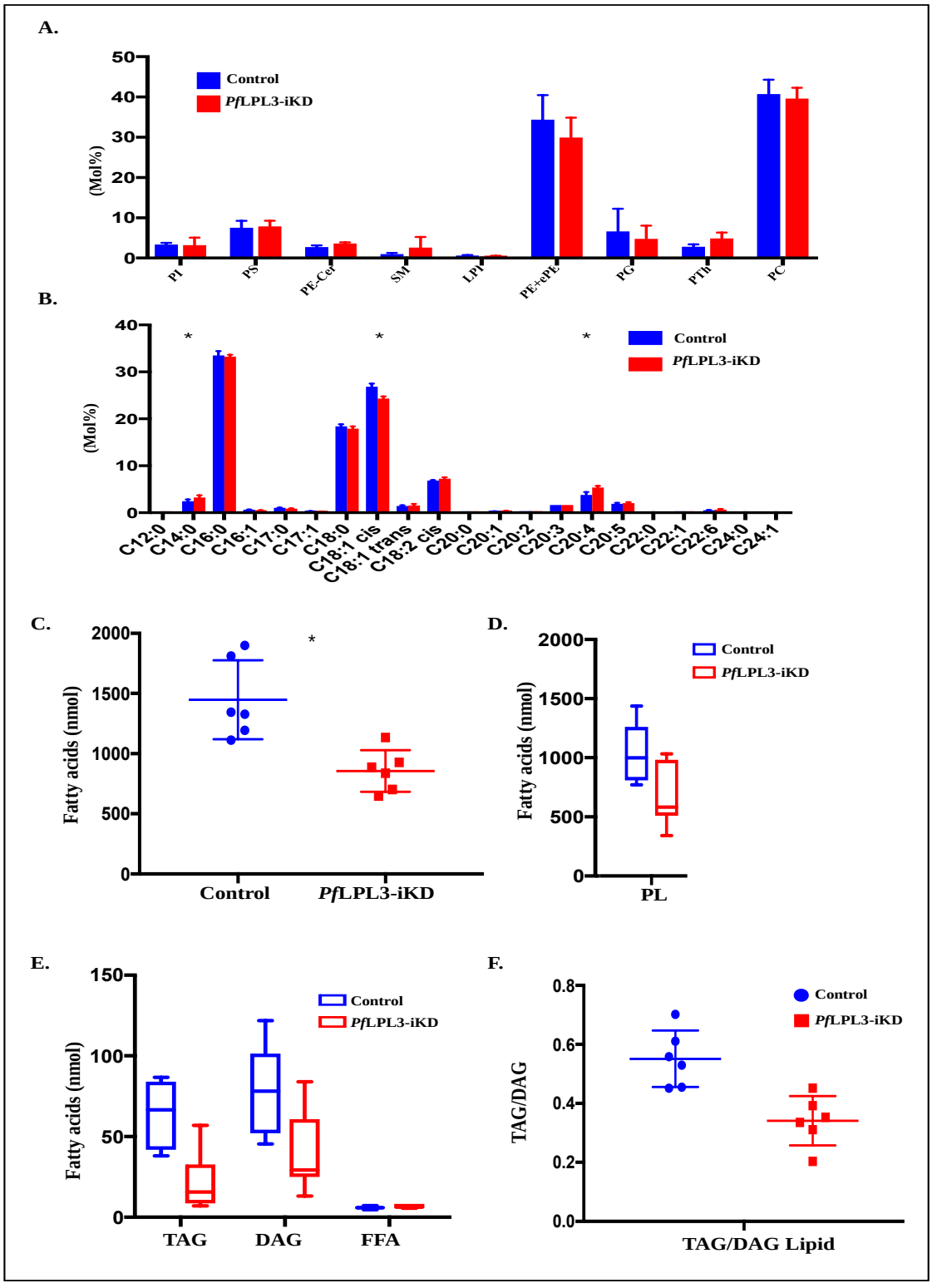

Figure 26: Effect of PfLPL3 knock-down on lipid profile of the *Pf*LPL3 parasites: Total lipids isolated from *Pf*LPL3-iKD were analyzed by LC-MS and abundance was

confirmed with control set. (A) Graphical representation of several phospholipids composition in total phospholipids. (B) Graph showing that the composition of different fatty acids is not much altered in comparison to the control set. (C) Graphical representation of phospholipid abundance showing that there is a slight decrease in the phospholipid content in *Pf*LPL3-iKD parasites. Graph showing that the decrease in the Fatty acid amounts (D) but no alteration in the fatty acids composition (E) in *Pf*LPL3-iKD parasites in comparison to control. (F) Graph showing the decrease in the TAG to DAG ratio in *Pf*LPL3-iKD parasites.

Overall, our results suggest that *Pf*LPL3 lysophospholipase is essential for the parasite, and it plays an important role in fatty acid, neutral lipid as well as phospholipids synthesis, which are crucial for the membrane synthesis required during the schizogony of the parasite.

4.2.2 Functional Characterization of *Pf*LPL20

For functional characterization of *Pf*LPL20, we utilized GFP-targeting as well as *glmS* mediated gene knock-down strategies. The transgenic parasite lines were also used for immunoprecipitation, metabolic study, and transcriptomic analyses to explore role of *Pf*LPL20 in maintaining the lipid homeostasis in *P. falciparum.*

4.2.2.1 Generation of *Pf*LPL20-pSSPF2-GFP line for localization study

To generate transgenic parasite line expressing GFP fusion protein, full length *PfLPL20* gene was amplified using primers 1294A and 1295A (Figure 27B.) and cloned in to pSSPF2-GFP vector (Figure 27C). All cloned fragments of the final plasmid construct were analyzed using several combinations of the restriction enzymes digestion to confirm for correct arrangement and integrity of various expression cassettes. (Figure 27D) *P. falciparum* 3D7 parasites were transfected with plasmid construct and transgenic parasites were selected on blasticidin drug.

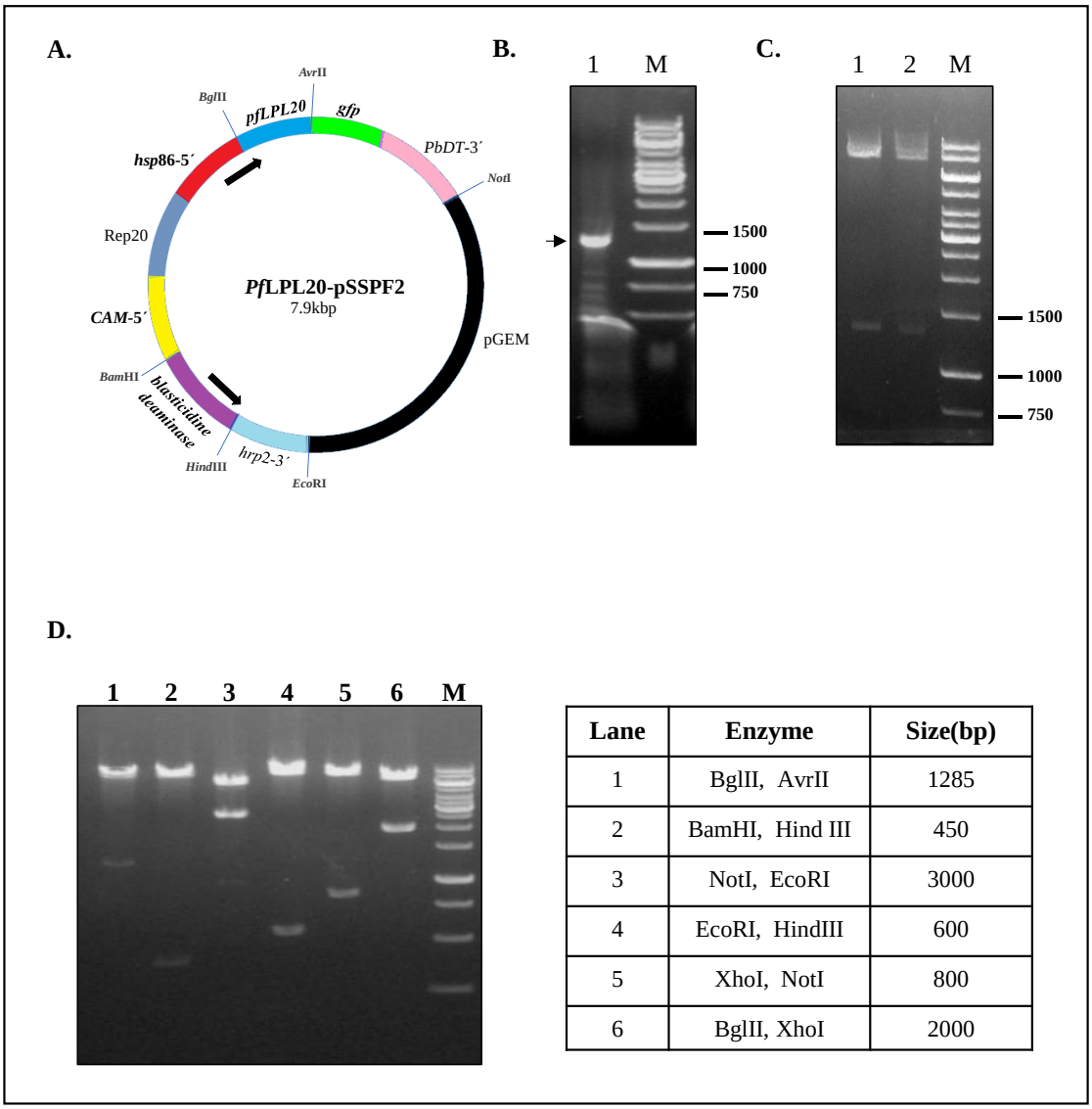

Lane	Enzyme	Size(bp)
1	BglII, AvrII	1285
2	BamHI, Hind III	450
3	NotI, EcoRI	3000
4	EcoRI, HindIII	600
5	XhoI, NotI	800
6	BglII, XhoI	2000

Figure 27: Generation of transfection plasmid construct for expression of *Pf*LPL20-GFP fusion protein: (A) Schematic of the pSSPF2 vector map showing different vector cassettes and restriction sites. (B) Agarose gel showing PCR amplified *Pf*LPL20 gene. (C) Agarose gel showing restriction digestion of *Pf*LPL20-pSSPF2-GFP plasmid using restriction enzymes *Bgl*II and *Avr*II, excised fragment was observed at the expected size of 1285 base pair. (D) Agarose gel electrophoresis of the *Pf*LPL20-pSSPF2-GFP plasmid digested with different sets of restriction enzymes to analyze different expression cassettes in the vector. Table showing different combination of restriction enzymes used to check vector cassette along with their respective fallout sizes.

The transgenic parasites were studied for localization of *Pf*LPL20-GFP fusion protein by fluorescence/confocal microscopy. Expression of the chimeric protein (~70kDa) in transgenic parasites was confirmed by western blotting (Figure 28A). The chimeric protein was found to be expressed in all developmental stages, except young ring-stage, during asexual life-cycle of the parasite, under the control of *P. falciparum* calmodulin promoter (Cam5'UTR). As the parasite developed through the trophozoite and schizont stages, fluorescence signal was observed in vesicular structures in the parasite cytosol. During trophozoite stages, *Pf*LPL20 was present in distinct foci/vesicles at the parasite periphery, close to the parasite membrane; in addition, some of these vesicles were also distributed in the parasite cytosol (Figure 28B); in late-trophozoite and schizont stages, the fluorescence was observed in 2-3 large vesicular structure, in most of the parasites these structures were present in close proximity of the food-vacuole (Figure 28B). Size and location of these large vesicular structures resemble the food-vacuole associated lipid-storage bodies in the parasites. We assessed localization of *Pf*LPL20 with respect to lipid storage body by co-staining the transgenic parasites using Nile red. The Nile Red is a hydrophobic probe that can stain lipid storages in cells and concentrate in stores of neutral lipids such as TAG (Fowler and Greenspan, 1985). In trophozoite and schizont stage parasites, the Nile Red stained 1-2 vesicular structures strongly associated with food vacuole. The Nile Red stained lipid bodies showed complete overlap with *Pf*LPL20-GFP fusion protein near the food-vacuole, suggesting that the *Pf*LPL20 localize in the neutral lipid storage bodies near the parasite food vacuole (Figure 28C). A 3D reconstruction of *Pf*LPL20-GFP (Figure 29A) and *Pf*LPL20-GFP co-stained with Nile Red (Figure 29B) at the schizonts stage parasite clearly shows localization of *Pf*LPL20 in the lipid body.

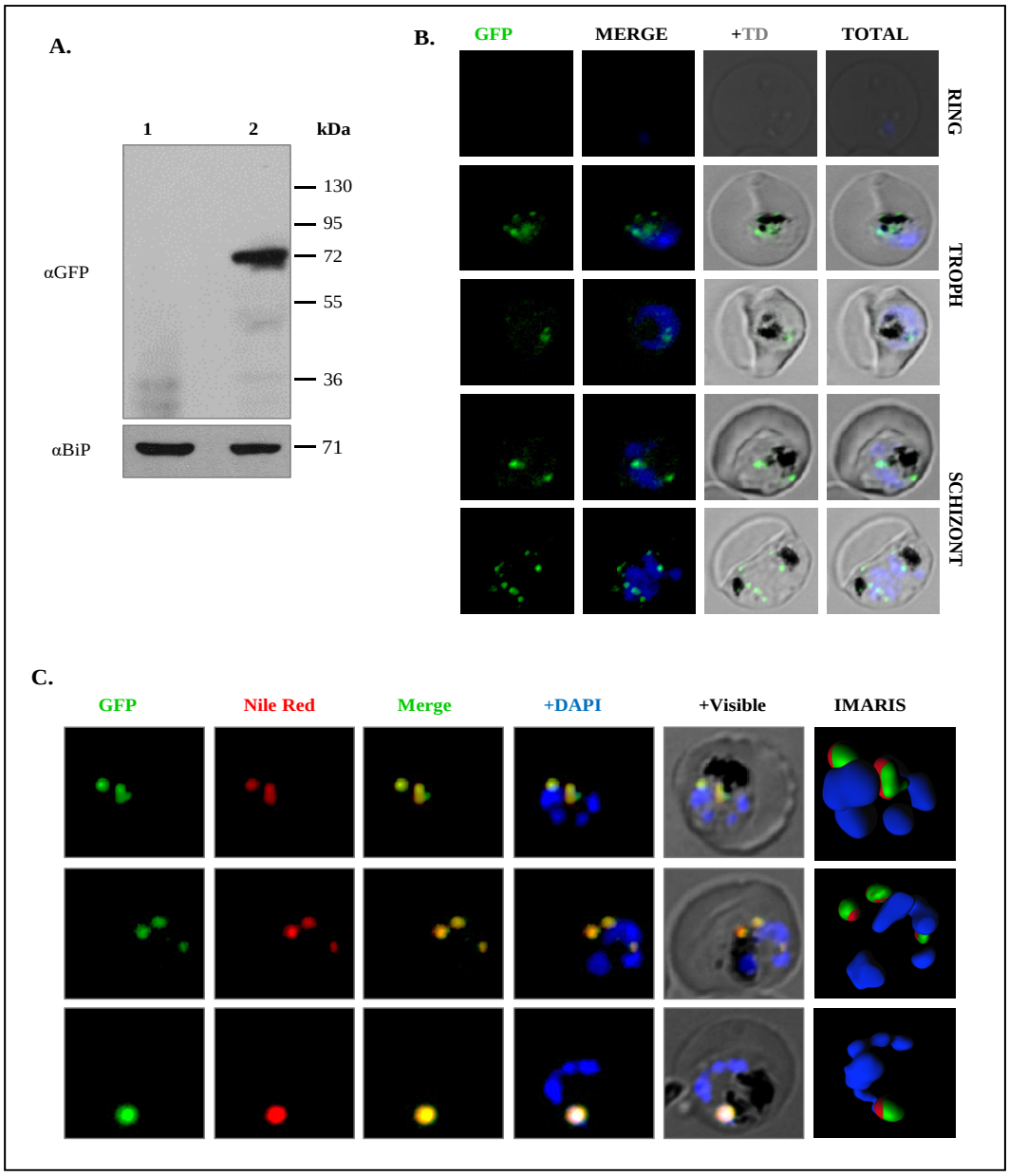

Figure 28: Generation of transgenic parasite line expressing *Pf*LPL20-GFP fusion protein and sub-cellular localization of *Pf*LPL20: (A) Western blot analysis of lysate of transgenic parasites using anti-GFP antibody shows a band at ~70 kDa (Lane 2), which was not detected in the wild-type 3D7 parasite lysate (Lane1); a parallel blot probed with anti-BiP antibodies to show equal loading. (B) Confocal microscopy images of the transgenic parasites at ring, trophozoite and schizont stages expressing fusion protein. *Pf*LPL20-GFP fusion protein was present in the vesicular structures near parasite boundary, in the cytosol and as a large multi-vesicle like structure near the food-vacuole. (C) Co-staining of transgenic parasites with neutral lipid marker (Nile red) shows that the *Pf*LPL20 (green) associates with neutral lipid storage body near the food-vacuole. Nucleus was stained in blue with DAPI. 3D-images was generated by series of Z-stack images using IMARIS software.

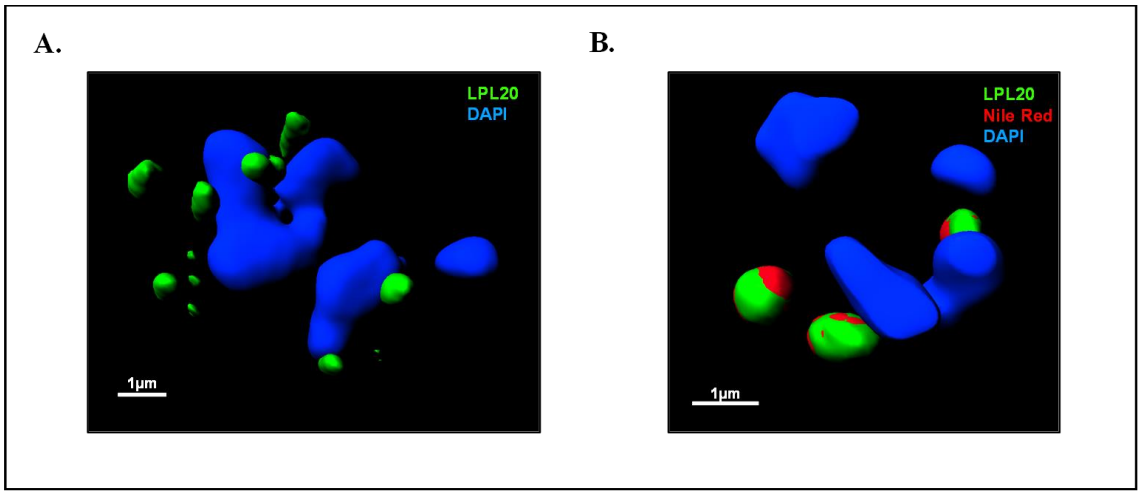

Figure 29: Three-dimensional reconstructed images of a schizont stage transgenic *P. falciparum* using IMARIS: (A) The GFP signal was observed in vesicular structures near the PV and the food vacuole. (B) *Pf*LPL20-GFP fusion proteins stained with Nile red (red) shows colocalization with neutral lipids. The parasite nuclei were stained with DAPI (blue).

4.2.2.2 Endogenous tagging of *Pf*LPL20 gene and localization of *Pf*LPL20-GFP fusion protein in transgenic parasites

We tagged the endogenous *Pf*LPL20 for its localization studies as well as to study its functional essentiality by conditional knock-down strategy. We used GFP-*glm*S ribozyme system for C-terminal tagging of the native *PfLPL20* gene by single cross-over, so that the fusion protein gets expressed under the control of native promoter. Briefly, a C-terminal fragment of the *Pf*LPL20 gene was amplified using specific primers 1224A & 1225A (Figure 30B), amplified fragment was cloned in to pGFP-*glmS* vector (Figure 30C) to generate transgenic construct, all cloned fragments of the final plasmid construct were analyzed using several combinations of the restriction enzymes digestion to confirm correct arrangement of various expression cassettes (Figure 30D). The 3D7 strain of *P. falciparum* parasites were transfected with plasmid construct and selected over blasticidin drug; drug on/off cycles were applied for selection of the parasite having integration of the plasmid into parasite genome.

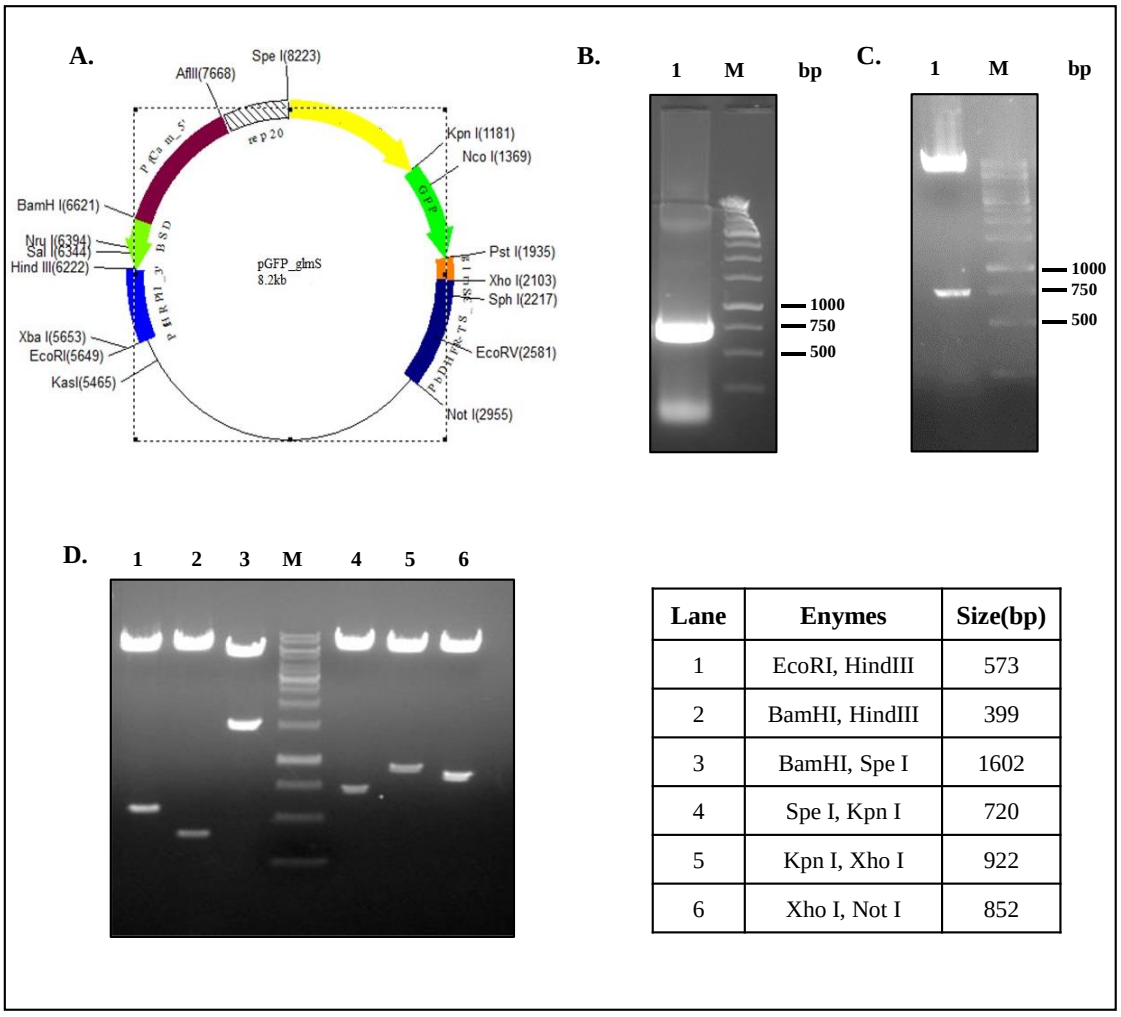

Lane	Enymes	Size(bp)
1	EcoRI, HindIII	573
2	BamHI, HindIII	399
3	BamHI, Spe I	1602
4	Spe I, Kpn I	720
5	Kpn I, Xho I	922
6	Xho I, Not I	852

Figure 30: Generation of transfection plasmid construct for *Pf*LPL20GFP-*glmS* parasite line: (A) Schematic of the pGFP-*glmS* vector map showing different vector and cassettes restriction sites for restriction enzymes. (B) Agarose gel showing PCR amplified C-terminal of the *Pf*LPL20 gene. (C) Agarose gel showing restriction digestion of *Pf*LPL20-GFP-*glmS* plasmid construct with SpeI & KpnI enzymes, showing excision of cloned fragment. (D) Agarose gel electrophoresis of the *Pf*LPL20-GFP-*glmS* plasmid construct with different sets of restriction enzymes to analyze the vector cassettes. Table showing different combination of restriction enzymes used to analyze different expression cassette along with respective size of excised fragments.

Transgenic integrated parasite line, *Pf*LPL20-GFP-*glmS*, was obtained after several rounds of drug-selection cycle (Figure 31B); C-terminal integration was confirmed in selected clonal population by PCR based analyses using primers 2200F & 1234A (Figure 31B). Expression of fusion protein of ~70kDa was detected by western blot analysis using anti-GFP antibody (Figure 31C); this band was not detected in wild type 3D7 parasites.

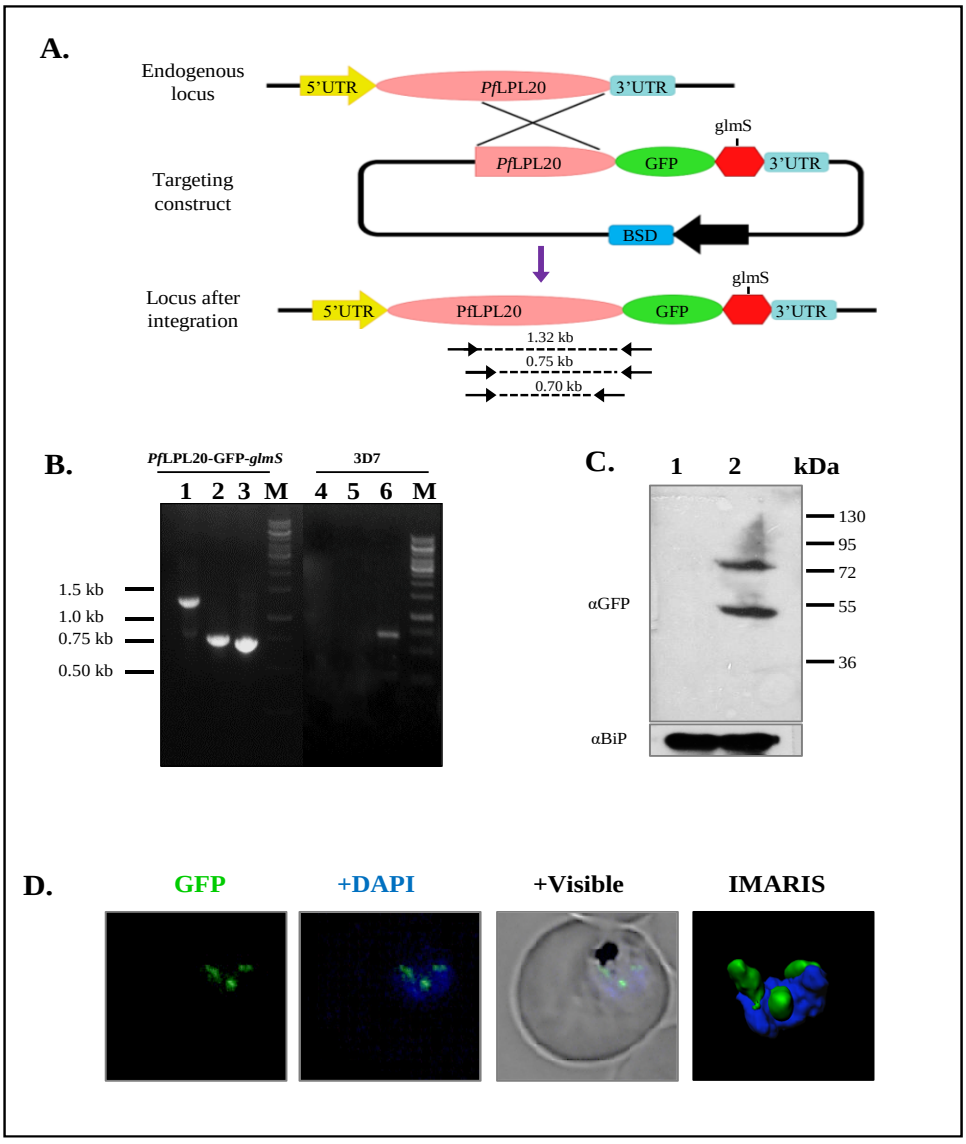

Figure 31 : Generation of transgenic parasite line with GFP-*glmS* tag in the *pfLPL20* gene locus for transient knock-down: (A) Schematic representation of GFP-*glm*S reverse genetic approach showing the integration of *Pf*LPL20-GFP-glmS plasmid at the C-terminus of the endogenous *pfLPL20* gene locus. (B) PCR based analyses to confirm integration of plasmid in the target gene locus using total DNAs of the transgenic parasite culture (purified clonal parasite population) and wild type 3D7 parasite lines; locations of primers used, and length of respective amplicons are marked in the schematic diagram. Lane 1 and 4 (primers 2200F and 1234A) showing amplicon only in the integrants; lane 2 and 4 (primers 1224A and 1234A) show amplicon in integrants or episome parasites; lane 3 and 6 (primers number 1224A and 1225A) show amplification in both integrants and the wild-type line. (C) Western blot analysis of lysate of transgenic and wild-type parasites using anti-GFP antibody. The fusion protein band (~70kDa) was detected in the transgenic parasites only (Lane 2) and not in the wild-type parasite (Lane 1). Blot ran in parallel and

probed with anti-BiP was used as loading control. (D) Fluorescent microscopic images of transgenic parasites. Fusion protein signal was observed in vesicular structures in transgenic parasites. The parasite nuclei were stained with DAPI and parasites were visualized by confocal laser scanning microscope.

4.2.2.3 *Pf*LPL20 is dispensable at the asexual stage of the parasite

To understand the functional significance of *Pf*LPL20 and its possible involvement in lipid metabolism, we utilized the transgenic *Pf*LPL20-GFP-*glmS* parasite line for *glmS* ribozyme mediated inducible knock-down of *Pf*LPL20 expression. Inducible knock-down (iKD) was assessed by quantification of the corresponding mRNA and proteins levels of *Pf*LPL20-GFP in parasite cultures grown in presence of glucosamine (*Pf*LPL20-iKD set) as compared to controls (Figure 32A). As shown in Figure 32B, glucosamine treatment significantly (>70%) reduced the protein level of fusion protein as assessed by western blot analysis using anti-GFP antibody. To assess the effect of this *Pf*LPL20 knock-down on parasite growth, synchronized parasite cultures were grown in presence or absence of glucosamine, and new ring stage parasitemia was calculated in two subsequent cycles. However, there was no difference in the parasite growth after *Pf*LPL20 knock-down as compared to controls (Figure 32C). These results indicated dispensability of this gene for the asexual blood stage parasite cycle.

Further, to study the effect of selective degradation of *Pf*LPL20 on parasite development cycle, Giemsa stained smears of the parasite were prepared at different time points during the assay. In control set, during each intra-erythrocytic cycle the parasites developed from ring to trophozoites to mature schizonts and subsequently merozoites released from these schizonts invaded new erythrocytes, which effectively increased the total parasitemia. In *Pf*LPL20-iKD set, the parasites developed from ring to trophozoites stages, however a number of trophozoites showed an interruption in further development (Figure 32D). It was observed that this growth interruption was only transient, which led to slight delay in parasite development, however, all the parasites were able to develop into mature stages and overall parasite growth and multiplication was similar as in case of control set.

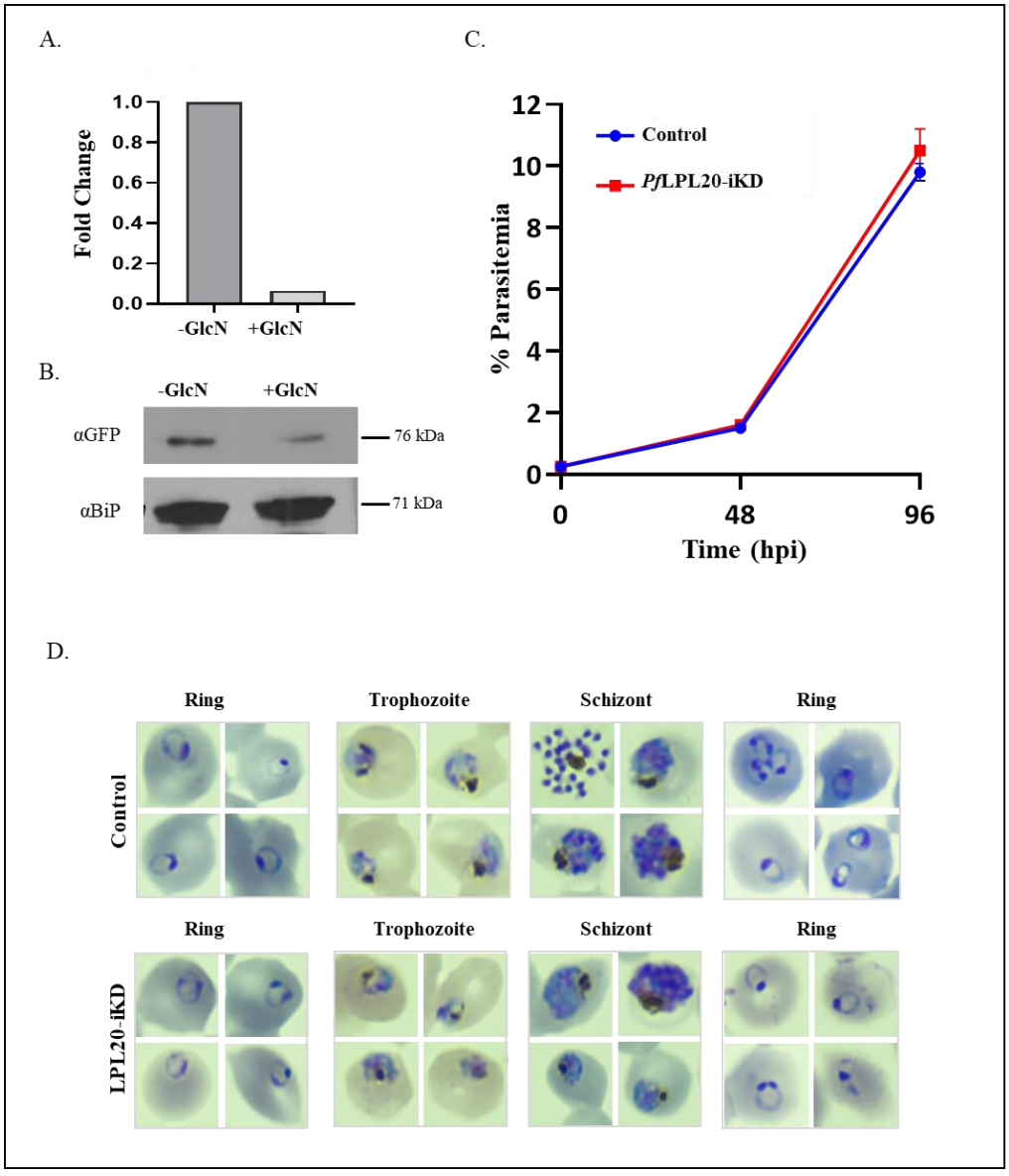

Figure 32: Inducible knock-down showing dispensability of *Pf*LPL20 in asexual blood stages of the parasite: (A) Real time PCR data showing reduction in the transcript levels of *Pf*LPL20 in transgenic parasite grown in presence of glucosamine (+GlcN) as compared to control (-GlcN). (B) Western blot analysis using anti-GFP antibody showing reduction in the *Pf*LPL20 fusion protein levels in transgenic parasites grown in presence of 2.5 mM glucosamine. (C) Graph showing reduction in the *Pf*LPL20-GFP-*glmS* parasite growth in presence of 2.5 mM glucosamine. Tightly synchronized ring stage parasite cultures of transgenic parasites were grown with or without glucosamine (Control and *Pf*LPL20-iKO, respectively), and their growth was monitored as formation of new rings estimated at 48h and 96h. (D) Morphological analysis of the *Pf*LPL20 knock-down parasites at ring, trophozoite and schizont stage. *Pf*LPL20-iKD parasite showed slight delay in development into schizont as compared to control set, however all the parasites developed into schizonts, formed segregated merozoites and developed new ring stage parasites.

4.2.2.4 Identification of interacting partners of *Pf*LPL20 in the parasite

To identify the interacting partners of *Pf*LPL20, we carried out immunoprecipitation assay using both *Pf*LPL20-GFP-*glmS* and *Pf*LPL20-pSSPF2-GFP parasites. GFP-Trap beads were used to pull down the interacting protein complex, eluted proteins were digested with trypsin and resultant peptides were subjected to mass spectrometry analysis for their identification. Following proteins were detected in both sets of co-immunoprecipitation: *Pf*LPL20, *Pf*PMT, *Pf*SAMS, *Pf*OAT (Phosphoethanolamine-N-methyltransferase, S-adenosylmethionine synthetase, Ornithine amino-transferase of SDPM pathway (Table).

Table 3: Interacting partners of *Pf*LPL20 in the *P. falciparum.*

Accession No	Gene	Number of peptides pSSPF2-GFP/GFP-glmS	Score
PF3D7_0702200	Lysophospholipase 20	1/4	27.55, 30.00
PF3D7_1343000	Phosphoethanolamine-N-methyltransferase	4/6	10.64, 40.22
PF3D7_0922200	S-adenosylmethionine synthetase	4/6	22.05, 23.90
PF3D7_0608800	Ornithine amino transferase	3/14	8.09, 51.34

4.2.2.5 *Pf*LPL20 knock-down effects homeostasis of phosphatidylcholine synthesis pathways

As described earlier, there are two pathways for the PC synthesis in *P. falciparum*; 1. CDP-Choline branch of Kennedy pathway and 2. Serine Decarboxylase-Phosphoethanolamine Methyltransferase (SDPM) Pathway. In both pathways generation of the phosphocholine is the rate limiting step. Since *Pf*LPL20 is involved in cleavage LPC, hence its knock-down may deplete the production of choline substrate required for PC synthesis and thus mimic LPC depleted conditions; therefore, we assessed if this influence the expression level of genes of PC- biosynthesis as suggested by Brancucci et. al. We carried quantitative PCR and metabolomic studies to understand the role of *Pf*LPL20 in phosphocholine metabolism.

Real time quantitative PCR based analyses was carried out for genes *PfSAMS*, *PfPMT*, *PfEK* as well as for *PfLPL20*. As shown in Figure 33A, there was significant reduction (>90%) of the *PfLPL20* in the *Pf*LPL20-iKD set as compared to control set; in addition, expression level of *Pf*SAMS was significantly increased (~3.5 fold) in the *Pf*LPL20-iKD set. There was no change in the expression levels of *PfPMT* and *PfEK*.

4.2.2.6 *Pf*LPL20-iKD led to accumulation of phosphocholine in parasite

The upregulation of *PfSAMS* in *Pf*LPL20-iKD conditions suggest that SDPM pathway may have switched to increase in the synthesis of choline-phosphate, which could be utilized for PC synthesis by Kennedy pathway. We estimated the levels of the phosphocholine and choline in *Pf*LPL20-iKD set as compared to control set. The GC-MS analysis showed that there was no significant change in the choline levels for the two sets, however, phosphocholine levels were significantly high in *Pf*LPL20-iKD set as compared to control (Figure 33B). This data correlate with upregulation of SDPM pathway in the *Pf*LPL20-iKD conditions.

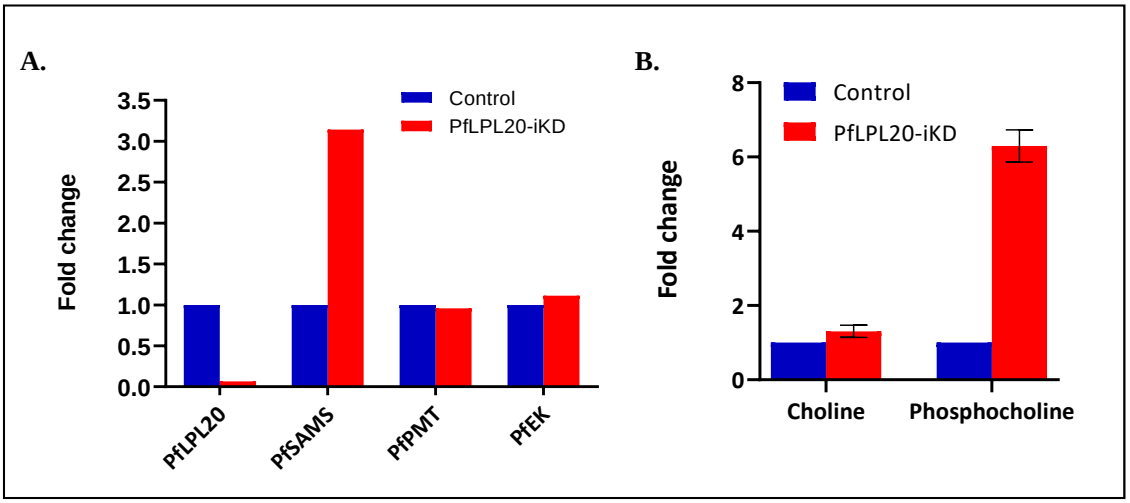

Figure 33: Knock-down *Pf*LPL20 renders parasite to upregulate alternate SDPM pathway for phosphocholine synthesis: (A) Graphical representation of relative transcript levels of different genes of the SDPM pathways in *Pf*LPL20-iKD parasites as compared to control set. Expression of *Pf*SAMS was altered significantly while there was no change in the expression of *Pf*PMT and *Pf*EK. (B) Bar graph showing relative levels of choline and phosphocholine in *Pf*LPL20-iKD parasites in comparison to control set. (PMT: Phosphoethanolamine-N-methyltransferase, SAMS: S-adenosylmethionine synthetase, SAHH: S-adenosyl-L-homocysteine, EK: ethanolamine kinase).

Overall, our results indicate *Pf*LPL20 play role in PC biosynthesis through catabolism of LPC acquired form host milieu to provide choline and phosphocholine; under the *Pf*LPL20 depleted conditions, the parasite switches to an alternate SDPM pathway for phosphocholine synthesis which is utilized for PC biosynthesis. These data provide new information on membrane phospholipid biosynthetic pathways of the malaria parasite, which could be used to design future therapeutic approach (Figure 34).

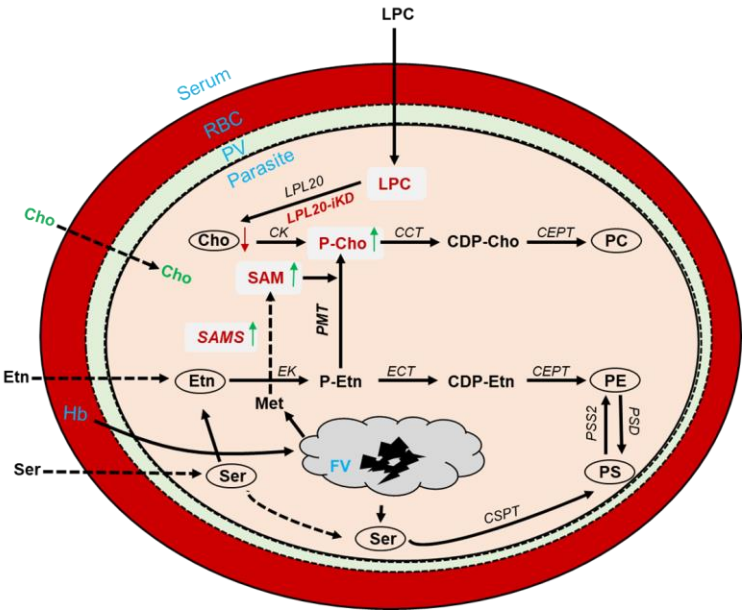

Figure 34: Schematic diagram showing pathways of biosynthesis for major phospholipids (PC,PE,PS) in *Plasmodium* and effect of *Pf*LPL20-iKD on these pathways: The parasite is able to scavenge both choline and LPC from host milieu; however, the choline generated from LPC catabolism is phosphorylated to generate phosphocholine which enters in Kennedy pathway for PC synthesis. Ethanolamine and Serine taken up from host milieu are phosphorylated into P-Etn and utilized for synthesis of PE and PS. Methionine and Serine are also generated from catabolism of hemoglobin in the food-vacuole. In *Pf*LPL20-iKD conditions, the choline generated from LPC is reduced, the SAMS gets upregulated which leads to higher production of SAM which is utilized by PMT to generate phosphocholine to compensate loss of choline/phosphocholine. LPC, Lysophosphatidylcholine; LPL20 ; lysophospholipase 20; PL, Phospholipase, Cho, choline; CK, choline kinase; CCT, CTP:phosphocholine cytidylyltransferase; CDP-Cho, CDP-choline; CEPT, choline/ethanolamine-phosphotransferase; PC, Phosphatidylcholine; Met, Methionine; SAMS, SAM synthetase; SAM, S-adenosylmethionine; PMT, Phosphoethanolaminemethyltransferase; Etn, Ethanolamine; EK, ethanolamine kinase; P-Etn, phosphoethanolamine; ECT, CTP:phosphoethanolamine cytidylyltransferase; CDP-Etn, CDPethanolamine; CEPT, choline/ethanolaminephosphotransferase; PE, Phosphoethanolamine; Ser, Serine; CSPT, CDP-diacylglycerol-serine-O-phosphatidyltransferase; PSS2, phosphatidylserine synthase by base exchange type 2; PSD, phosphatidylserine decarboxylase, FV, food vacuole; Hb, hemoglobin.

4.2.3 Functional Characterization of *Pf*LPL4

4.2.3.1 Generation of *Pf*LPL4-GFP-DD transgenic parasite line

To understand the functional significance of *Pf*LPL4, we used FKBP degradation domain (DD) system for transient knock-down at protein level. In this strategy C-terminal of the gene was tagged with DD domain using single cross over homologous recombination. Under normal conditions, the DD-tagged proteins are identified by cellular proteasomal machinery and selectively degraded in the cell. However, this degradation process can be stopped by adding a ligand, Shield1 (Shld1), which binds to the DD domain and stabilizes the tagged protein (Banaszynski et al., 2006; Herm-Gotz et al., 2007). Stable fusion protein can thus be expressed in presence of the shield1 molecule. Therefore, shield1 removal can be used for transient knockdown of tagged proteins in the cell (Figure 35).

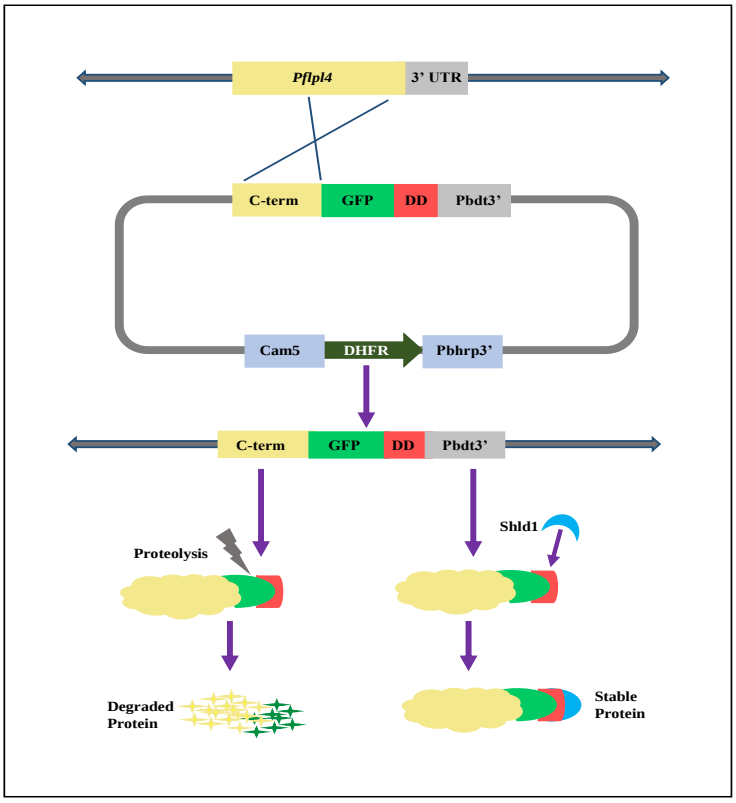

Figure 35: Schematic diagram showing reverse genetic approach utilized for degradation domain mediated transient knock-down of *Pf*LPL4: The C-terminal of *Pf*LPL4 gene was tagged with GFP-DD by single cross-over homologous recombination. The Fusion protein having GFP-DD tag gets rapidly degraded in the cell, while in presence of shld1 molecule, the fusion protein gets stabilized.

Briefly, C-terminal fragment of the *PfLPL4* was PCR amplified from *P. falciparum* genome using gene specific primers 1189A & 1063A (Figure 36B) and cloned into pARL$^{(a+)}$-GFP-DD vector using *Kpn*I & *Avr*II restriction sites (Figure 36C) to generate transgenic construct, all cloned fragments of the final plasmid construct were analyzed using several combinations of the restriction enzymes digestion to confirm correct arrangement of various expression cassettes (Figure 36D). Parasites were transfected with plasmid construct and selected over WR-99210 drug; drug on/off cycles were applied to promote integration of the plasmid into parasite genome. Integrated parasite line, *Pf*LPL4-GFP-*DD*, was obtained after several rounds of drug-selection cycle. To obtain pure integrated parasite population, clonal selection was done in 96 well plate by using serial dilution method and four pure clones were isolated. Western blot analysis was done to assess the integration of all clones and expression of fusion protein in the parasite. As shown in (Figure 37), clones (H 7, H 11) showed expression of the fusion protein (~106kDa). This confirmed the successful integration of the plasmid in parasite genome.

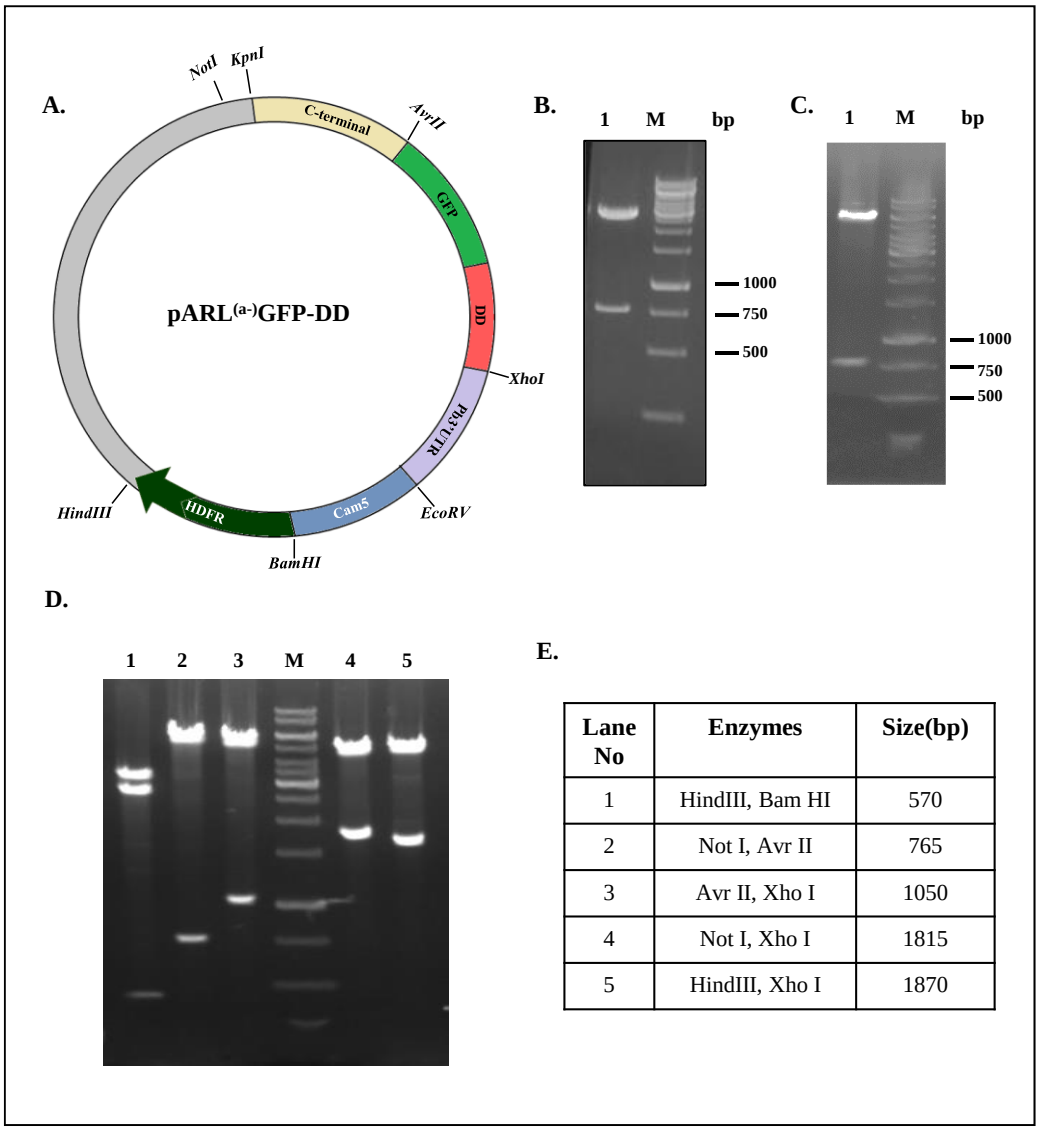

Lane No	Enzymes	Size(bp)
1	HindIII, Bam HI	570
2	Not I, Avr II	765
3	Avr II, Xho I	1050
4	Not I, Xho I	1815
5	HindIII, Xho I	1870

Figure 36: Generation of *Pf*LPL4-GFP-DD plasmid construct for *Pf*LPL4-GFP-DD transgenic parasite line: (A) Schematic of pARL$^{(a-)}$GFP-DD vector showing different vector cassettes and restriction sites for restriction enzymes. (B) Agarose gel showing restriction digestion of C-term cloned in pJET vector. (C) Agarose gel showing restriction digestion of *Pf*LPL4-GFP-DD plasmid construct with NotI & AvrII enzymes, showing excision of cloned fragment, excised fragment was observed at the expected size of ~765 base pair. (D) Agarose gel electrophoresis of the *Pf*LPL4-GFP-DD plasmid construct with different sets of restriction enzymes to analyse the vector cassette. Table showing different combination of restriction enzymes used to check different expression cassette along with respective size of excised fragments.

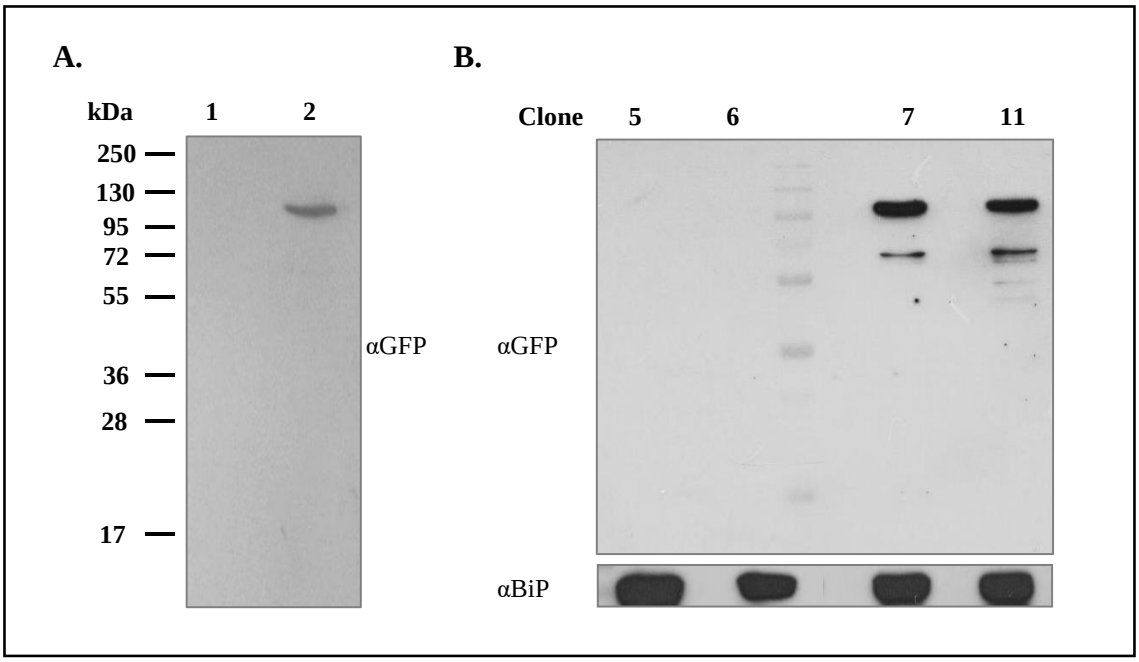

Figure 37: Expression of *Pf*LPL4-GFP-DD fusion protein in transgenic parasite line and clonal selection: (A) Western blot analyses of transgenic parasite lysate using anti-GFP antibody showing a band at expected size of 108kDa, which was not detected in wild type 3D7 parasite lysate (Lane 1: 3D7 lysate, Lane2: Transgenic parasite lysate). (B) western blot of all four parasite clones showing the expression of fusion protein only in two clones (clone 7,11). BiP was used as loading control.

4.2.3.2 Localization study of *Pf*LPL4 in parasite

The *Pf*LPL4-GFP-DD parasite was analyzed for localization by fluorescence microscopy to assess localization of *Pf*LPL4. However, the transgenic parasites did not show any fluorescence even at higher laser exposure. Since the fusion protein was found to be expressed in these parasites by western blot analysis, the absence of any fluorescence could be due to quenching of the GFP by fusion protein. Therefore, these parasites could not be used for localization studies.

4.2.3.3 *Pf*LPL4 is non-essential at the asexual stage of the parasite

To understand the functional significance of *Pf*LPL4 and its possible involvement in parasite survival, we used the *Pf*LPL4-GFP-DD parasite line for transient knock-down of *Pf*LPL4 expression using DD system. Synchronized ring stage parasites were grown in presence or absence of Shld1 and parasites were harvested at the schizonts stage. Parasite

lysates were analyzed by western blot analysis to assess the knock-down of *Pf*LPL4 expression level. As shown in figure 38A, expression of the *Pf*LPL4-GFP fusion protein was observed in (+) shld1 set, whereas fusion protein level was drastically reduced in (–) shld1 set, suggesting degradation and downregulation of *Pf*LPL4. To assess the effect of this *Pf*LPL4 knock-down on parasite growth, synchronized parasite cultures were grown in presence or absence of shild1, and new ring stage parasitemia was assessed in two subsequent cycles. However, we could not observe any change in the parasite growth after *Pf*LPL4 knock-down as compared to control (Figure 38B & C), which clearly indicates the dispensability of this gene for the asexual blood stage parasite.

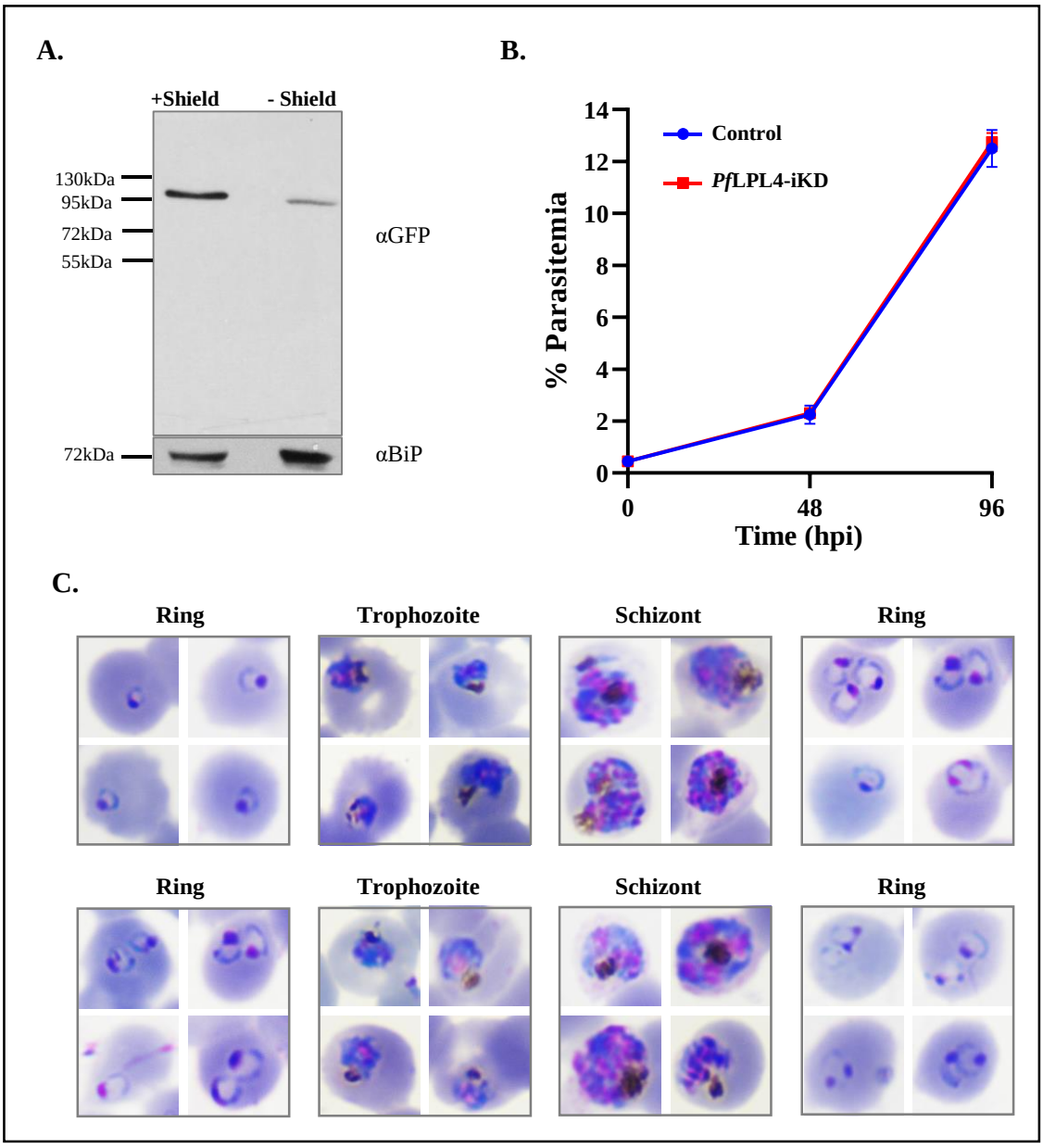

Figure 38: *Pf*LPL4 is non-essential for the asexual blood stage parasite: (A) Western blot of transgenic parasite grown in presence and absence of shld1 showing 80% reduction in the fusion protein expression. BiP was used as a loading control. (B) Line graph showing the *Pf*LPL4-GFP-DD parasite growth in presence and absence of the Shld1. Formation of new rings were estimated after 2nd and 4th day of treatment. There was no difference in the parasitemia of both *Pf*LPL4-iKD and control parasites. (C) Morphological analysis of the control and the *Pf*LPL4 knock-down parasites at ring, trophozoite and schizont stage. *Pf*LPL4-KD parasite showed no defect in the parasites morphology as observed from Giemsa smears.

4.3 Identification of inhibitors of *Plasmodium falciparum* lysophospholipases

One of the major aims to be achieved by understanding biology of the parasite, is to identify functionally important metabolic pathways as drug targets, and subsequently identify their specific inhibitors to develop new antimalarials. We elucidated functional roles of *P. falciparum* lysophospholipases as well as their functional essentiality for parasite growth and survival. We have carried out functional studies for three lysophospholipases using several reverse genetic approaches and metabolic studies; our results identified *Pf*LPL3 to be an essential enzyme for the asexual blood stage parasites, which makes it a potential drug-target. Therefore, we tried to identify specific inhibitors for this enzyme using *in vitro* activity assay-based screening of Malaria Box compound library. We identified specific inhibitors of *Pf*LPL3 having potent parasiticidal efficacies. These results are described below.

4.3.1 Identification of specific inhibitors for enzyme activity of *Pf*LPL3

Purified recombinant *Pf*LPL3 was used for biochemical characterization of *Pf*LPL3 using fluorescence-based activity assay as described in section 4.1.2. This assay was further standardized for high-throughput screening of compound library.

4.3.1.1 Standardization of a robust activity assay and screening of compound library on *Pf*LPL3

The enzymatic activity assay was standardized in 96-well format, robustness of the assay was assessed using HML test for a period of 2 days, and the Z-value was calculated for statistical assessment. In HML assay, three different reaction wells are set up : the **H**igh activity well i.e. lysophospholipase activity well at maximum concentration of protein (20µg); **M**edium activity well i.e the activity in presence of the half amount (10µg) of the protein ; and the **L**ow activity well that is the substrate control only without the protein. The assay was repeated for two consecutive days. The Z-value was estimated as ~0.9, which indicates robustness of the assay (Figure 39). This assay was utilized to screen drug-like compound library, to identify *Pf*LPL3 specific inhibitors. The anti-malarial compound

library called as 'Malaria Box' was obtained from **M**edicines for **M**alaria **V**enture (MMV), Switzerland (Spangenberg et al., 2013). The MMV Malaria box library consists of 200 drug-like and 200 probe-like compounds. Each compound of the library was assessed in a primary screening at final concentrations of 5µM in *Pf*LPL3 lysophospholipase activity assay (Figure 40).

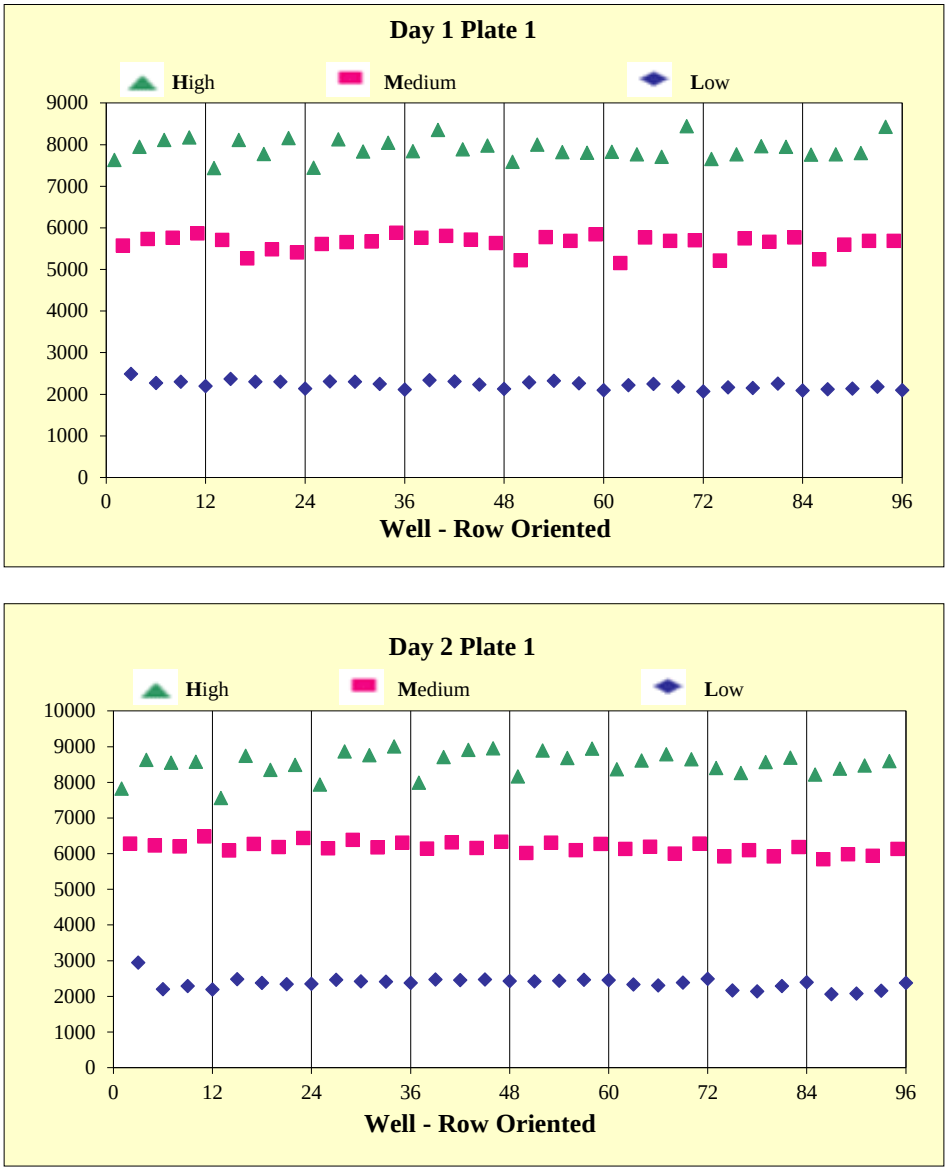

Figure 39 : Assessment of robustness of *Pf*LPL3 lysophospholipase activity assay: Robustness of the activity assay was assessed by estimating Z-value carried out in HML format in 96-well plate for two consecutive days, as given the Z-value was found to be ~0.9.

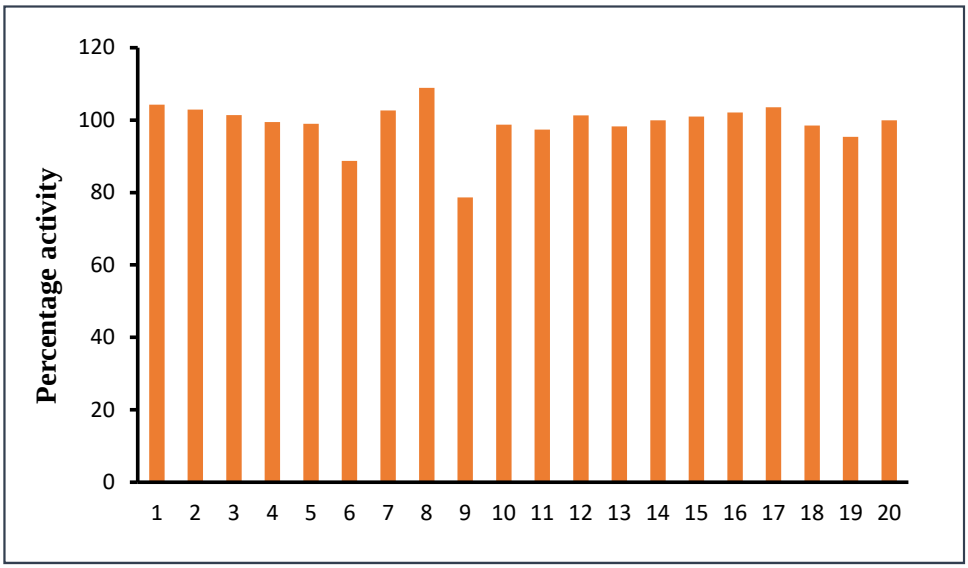
Percentage activity
120
100
80
60
40
20
0
1 2 3 4 5 6 7 8 9 10 11 12 13 14 15 16 17 18 19 20

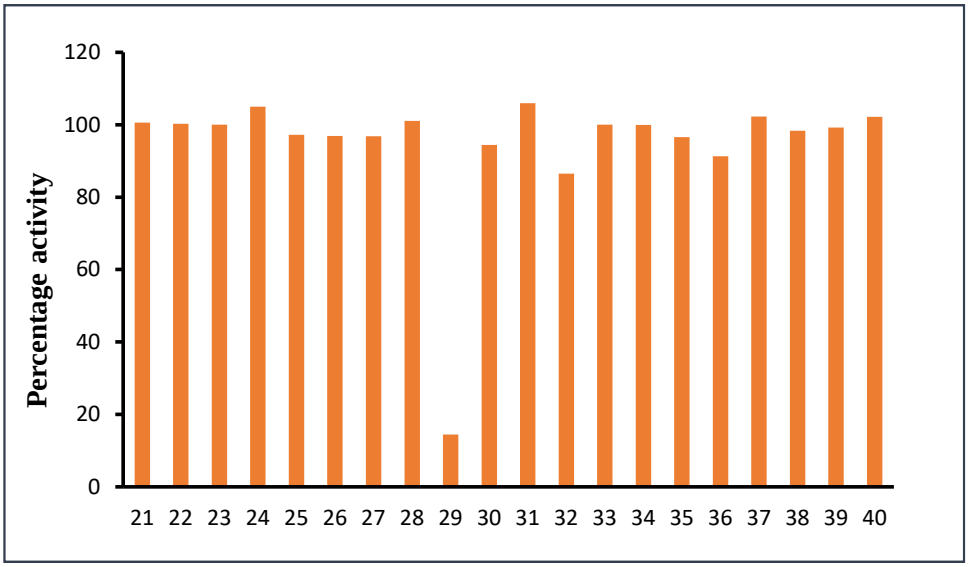
Percentage activity
120
100
80
60
40
20
0
21 22 23 24 25 26 27 28 29 30 31 32 33 34 35 36 37 38 39 40

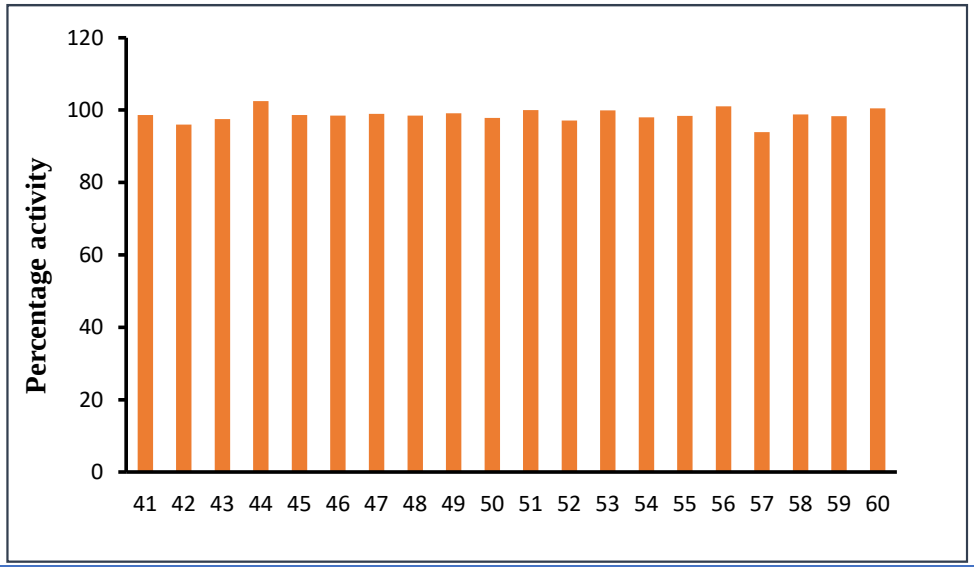
Percentage activity
120
100
80
60
40
20
0
41 42 43 44 45 46 47 48 49 50 51 52 53 54 55 56 57 58 59 60

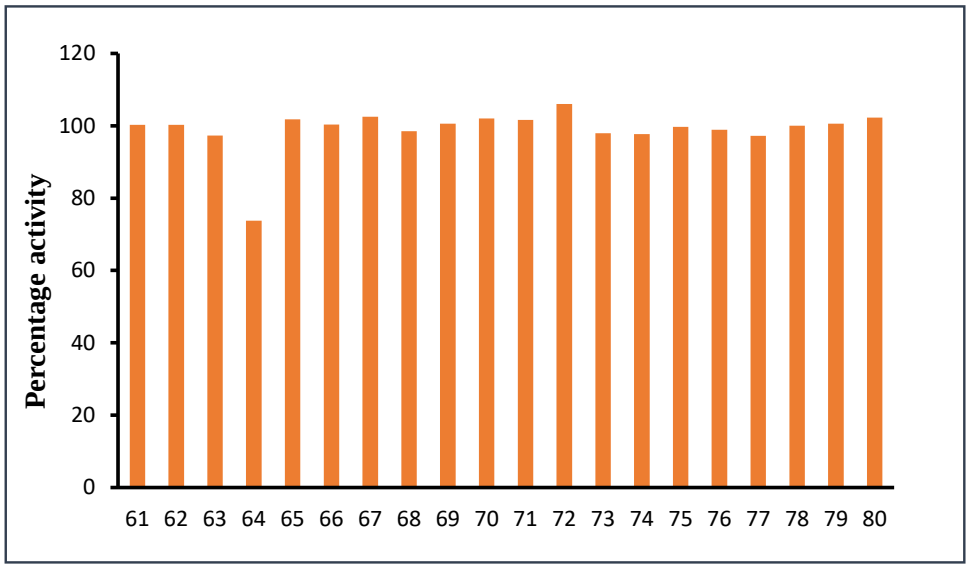
Percentage activity
120
100
80
60
40
20
0
61 62 63 64 65 66 67 68 69 70 71 72 73 74 75 76 77 78 79 80

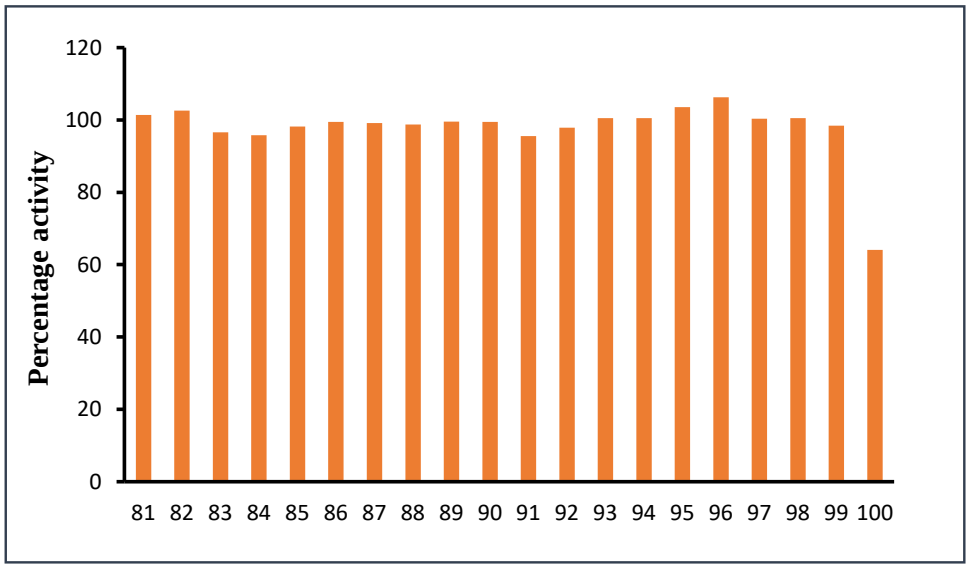
Percentage activity
120
100
80
60
40
20
0
81 82 83 84 85 86 87 88 89 90 91 92 93 94 95 96 97 98 99 100

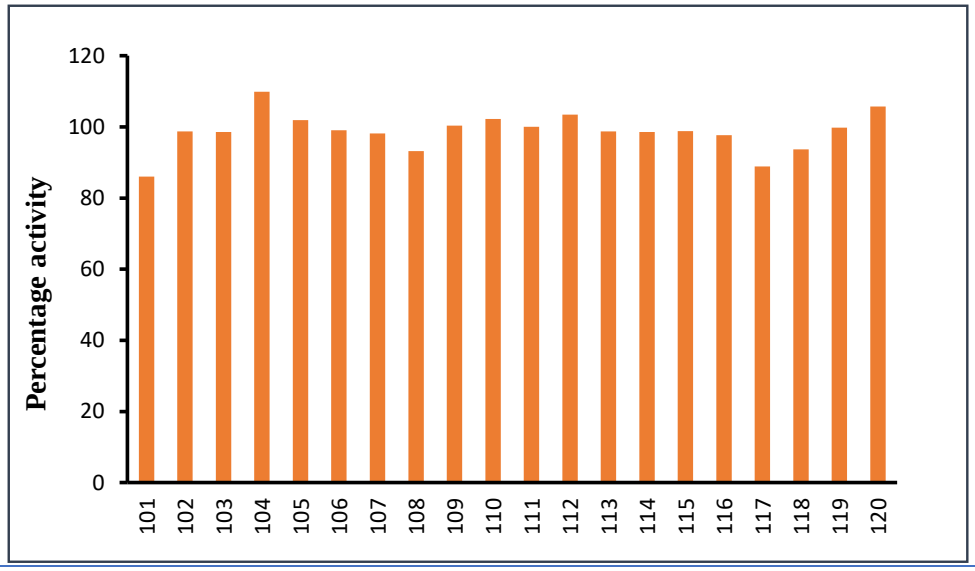
Percentage activity
120
100
80
60
40
20
0
101 102 103 104 105 106 107 108 109 110 111 112 113 114 115 116 117 118 119 120

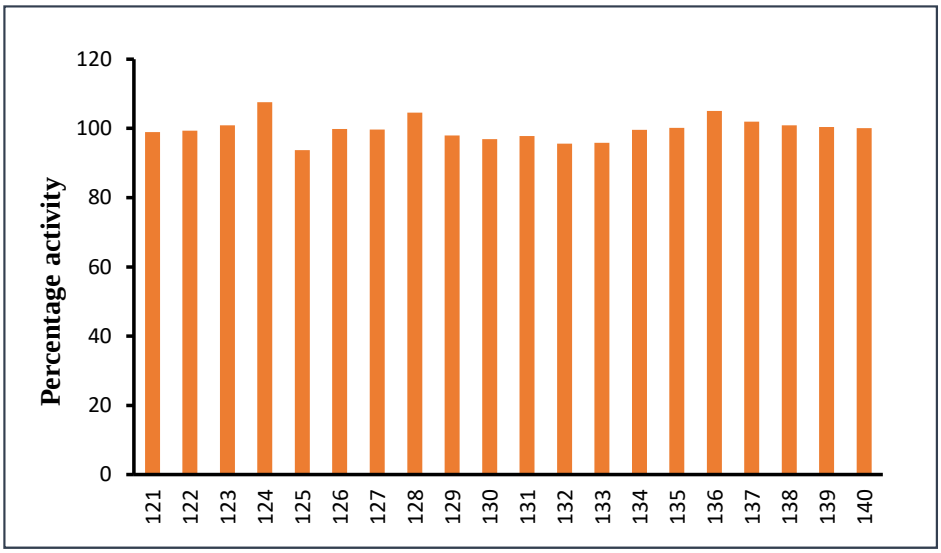
Percentage activity
120
100
80
60
40
20
0
121 122 123 124 125 126 127 128 129 130 131 132 133 134 135 136 137 138 139 140

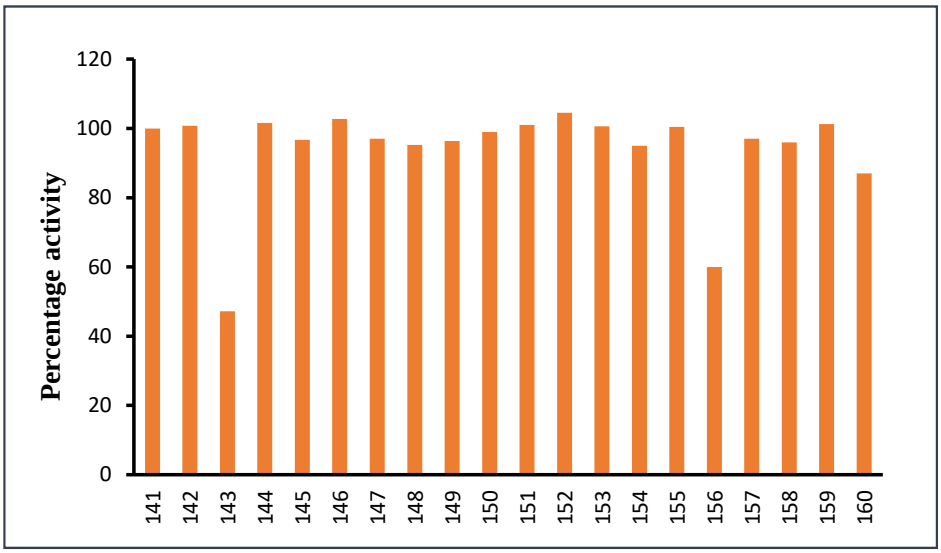
Percentage activity
120
100
80
60
40
20
0
141 142 143 144 145 146 147 148 149 150 151 152 153 154 155 156 157 158 159 160

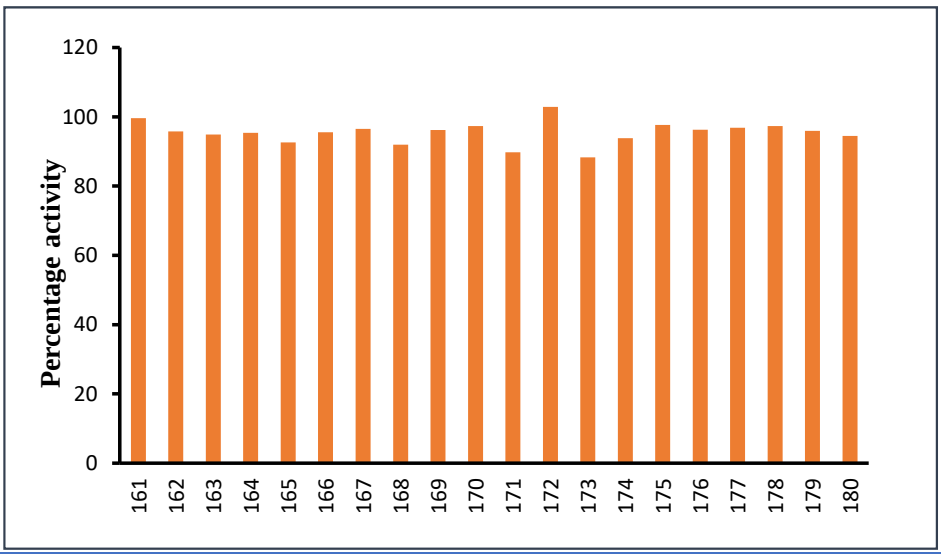
Percentage activity
120
100
80
60
40
20
0
161 162 163 164 165 166 167 168 169 170 171 172 173 174 175 176 177 178 179 180

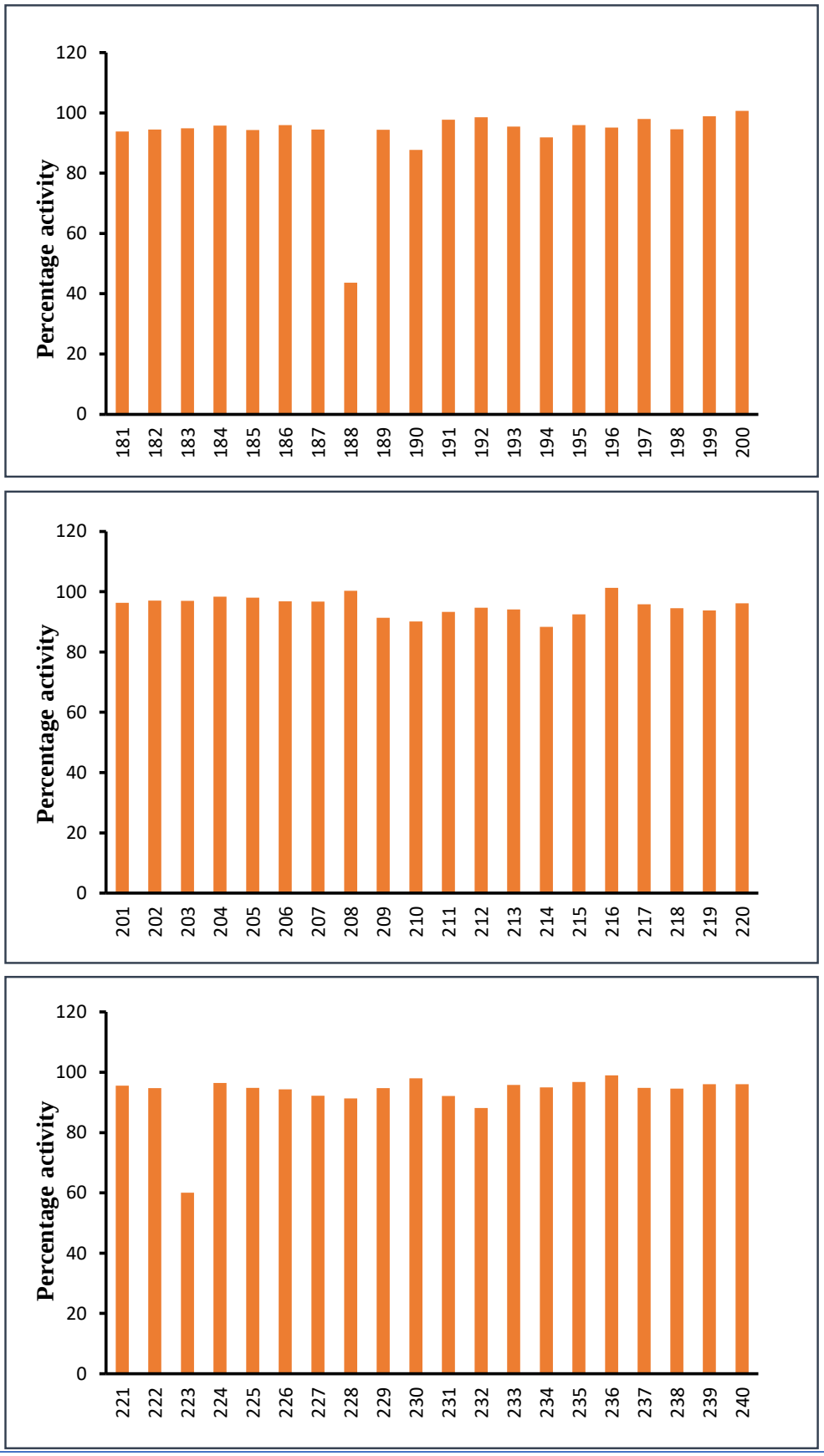
Percentage activity
0
20
40
60
80
100
120
181 182 183 184 185 186 187 188 189 190 191 192 193 194 195 196 197 198 199 200
Percentage activity
0
20
40
60
80
100
120
201 202 203 204 205 206 207 208 209 210 211 212 213 214 215 216 217 218 219 220
Percentage activity
0
20
40
60
80
100
120
221 222 223 224 225 226 227 228 229 230 231 232 233 234 235 236 237 238 239 240

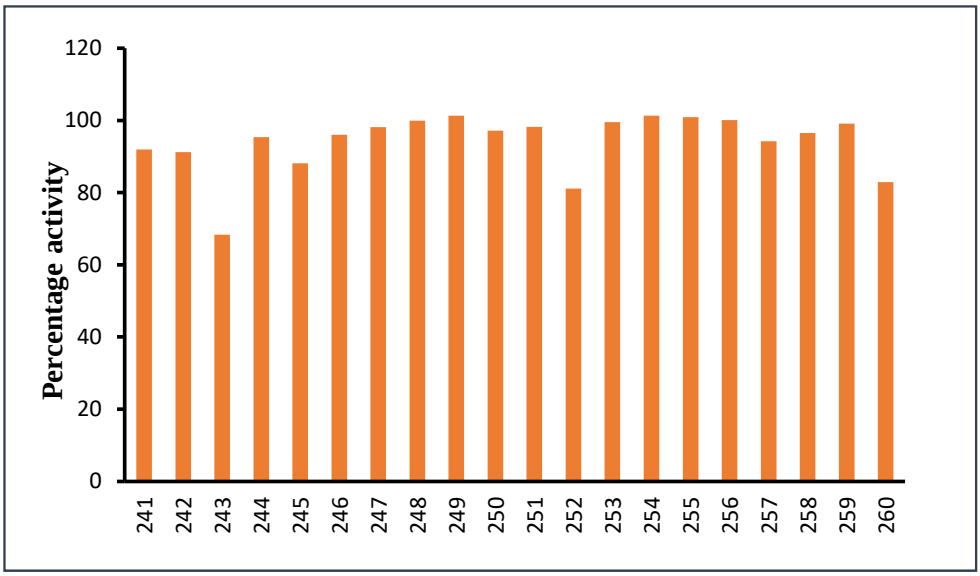
Percentage activity
120
100
80
60
40
20
0
241 242 243 244 245 246 247 248 249 250 251 252 253 254 255 256 257 258 259 260

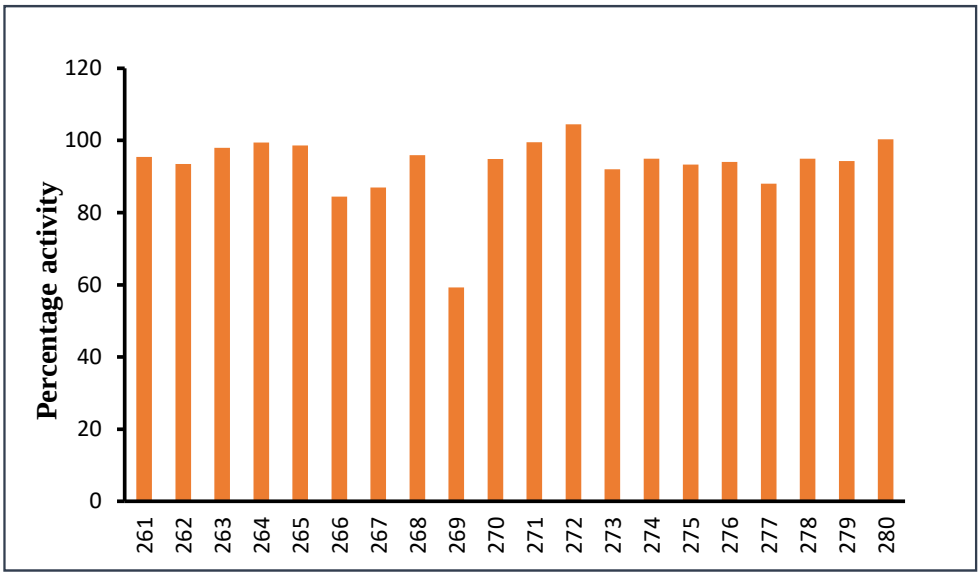
Percentage activity
120
100
80
60
40
20
0
261 262 263 264 265 266 267 268 269 270 271 272 273 274 275 276 277 278 279 280

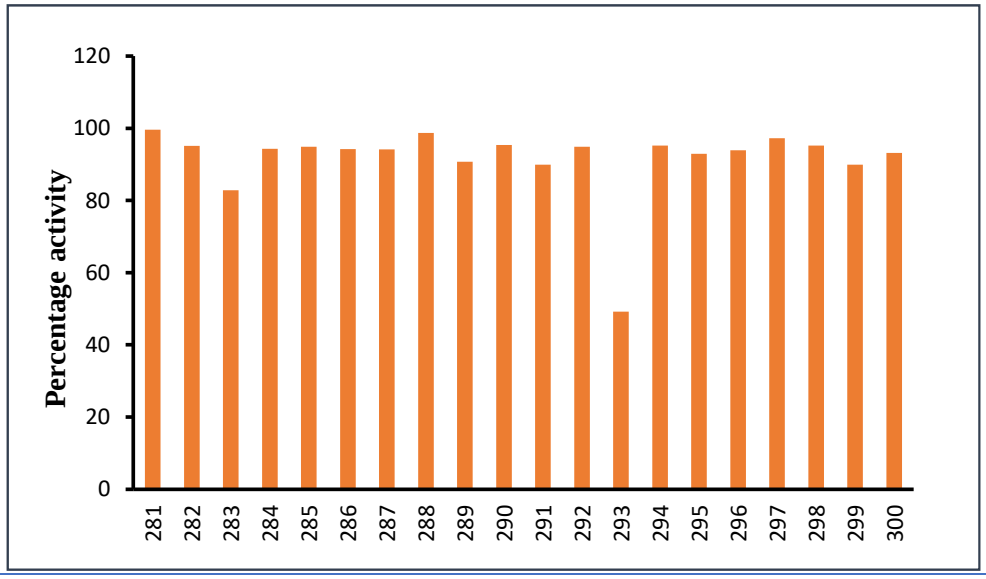
Percentage activity
120
100
80
60
40
20
0
281 282 283 284 285 286 287 288 289 290 291 292 293 294 295 296 297 298 299 300

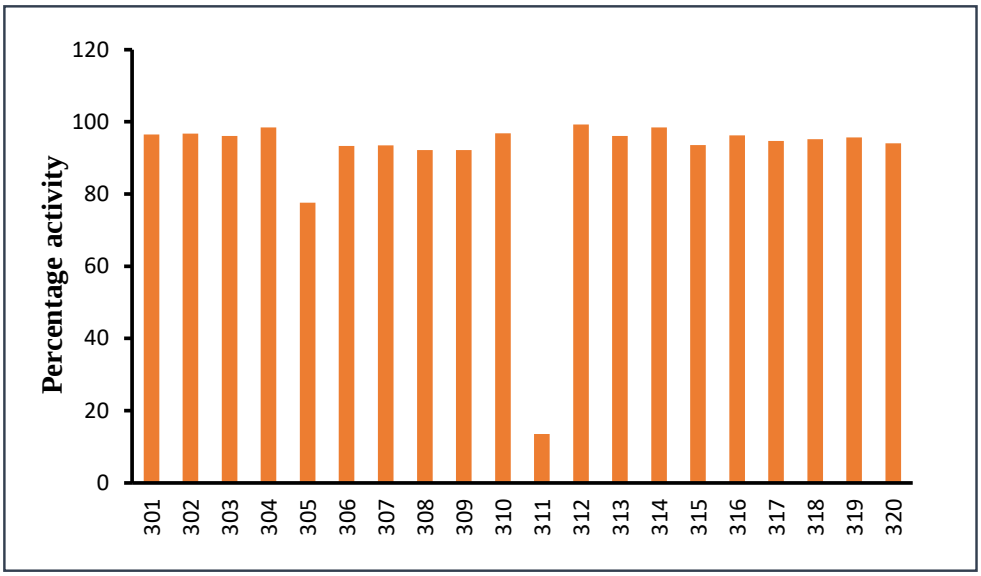
Percentage activity
120
100
80
60
40
20
0
301 302 303 304 305 306 307 308 309 310 311 312 313 314 315 316 317 318 319 320

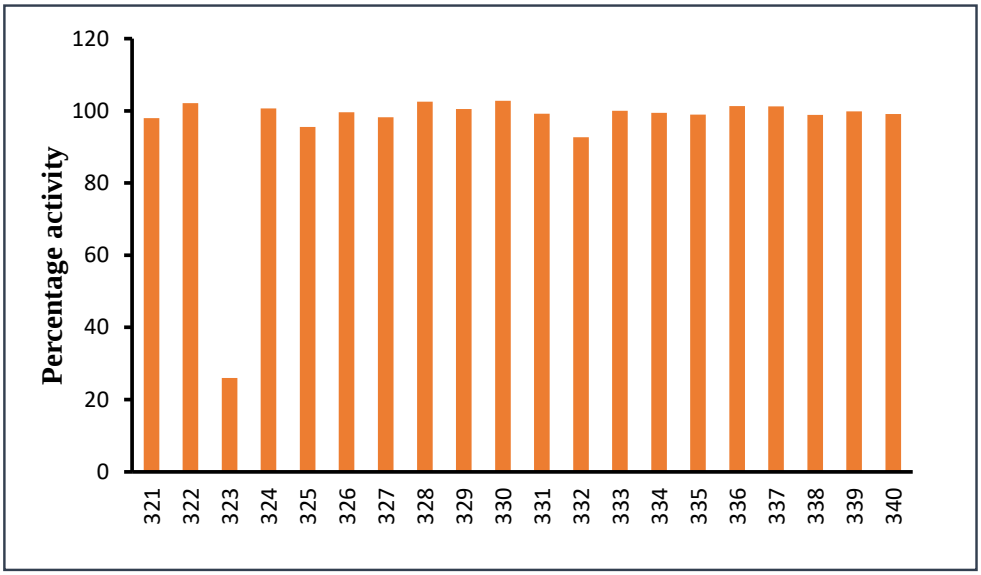
Percentage activity
120
100
80
60
40
20
0
321 322 323 324 325 326 327 328 329 330 331 332 333 334 335 336 337 338 339 340

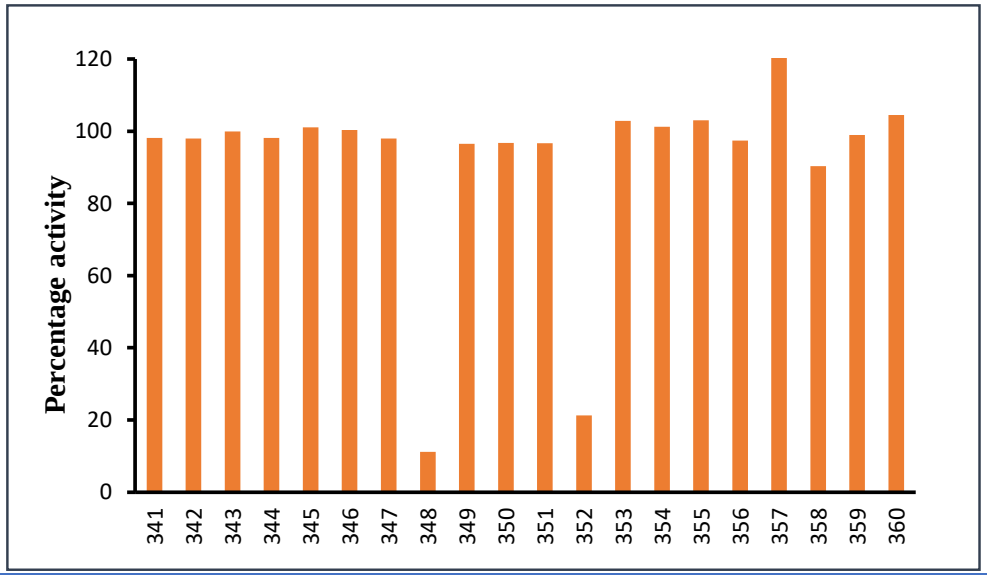
Percentage activity
120
100
80
60
40
20
0
341 342 343 344 345 346 347 348 349 350 351 352 353 354 355 356 357 358 359 360

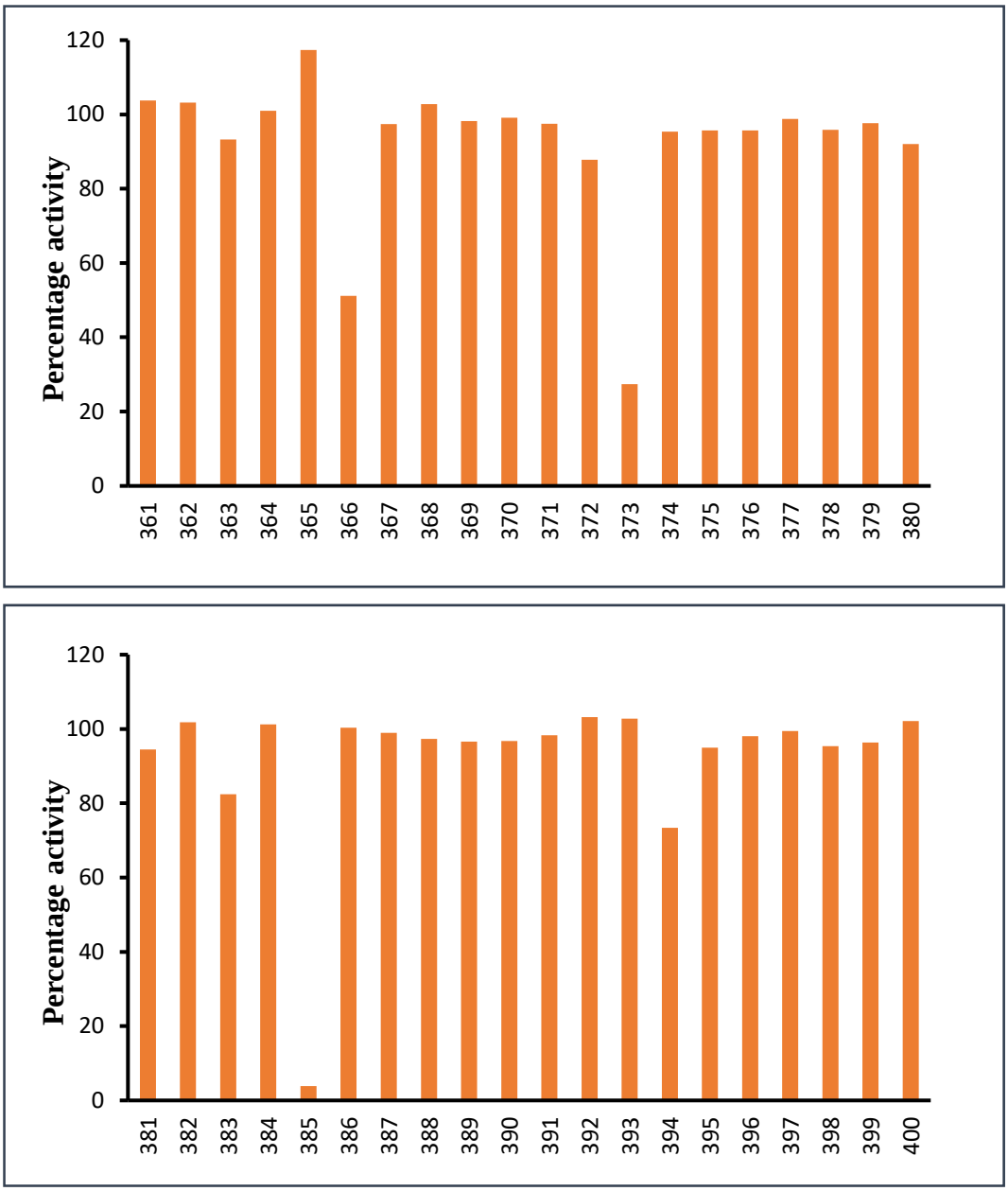

Figure 40: Primary screening of malaria box compound library using *in-vitro Pf*LPL3 lysophospholipase activity assay. Percentage activity in presence of each compound at 5µM final concentration is plotted in comparison to activity with DMSO control.

In primary screening two compounds (348 and 385) showed >70% enzyme activity inhibition at 5µM concentration and were named as PCB6 and PCB7 and selected for further studies (Figure 40). These compounds were assessed for their inhibitory potential in a concentration gradient to estimate Ki and IC_{50} value. The IC_{50} values of these

compounds were estimated to be 1.23 µM and 0.90 µM respectively; their *K*i were found to 0.634 µM and 0.464 µM, respectively. These two compounds were selected for further *in-vivo* experiments.

Table 4: MMV compounds identified as *Pf*LPL3 inhibitors and their efficacies on enzymatic activities (IC_{50}) and *P. falciparum* growth (EC_{50})

Plate	MMV-ID	Lab-ID	EC_{50}(µM)	IC_{50}(µM)
P4-10G	MMV676182	PCB 6	1.26	1.23
P5-2C	MMV676398	PCB 7	0.92	0.9

4.3.1.2 *Pf*LPL3 inhibitors block *P. falciparum* schizont development: The "Malaria Box" compounds are known to show anti-parasiticidal efficacies with EC_{50} at ~1.0 µM. We confirmed the EC_{50} of PCB6 and PCB7 compounds to be 1.26 µM and 92 µM respectively (Figure 41A and B). Further, IC_{50} and EC_{50} values are very similar for each of the compound, PCB6 and PCB7, suggesting specificity of these compounds to the selected target in the cell. To assess the effect of these compounds on parasite development cycle, synchronized parasites culture was treated with each compound at EC_{50} and parasite development was monitored at different time points of the asexual blood stage parasite cycle. It was found that for both compounds, PCB 6 and PCB 7, the treated parasites developed from ring to trophozoites normally as in case of solvent control, however >50% of these trophozoites were not able to develop into mature schizonts and appeared as stressed parasites. These results were similar to the morphological effect observed in *Pf*LPL3 knock-down experiments (Figure 41C). Thus, these results clearly show the specificity of the selected compounds for *Pf*LPL3. Overall, we identified two specific inhibitors of *Pf*LPL3 which have effective parasiticidal efficacies.

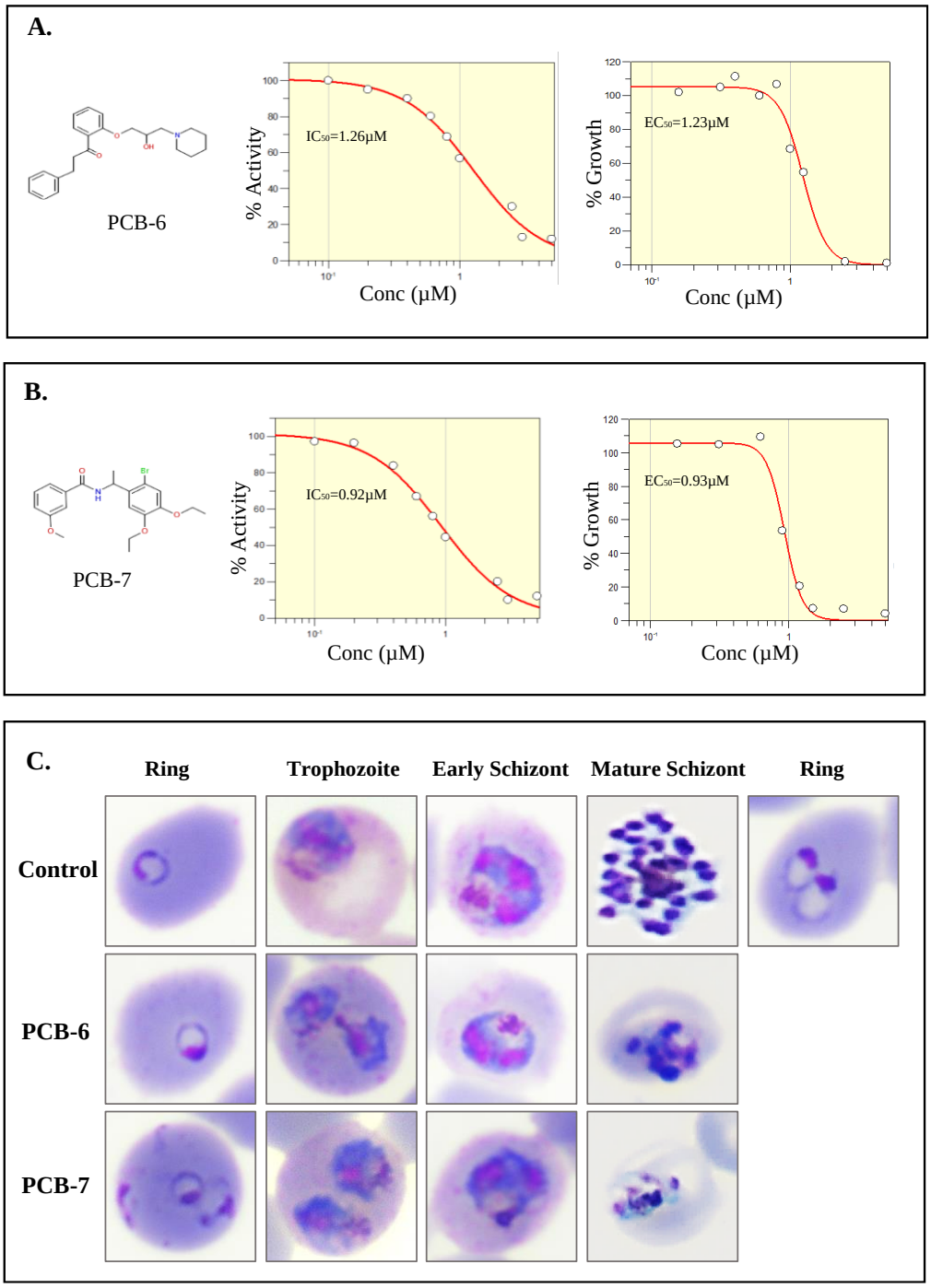

Figure 41: Identification of *Pf*LPL3 specific inhibitors from MMV Malaria Box: A robust *in vitro* activity assay was used to screen the 'Malaria Box' and potent inhibitors of *Pf*LPL3 were identified having parasiticidal efficacies. Concentration dependent inhibition of enzymatic activity and asexual stage parasite growth by PCB-6 (A) and PCB-7 (B) compounds, respectively. The IC_{50} and EC_{50} values for the compounds are indicated. (C) Effect on the morphology of 3D7 parasites at different time points after treatment with *Pf*LPL3 inhibitors.

4.3.2 *In silico* studies to assess binding mode of *Pf*LPL3 inhibitors

We also carried out the in-silico docking/interactions studies of the selected compounds with the active site of *Pf*LPL3. These studies may help to develop more potent derivates of the inhibitors.

4.3.2.1 Generation of three-dimensional homology model of *Pf*LPL3

To predict three-dimensional structure, *Pf*LPL3 was subjected to NCBI BLAST to identify the PDB template, however we could not find any template showing more than 30% identity with a significant query coverage score which is required for homology modeling. We used I-TASSER tool to predict 3D structure of *Pf*LPL3. The I-TASSER predicted the best 3D model by using 6EIC, (Monoglyceride Lipase from *Mycobacterium Tuberculosis)* as a template with TMC scores 0.56 and -1.26 respectively. The RAMPAGE generated Ramachandran plot of *Pf*LPL3 structural model showed that the 11.7% residues were in outlier region, which were further reduced to 1.9% by using molecular simulations in Gromacs version 8 tool (Figure 42A). The predicted secondary structure was found to be in coherence with the secondary structure analysed by PSI-pred (Figure 42C). Sequence analysis and alignment with 6EIC shows the conservation of both the G-X-S-X-G motifs. In the predicted 3D structure one motif was found to be located towards the periphery and another is present in the core as shown in (Figure 43B).

Figure 42 : Sequence alignment and structure prediction of *Pf*LPL3: (A) Predicted 3D structure of *Pf*LPL3 using I-TASSER and Cartoon representation of superimposition of model LPL3 (green) with Template 6EIC chain B (yellow), (B) Multiple sequence alignment of LPL3 with different chains of template 6EIC using CLUSTALΩ tool. (C) Predicted secondary structure of *Pf*LPL3 using PSI-pred tool.

4.3.2.2 Ligand binding pocket prediction and docking

To identify the binding pocket residues, *Pf*LPL3 was subjected to Fpocket tool which identified 10 possible binding pockets for *Pf*LPL3. The pocket with the highest score was selected which consist of residues; His 47, Gly 48, Gly 98, Ile 206, Ala 208, Ser 240, Ser 243, Ala 270, Val 332 and Glu 336 (Figure 43). The ligands were well docked within the

pocket which was further confirmed by molecular simulations. The complex was found to be stable for 10 nano seconds with the levels off to ~0.45 nm (4.5 Å).

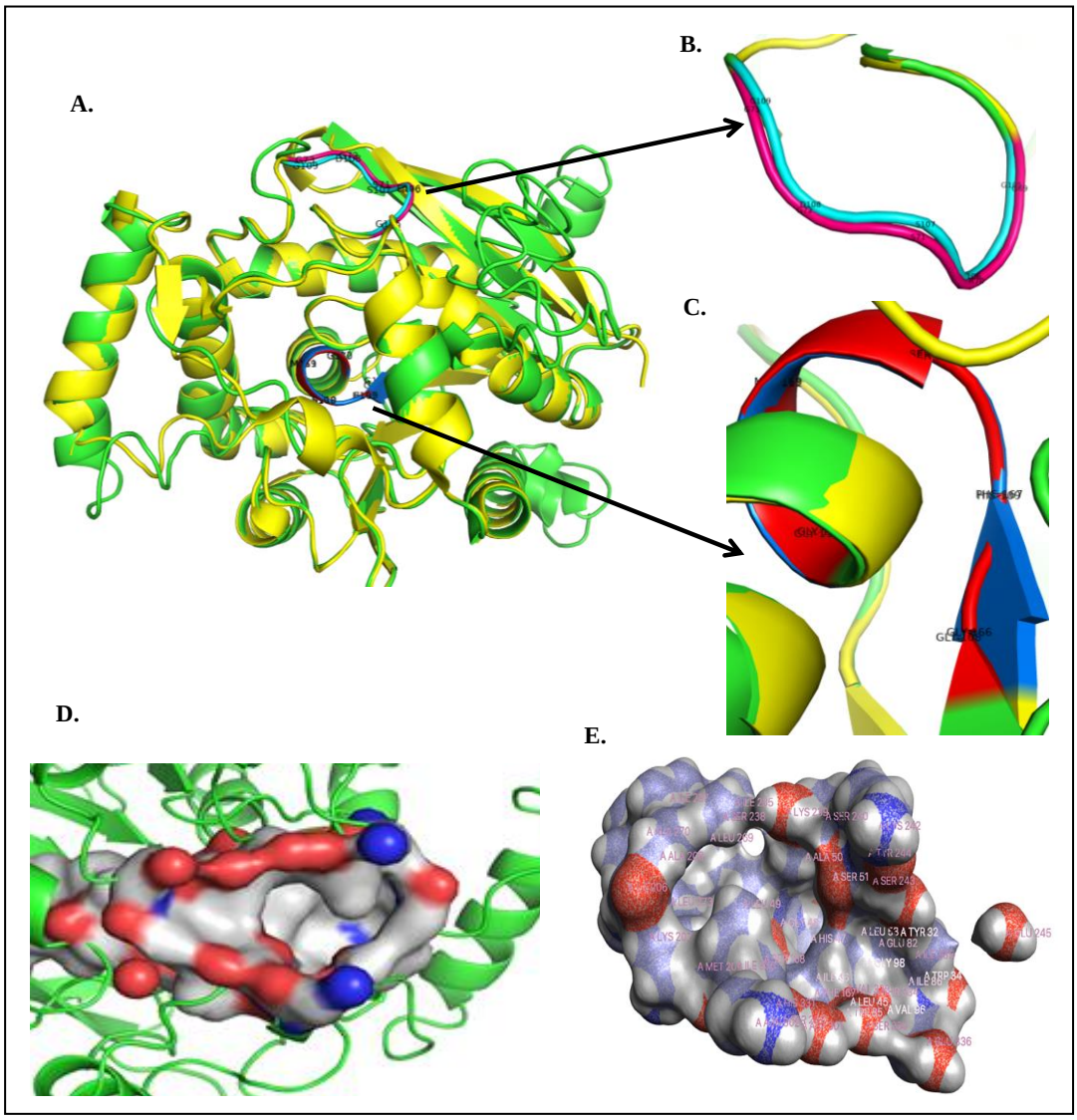

Figure 43: Structural analysis to provide active site binding pocket: (A) Structural alignment of the predicted tertiary structure with template. (B) and (C) Temporal position of the conserved GXSXG motif in the predicted 3D structure. (D) and (E) Predicted ligand binding pocket of *Pf*LPL3 with residues labelled.

The ligands were subjected to force-field analysis for better understanding of the binding modes (electropositive, electronegative, hydrophobic and Van der Waals forces) of interactions involved in docking. The model was then docked with keeping the binding pocket and catalytic residues as the center for the grid generation using default docking

parameters (Figure 44 and 45). The binding energies of the protein *Pf*LPL3 when docked with following inhibitors is listed in Table 5.

Table 5: Binding energies of the protein *Pf*LPL3 docked with selected inhibitors.

S.No	Inhibitor	Binding energy	VS Score	Rank Score
1	PCB6	-8.939	-9.863	-7.415
2	PCB7	-7.173	-8.296	-6.721

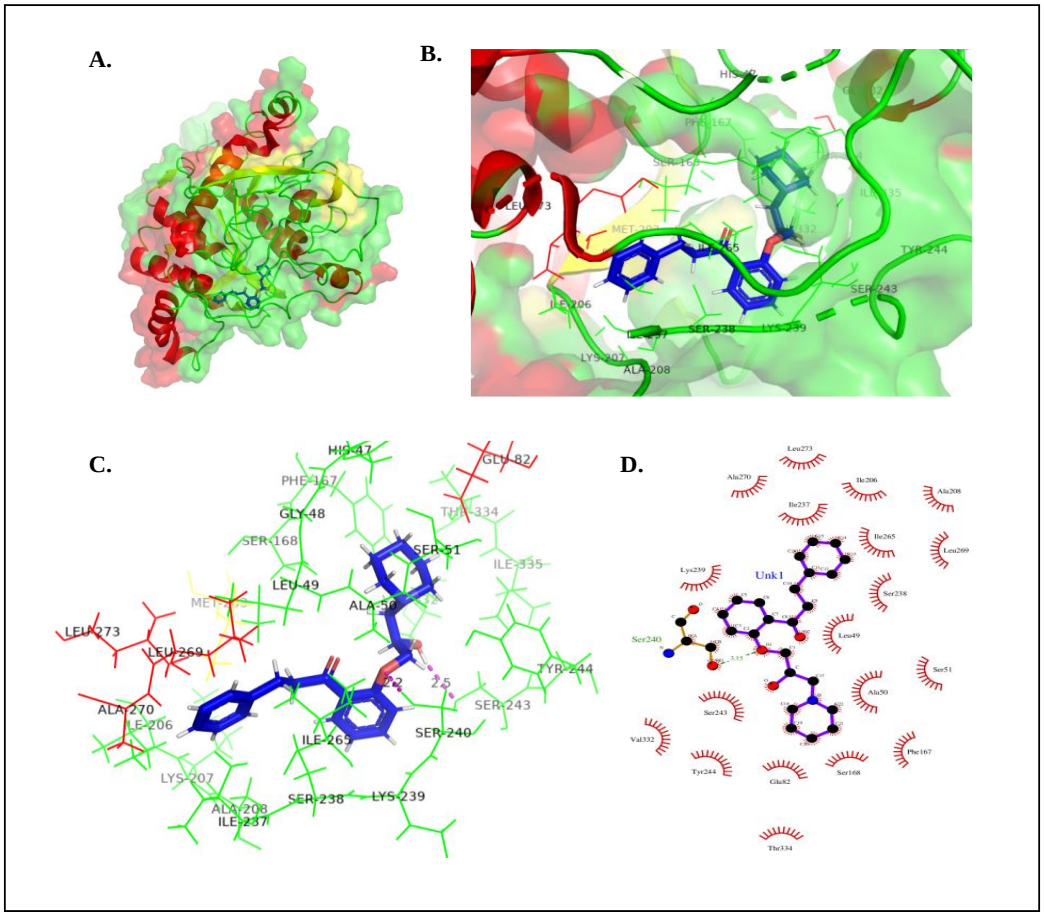

Figure 44: Docking of PCB-6 in the binding pocket of *Pf*LPL3: (A) Cartoon representation of model *Pf*LPL3 surface view (green) in a docked pose with PCB-6 (Blue); (B) Representation of interacting residues of *Pf*LPL3 in a docked conformation with PCB-6; (C) Interacting residues of *Pf*LPL3 with PCB-6 expanded around 4Å; (D) Ligplots to show *Pf*LPL3 residues forming hydrogen bond and hydrophobic interactions with the PCB-6 for protein–ligand complexes.

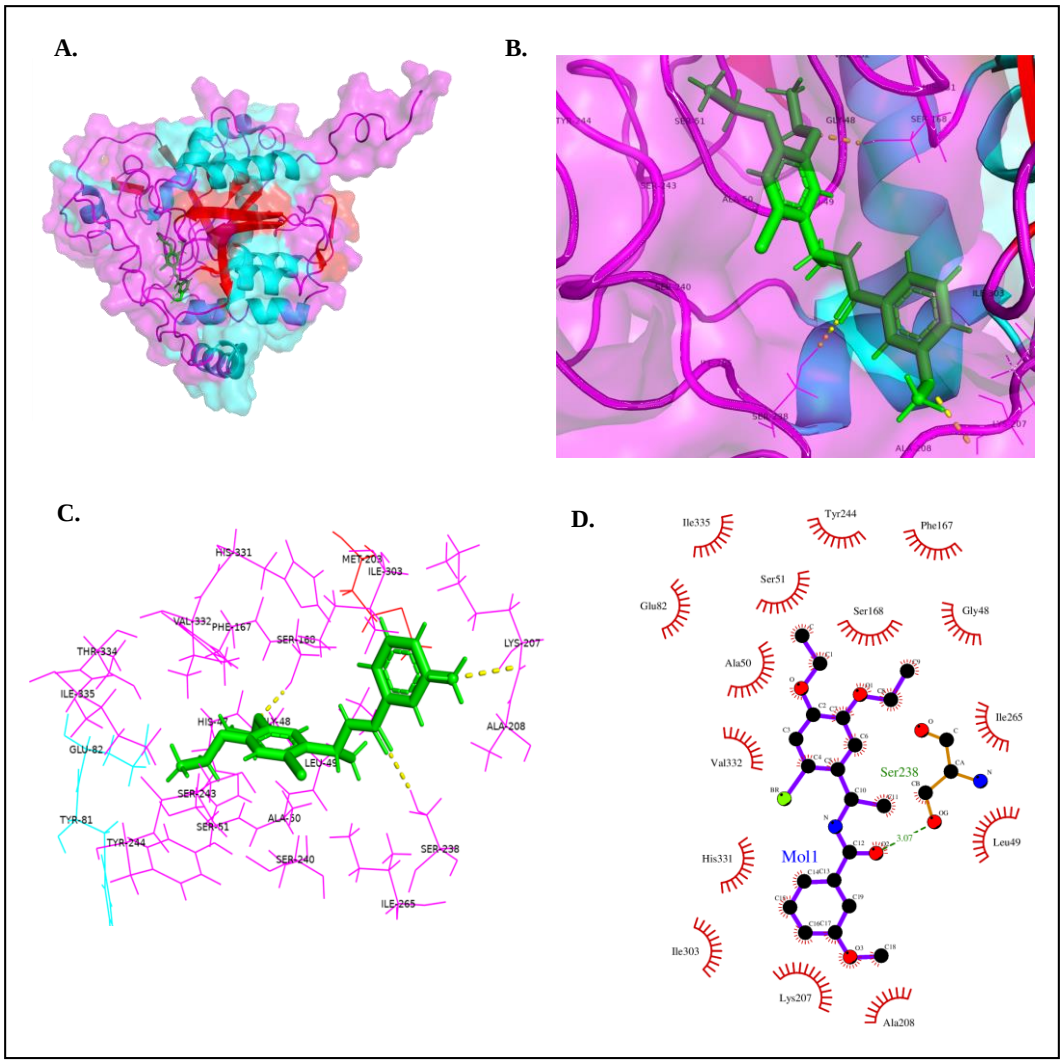

Figure 45: Docking of PCB-7 in the binding pocket of *Pf*LPL3: (A) Cartoon representation of model *Pf*LPL3 surface view (violet) in a docked pose with PCB-7 (Green); (B) Representation of interacting residues of *Pf*LPL3 in a docked conformation with PCB-7; (C) Interacting residues of *Pf*LPL3 with PCB-7 expanded around the 4Å; (D) Ligplots to show *Pf*LPL3 residues forming hydrogen bond and hydrophobic interactions with the PCB-7 for protein–ligand complexes.

Chapter 5 Discussion

5. Discussion

The asexual growth cycle of malaria parasite involves extensive synthesis of membranes, especially required for development of new membrane-bound organelles as well as for the assembly of new merozoites after cell division, which requires large amount of lipids/ phospholipids in the parasite (Amiar et al., 2016; Vaughan et al., 2009; Yu et al., 2008). To fulfill these large requirements of lipids, the parasite *de novo* synthesize as well as scavenge lipids/phospholipids from host milieu during the erythrocytic cycle. Indeed, there is huge increase in phospholipids, neutral lipids and fatty acids content in the parasite as it develops inside the host erythrocyte (Vial et al., 1982). Several studies showed that the metabolic pathways linked with synthesis, catabolism and trafficking of lipids, are essential for parasite survival (Ben Mamoun et al., 2010; Choubey et al., 2007; Hanada et al., 2002; Mitamura and Palacpac, 2003). Phospholipids are known to play important roles in the progression of the life cycle of every parasite and its pathogenesis, whereas lysophospholipids are the major building blocks for the synthesis of phospholipids during cell-cycle (Brancucci et al., 2017).

In our attempts to further understand lipid homeostasis and membrane synthesis in the parasite, we explored the role of putative lysophospholipases (LPLs) in *P. falciparum* during asexual life cycle. Lysophospholipases, that hydrolyze lysophospholipids during the phospholipid catabolism, are present across all the kingdoms, highlighting their importance in living cell. *P. falciparum* infected RBCs shows significant lysophospholipase like activity as compared to uninfected RBCs (Zidovetzki et al., 1994), suggesting functional relevance of these enzymes for parasite growth and segregation. We have carried out biochemical and functional characterization of three putative lysophospholipases, labelled as *Pf*LPL3 (PF3D7_1476800), *Pf*LPL4 (PF3D7_0731800), and *Pf*LPL20 (PF3D7_0702200). The *P. falciparum* genome codes for a large family of about 14 LPLs, however, their functional roles are not characterized. All the LPLs harbors α/β hydrolase domain having GXSXG conserved motif. All the three selected LPLs also contain this conserved motif along with serine, histidine, and aspartic acid as catalytic site residues. In the first part of the thesis we have characterized enzymatic properties of these enzymes.

All the three targets were expressed as recombinant protein and purified. These recombinant enzymes were assessed in enzymatic assays using LPC substrate; in this assay the LPC first gets hydrolyzed to glycerophosphocholine by LPL, which is subsequently hydrolyzed by glycerophosphodiesterase to release choline which is estimated by a fluorescent based assay. All the three *P. falciparum* LPLs showed LPL activity in this assay with *Km* values comparable to LPLs from other organisms (Fujimori et al., 1993).

Intracellular growth and segregation of *Plasmodium* requires lipid synthesis which is essentially needed for new membrane development; phospholipids are *de-novo* synthesized by the parasite; however, their precursors are scavenged from the host milieu. It has been shown that depletion in the serum LPC leads to decrease in the number of merozoites in rodent malaria model (Brancucci et al., 2017). Host scavenged LPC is essential for Phosphatidylcholine (PC) synthesis in the parasite; PC is generated by Kennedy pathway from cytidine diphosphate (CDP)-choline (Gibellini and Smith, 2010; Hanada et al., 2002; Tischer et al., 2012), whereas in absence of choline, PC is generated via triple methylation of PE using ethanolamine and serine as external precursors (Bobenchik et al., 2011; Pessi et al., 2005). It was earlier proposed that choline acquired from serum gets directly incorporated in to PC, however, recent study showed that majority of the choline incorporated into PC is generated from LPC (Brancucci et al., 2017), highlighting the role of LPLs in PC synthesis. Therefore, these three LPLs with putative activity of hydrolysis of LPC may be crucial for the parasite.

In second part of this research work under this thesis, we studied the functional role and essentiality of these target genes in the parasite. Enormous research has been carried out to develop different reverse genetic approaches for gene function analysis in malaria parasites (de Koning-Ward et al., 2015). Since, it is difficult to knockout an essential gene in the parasite, several tools have been developed for transient knock-down of target gene (Armstrong and Goldberg, 2007; Meissner et al., 2005). We utilized various research approaches including gene knock-down, GFP-tagging, metabolic studies, and the transcriptomic analysis to understand the functional roles of these LPLs. To understand role of *Pf*LPL3 in the parasite, we tagged the native gene at the C-terminus with GFP and a *glmS* ribozyme system (Prommana et al., 2013). The transgenic parasite lines expressing

fusion protein was then used for localization as well as gene knock-down studies. Our studies suggested localization of *Pf*LPL3 in the Parasitophorous Vacuole (PV) region and even extending into the Tubulovesicular networks (TVN); the PV regions are at the interphase of host-parasite interaction during intracellular growth, and these interphase are site of active transport of material from host to parasite through Parasitophorous Vacuolar Membrane (PVM) (Desai et al., 2000; Nguitragool et al., 2011). The PVM act as a molecular sieve for the parasite whereas the Tubulovesicular networks (TVN) are extensions of PVM which increases the surface area of the PVM to facilitate nutrient uptake and protein transport. Presence of *Pf*LPL3 in PV is very interesting, which may suggest that PV/TVN regions are also site of phospholipid uptake and metabolism. Indeed, it has been shown that lysophosphatidylcholine present in blood plasma acts as a precursor for choline and fatty acids synthesis in the parasite (Brancucci et al., 2017; Wein et al., 2018), highlighting host lipid scavenging, metabolism, and utilization by the parasite. For utilization of host lysophosphatidylcholine, the parasite needs to remove their acyl chain using lysophospholipases to generate glycerophospholipids; further, the glycerophosphodiesterase acts downstream of LPL to remove the choline moiety from glycerophospholipids. Recent study showed tripartite distribution of glycerophosphodiesterase in the cytosol, PV, and food vacuole (Denloye et al., 2012). Presence of Phospholipase A (Burda et al., 2015), glycerophosphodiesterase as well as lysophospholipase, *Pf*LPL3, in the PV of the parasite strongly suggests that it is site of catabolism of exogenously imported phospholipids in to fatty acids and choline; these metabolites get further transported to the parasite cytosol by choline transporters, which are shown to be present in the parasite plasma membrane (Biagini et al., 2004; Lehane et al., 2004).

We have used the inducible *glm*S ribozyme system for conditional knock-down *Pf*LPL3 to explore its role in parasite life cycle. Transient down regulation of *Pf*LPL3 caused growth retardation of transgenic parasites; the parasite developmental-stage profile after *Pf*LPL3 knock-down showed that the development of trophozoites into schizonts was severely disrupted in these parasites. Trophozoite stage of the parasite is metabolically most active stage in which parasite generates and utilizes the available raw materials for

cytokinesis and karyokinesis. There is a drastic increase in the synthesis of lipids for membrane synthesis required for development of segregating organelles as well as formation of daughter merozoites. Hindrance in schizont development due to *Pf*LPL3-iKD suggests role of *Pf*LPL3 in parasite growth cycle. Although, some of the parasites in the *Pf*LPL3-iKD set were able to develop from trophozoite into schizonts, however, these schizonts have compromised on number of merozoites developed, although these merozoites have properly developed membrane. In *P. berghei*, a phospholipase (*Pb*PL) is shown to be present in parasitophorous vacuole, and its depletion caused defect in the egress from the host hepatocytes (Burda et al., 2015).

Our lipidomic analysis revealed that there was decrease in the total fatty-acid content combined with minor decrease in the phospholipid content after inducible knock-down (iKD) of *Pf*LPL3; however, there was no difference in phospholipid composition. These results indicated that *Pf*LPL3-iKD effect the hydrolysis of phospholipids and fatty-acids production. Indeed, lysophospholipases are known to cleave the fatty acid chain from the complex lipids, lysophospholipids; the fatty-acids (FAs) produced by this cleavage are ultimately utilized in generation of neutral lipids, Diacylglycerol and Triacylglycerol (DAG and TAG) in the parasite. Indeed, there was significant reduction in relative amount of DAG and TAG upon depletion of *Pf*LPL3; further, there was a reduction in the ratio of TAG to DAG. These results confirmed that *Pf*LPL3 is particularly involved in lipid recycling which ultimately effects the synthesis of TAG.

These neutral lipids play important role in eukaryotic cell cycle; DAG is known to activates protein kinase C by acting as second messenger (Goni and Alonso, 1999), it also serves as a precursor for synthesis of TAG and major phospholipids. TAG is stored into cytosolic lipid droplets that detoxify and sequester FAs. Whereas, TAG degradation by specific lipase can release these FAs to be utilized for membrane assembly (Athenstaedt and Daum, 2006). In asexual stage parasites, neutral lipids are stored in a lipid-body associated with the food-vacuole (Jackson et al., 2004; Vielemeyer et al., 2004). During parasite growth, hydrolysis of TAG can rapidly produce FAs to utilize in membrane synthesis (Palacpac et al., 2004). A general lipase inhibitor, Orlistat, was suggested to block utilization of stored TAGs, which inhibited parasite growth and caused developmental

arrest in late stages (Gulati et al., 2015). In similar way, reduction in TAG levels in *Pf*LPL3-iKD conditions, caused arrest of parasite in late stages, in addition, some of the parasite showed reduced number of merozoites, which also point at hindrance in membrane biogenesis.

To understand the functional role of *Pf*LPL20, we used GFP-*glm*S ribozyme system for conditional knock-down of the *PfLPL20* gene; we tagged *Pf*LPL20 at C-terminal with GFP-*glm*S tag. In addition, transgenic parasite line expressing *Pf*LPL20-GFP fusion protein was also generated for localization studies. Confocal microscopy analysis of both transgenic parasite lines (*Pf*LPL20-GFP and *Pf*LPL20-GFP-*glm*S) showed that *Pf*LPL20 is present in vesicular structures, which are associated with parasite membrane or distributed in parasite cytosol; during late developmental stages these vesicles get fused to a multi-vesicular structure in close proximity to the food-vacuole. These structures showed resemblance with the previously reported neutral lipid bodies (NLB) (Jackson et al., 2004; Palacpac et al., 2004), which act as a reservoir of diacylglycerols (DAG) and triacylglycerol (TAG). Co-localization of *Pf*LPL20 with neutral lipid labelling probes confirmed its presence in these lipid bodies. It is suggested that the parasite utilizes these stored lipids for membrane biogenesis during segregation. Localization of *Pf*LPL20 in small endocytic vesicles near parasitophorous vacuole and its subsequent localization in neutral lipid stores, may indicate its involvement in catabolism of lipids which are scavenged from the host. As discussed earlier, it has been shown that *P. falciparum* scavenge LPC from the host milieu which gets catabolized and utilized in PC synthesis required for membrane biogenesis. As expected from sequence homology and presence of catalytic active site, *Pf*LPL20 indeed showed catabolic activity on LPC substrate, which may suggest its role in phospholipid recycling in the parasite. Overall, the localization studies and biochemical characterization of *Pf*LPL20 indicate its association with the lipid homeostasis in the parasite.

The C-terminal *glm*S tag based system could induce >90% knock-down of *pfLPL20* transcript in the transgenic parasites; whereas, the parasite growth analysis showed that the inducible-knock-down did not affect parasite growth and multiplication, which may suggest that the enzyme is not essential for the survival of the asexual blood stage parasites.

Recent study using *piggyBac* transposon insertion-based mutagenesis also showed dispensability of *Pf*LPL20 (Zhang et al., 2018). One of the reasons for dispensability of an active enzyme in the cell could be compensation of its function by any other enzymes/pathway. Biochemical characterization showed that catabolism of LPC is the main function of *Pf*LPL20 which generates fatty acids and choline to be utilized by the parasite. Although parasite is able to import free choline from host milieu (Ancelin et al., 1991; Biagini et al., 2004), however, the scavenged choline is not utilized by the parasite for membrane synthesis . Detailed analysis of parasite stage development in the *Pf*LPL20 knockdown suggested transient morphological effects on trophozoite stages. These results may suggest the possibility that the *Pf*LPL20 function is compensated or switched over to another metabolic pathway in the parasite.

Extensive synthesis of membrane phospholipids is essential for parasite growth and segregation. Trophozoite and schizont infected RBCs show six-fold increase in the phospholipid content in comparison to uninfected RBCs; majority of this phospholipid content is phosphatidylcholine (PC), which is a major membrane phospholipid in *Plasmodium*. Under normal condition the parasite generate most of the required PC via CDP-Choline- dependent-Kennedy pathway using choline as a substrate (Ancelin and Vial, 1989; Carman and Henry, 1989; Kent, 1995; Lykidis and Jackowski, 2001). As discussed earlier, recent studies have shown that LPC imported from the serum is the main source of choline, which converts into phosphocholine to get utilized for PC bio-synthesis (Brancucci et al., 2017; Wein et al., 2018), thus lysophospholipase play key role in the membrane bio-synthesis. The parasite can also utilize triple methylation of the phosphoethanolamine (PE) to make phosphocholine which then enters in the same pathway to make PC (Figure 34). This involves activity of phosphoethanolamine methyltransferase (PMT), which transfer methyl group from S-adenosylmethionine (SAM) to PE. Further, it has been shown that under serum LPC depleted conditions, there is shift of PC synthesis towards PMT pathway using ethanolamine substrate. It was also shown that under LPC depleted conditions the expression of *Pf*PMT (phosphoethanolamine-methyltransferase), *Pf*SAMS (S-adenosylmethionine synthetase) and *Pf*EK (ethanolamine kinase) get upregulated (Brancucci et al., 2017). The *Pf*LPL20 knockdown conditions may reduce

catabolism of LPC resulting in reduction in availability of choline for Kennedy pathways, which may mimic the LPC depletion conditions. Therefore, we assessed transcript levels of different enzymes of PMT pathways under *Pf*LPL20 knockdown conditions. In *Pf*LPL20 knockdown conditions, there was a significant upregulation in the transcript level of *Pf*SAMS (SAM synthetase), whereas expression levels of *Pf*PMT and *Pf*EK were not altered. These results suggest that the transcript response under *Pf*LPL20 knockdown conditions was somewhat different as compared to LPC depleted conditions. Under serum LPC depletion condition upregulation of PMT transcript was reported (Brancucci et al., 2017); in addition, there was upregulation of AP2-G transcript levels which resulted in induction of gametocytes. It is also shown that in field-isolates, higher levels of plasma LPC has a negative influence on gametocyte production (Usui et al., 2019); therefore, it was suggested that the LPC depletion acts upstream of any event of sexual differentiation, but its exact role in induction sexual commitment remains unclear.

The upregulation of SAMS, under *Pf*LPL20-iKD conditions, would have increased conversion of L-methionine to SAM, causing accumulation of SAM and its higher availability for triple methylation step by *Pf*PMT; consequently, the PMT pathway would be upregulated to produce higher levels of phosphocholine. Indeed, quantitative estimation showed upregulation of phosphocholine levels in the *Pf*LPL20 knock-down conditions. These results thus confirm that under *Pf*LPL20 knockdown conditions, the alternate pathway gets upregulated to provide phosphocholine required for PC biosynthesis, which help asexual stage parasites to survive and multiply.

Overall, we have used the *glmS* mediated knock-down of *Pf*LPL20, which resulted in the upregulation of alternate pathway to generate phosphocholine synthesis in *Plasmodium falciparum*. Our results indicate *Pf*LPL20 play a role in PC biosynthesis through catabolism of LPC acquired from host milieu to provide choline which gets phosphorylated to form the phosphocholine; under the *Pf*LPL20 depleted conditions, the parasite switches an alternate SDPM pathway for phosphocholine synthesis, which is utilized for PC biosynthesis. Thus, parasite can compensate loss of one pathway of phosphocholine synthesis with another pathway, so that the parasite growth and segregation is maintained. These results may suggest that *Pf*LPL20 levels regulate

cooperation between two different pathways to generate phosphocholine required for PC synthesis. These data provide new information on membrane phospholipid biosynthetic pathways of the malaria parasite, which could be used to design future therapeutic approaches.

To understand the functional role of *Pf*LPL4, we used FKBP degradation domain system for conditional knock-down studies. We successfully generated the *Pf*LPL4-GFP-DD transgenic parasite line expressing *Pf*LPL4-GFP-DD fusion protein. Transient knock-down of *Pf*LPL4 results in the ~80 % reduction in the expression of the fusion protein. However, we could not observe any change in the parasite growth after *Pf*LPL4 knock-down as compared to control, which clearly indicate dispensability of this gene for the asexual blood stage parasite. *Pf*LPL4 was found to be exported to the RBC by the parasite and annotated as gametocyte exported protein 8 (GEXP08). Further studies are required to explore the functional role of this enzyme at the sexual blood and liver stages of the parasite.

One of the important motives to understanding the biology of the parasite is to identify functionally important metabolic pathways as drug targets and subsequently identify their specific inhibitors to develop new antimalarials. In the present research work, we carried out detailed gene functional analysis for three lysophospholipases of *P. falciparum.* Our results confirmed that one of these enzymes, *Pf*LPL3 is functionally essential for parasite survival and growth during asexual blood stage cycle. Thus, this enzyme is an important drug target. In the third part of the research work under this thesis, we tried to identify specific inhibitors for *Pf*LPL3, which could be developed in to new anti-malarials. We showed that *Pf*LPL3 harbor enzymatic activity for lysophospholipase; further, a robust *in-vitro* activity assay was established to screen the compound libraries. Medicine for Malaria Venture (MMV) established an open collaborative initiative in search of novel drugs for neglected tropical diseases; based upon extensive screening strategy, they identified a set of drug-like compounds having anti-malarial activity, and labelled this set as ‘Malaria Box’ (Spangenberg et al., 2013). These compounds are new leads to develop further; however, there is need to identify potential targets for these compounds in the parasite, which may help medicinal chemistry approaches to design diversity library and

identify potent antimalarial. We tested all compounds in the "Malaria Box" by using the *Pf*LPL3 activity assay, which identified two hit compounds, labelled as PCB6 and PCB7; both the compounds have parasiticidal efficacy and block the schizont development in *P. falciparum*, which is consistence with the gene knock down phenotype. Further, these compounds showed very close inhibition efficacy for enzyme activity with that of parasite growth inhibition efficacy (IC_{50} and EC_{50} values respectively). These results suggest that both the compounds can specifically target *Pf*LPL3 in the parasite. Hence, these can be further developed into potent antimalarials through medicinal chemistry campaign. Overall, in this study we established the functional role of *Pf*LPL3 in the development of the parasite and identified two specific inhibitors, which could be used further for the development of next generation of antimalarials.

Chapter 6 Summary

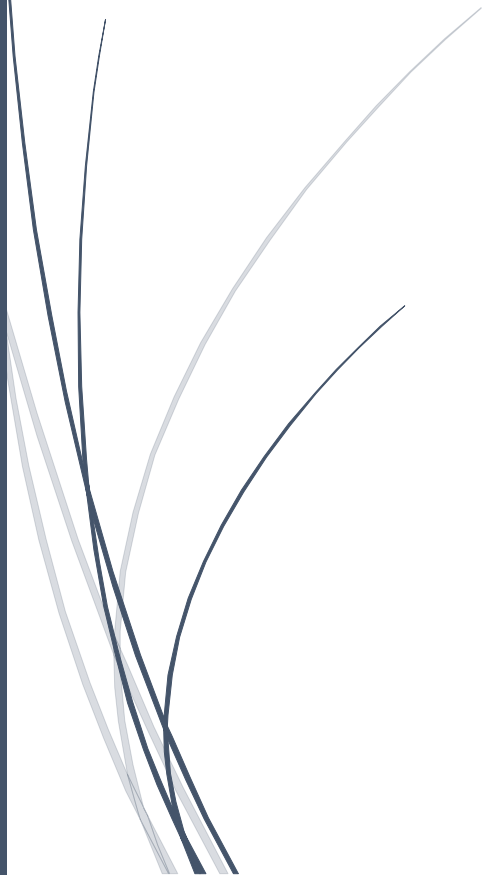

6. Summary

Phospholipid metabolism is crucial for membrane dynamics in malaria parasites during entire cycle in the host cell. The major phospholipid of parasite membranes, phosphatidylcholine (PC), is mainly synthesized through Kennedy pathways. The phosphocholine required for this synthetic pathway is generated by phosphorylation of choline derived from catabolism of lyso-phosphatidylcholine (LPC) scavenged from host milieu. Here we have biochemically characterized *P. falciparum* lysophospholipases (*Pf*LPL3, *Pf*LPL4 and *Pf*LPL20) which showed enzymatic activity on LPC substrate. We utilized GFP-tagging, reverse genetic approaches (*glmS* and FKBP degradation domain), metabolomics and transcriptomic studies to reveal the function of these lysophospholipases during the asexual blood stage cycle of *P. falciparum*.

*Pf*LPL3 was found to be localized in parasitophorous vacuole space at the parasite periphery, as well as in the tubulovesicular network space. *GlmS* mediated down-regulation of *Pf*LPL3 disrupted parasite lipid-homeostasis leading to significant disruption in parasite development from trophozoites to schizont; in addition, parasite which could develop into schizonts harboured reduced number of merozoites. Detailed lipidomic analyses confirmed role of *Pf*LPL3 in in generation of fatty acids, required as precursor for neutral lipid synthesis in the parasite. Our study thus proves an essential role of *Pf*LPL3 in lipid homeostasis/membrane-biogenesis for parasite growth and segregation during asexual cycle. We identified *Pf*LPL3 to be essential for the asexual blood stage parasites, which makes it a potential drug-target. Therefore, we tried to identify specific inhibitors to this enzyme using *in vitro* activity based screening of Malaria Box compound library, we identified two specific inhibitors of *Pf*LPL3 having potent parasitical efficacies. These compounds could be developed into new anti-malarials targeting lipid homeostasis machinery in the parasite.

For functional characterization of *Pf*LPL4, we utilized FKBP degradation domain (DD) and its conditional knock-down confirmed the dispensability of *Pf*LPL4 at the asexual blood stage of the parasite. Using GFP- targeting approach, *Pf*LPL20 was found to be localized in vesicular structures associated with the neutral lipid storage bodies, present

juxtaposed to the food-vacuole. The C-terminal tagged *glmS* mediated inducible knock-down of *Pf*LPL20 caused transient hindrance in the parasite development, however the parasites were able to multiply efficiently, suggesting that *Pf*LPL20 is either not essential for the parasite or there is an alternate pathway to compensate function of *Pf*LPL20. In *Pf*LPL20 depleted parasites, transcript levels of enzyme of SDPM pathway (Serine Decarboxylase-Phosphoethanolamine Methyltransferase) were altered along with upregulation of phosphocholine levels; these results show upregulation of alternate pathway to generate the phosphocholine required for PC synthesis through Kennedy pathway. These results highlight presence of alternate pathways for lipid homeostasis/membrane-biogenesis in the parasite.

Our study highlights functional roles of these selected LPLs in the parasite. These data could be useful to design future therapeutic approaches targeting phospholipid metabolism in the parasite. Further, we have identified two hit compounds targeting essential enzyme *Pf*LPL3: these can be developed as new anti-malarials using medicinal chemistry approaches.

Chapter 7

References

7. References

- Abdullah, S., and Karunamoorthi, K. (2016). Malaria and blood transfusion: major issues of blood safety in malaria-endemic countries and strategies for mitigating the risk of *Plasmodium* parasites. Parasitol Res *115*, 35-47.
- Amiar, S., MacRae, J.I., Callahan, D.L., Dubois, D., van Dooren, G.G., Shears, M.J., Cesbron-Delauw, M.F., Marechal, E., McConville, M.J., McFadden, G.I., *et al.* (2016). Apicoplast-Localized Lysophosphatidic Acid Precursor Assembly Is Required for Bulk Phospholipid Synthesis in *Toxoplasma gondii* and Relies on an Algal/Plant-Like Glycerol 3-Phosphate Acyltransferase. PLoS Pathog *12*, e1005765.
- Amino, R., Thiberge, S., Martin, B., Celli, S., Shorte, S., Frischknecht, F., and Menard, R. (2006). Quantitative imaging of *Plasmodium* transmission from mosquito to mammal. Nat Med *12*, 220-224.
- Ancelin, M.L., Parant, M., Thuet, M.J., Philippot, J.R., and Vial, H.J. (1991). Increased permeability to choline in simian erythrocytes after *Plasmodium knowlesi* infection. Biochem J *273 (Pt 3)*, 701-709.
- Ancelin, M.L., and Vial, H.J. (1989). Regulation of phosphatidylcholine biosynthesis in *Plasmodium*-infected erythrocytes. Biochim Biophys Acta *1001*, 82-89.
- Armstrong, C.M., and Goldberg, D.E. (2007). An FKBP destabilization domain modulates protein levels in *Plasmodium falciparum.* Nat Methods *4*, 1007-1009.
- Athenstaedt, K., and Daum, G. (1999). Phosphatidic acid, a key intermediate in lipid metabolism. Eur J Biochem *266*, 1-16.
- Athenstaedt, K., and Daum, G. (2006). The life cycle of neutral lipids: synthesis, storage and degradation. Cell Mol Life Sci *63*, 1355-1369.
- Banaszynski, L.A., Chen, L.C., Maynard-Smith, L.A., Ooi, A.G., and Wandless, T.J. (2006). A rapid, reversible, and tunable method to regulate protein function in living cells using synthetic small molecules. Cell *126*, 995-1004.
- Ben Mamoun, C., Gluzman, I.Y., Hott, C., MacMillan, S.K., Amarakone, A.S., Anderson, D.L., Carlton, J.M., Dame, J.B., Chakrabarti, D., Martin, R.K., *et al.*

(2001). Co-ordinated programme of gene expression during asexual intraerythrocytic development of the human malaria parasite *Plasmodium falciparum* revealed by microarray analysis. Mol Microbiol *39*, 26-36.

- Ben Mamoun, C., Prigge, S.T., and Vial, H. (2010). Targeting the Lipid Metabolic Pathways for the Treatment of Malaria. Drug Dev Res *71*, 44-55.
- Bhanot, P., Schauer, K., Coppens, I., and Nussenzweig, V. (2005). A surface phospholipase is involved in the migration of *Plasmodium* sporozoites through cells. J Biol Chem *280*, 6752-6760.
- Biagini, G.A., Pasini, E.M., Hughes, R., De Koning, H.P., Vial, H.J., O'Neill, P.M., Ward, S.A., and Bray, P.G. (2004). Characterization of the choline carrier of *Plasmodium falciparum*: a route for the selective delivery of novel antimalarial drugs. Blood *104*, 3372-3377.
- Biagini, G.A., Viriyavejakul, P., O'Neill P, M., Bray, P.G., and Ward, S.A. (2006). Functional characterization and target validation of alternative complex I of *Plasmodium falciparum* mitochondria. Antimicrob Agents Chemother *50*, 1841-1851.
- Blasco, B., Leroy, D., and Fidock, D.A. (2017). Antimalarial drug resistance: linking *Plasmodium falciparum* parasite biology to the clinic. Nat Med *23*, 917-928.
- Bobenchik, A.M., Augagneur, Y., Hao, B., Hoch, J.C., and Ben Mamoun, C. (2011). Phosphoethanolamine methyltransferases in phosphocholine biosynthesis: functions and potential for antiparasite therapy. FEMS Microbiol Rev *35*, 609-619.
- Bobenchik, A.M., Witola, W.H., Augagneur, Y., Nic Lochlainn, L., Garg, A., Pachikara, N., Choi, J.Y., Zhao, Y.O., Usmani-Brown, S., Lee, A., *et al.* (2013). *Plasmodium falciparum* phosphoethanolamine methyltransferase is essential for malaria transmission. Proc Natl Acad Sci U S A *110*, 18262-18267.
- Botte, C.Y., Yamaryo-Botte, Y., Rupasinghe, T.W., Mullin, K.A., MacRae, J.I., Spurck, T.P., Kalanon, M., Shears, M.J., Coppel, R.L., Crellin, P.K., *et al.* (2013). Atypical lipid composition in the purified relict plastid (apicoplast) of malaria parasites. Proc Natl Acad Sci U S A *110*, 7506-7511.

- Brancucci, N.M.B., Gerdt, J.P., Wang, C., De Niz, M., Philip, N., Adapa, S.R., Zhang, M., Hitz, E., Niederwieser, I., Boltryk, S.D., *et al.* (2017). Lysophosphatidylcholine Regulates Sexual Stage Differentiation in the Human Malaria Parasite *Plasmodium falciparum*. Cell *171*, 1532-1544 e1515.
- Burda, P.C., Roelli, M.A., Schaffner, M., Khan, S.M., Janse, C.J., and Heussler, V.T. (2015). A *Plasmodium* phospholipase is involved in disruption of the liver stage parasitophorous vacuole membrane. PLoS Pathog *11*, e1004760.
- Carman, G.M., and Henry, S.A. (1989). Phospholipid biosynthesis in yeast. Annu Rev Biochem *58*, 635-669.
- Choi, J.Y., Duraisingh, M.T., Marti, M., Ben Mamoun, C., and Voelker, D.R. (2015). From Protease to Decarboxylase: THE MOLECULAR METAMORPHOSIS OF PHOSPHATIDYLSERINE DECARBOXYLASE. J Biol Chem *290*, 10972-10980.
- Choi, J.Y., Kumar, V., Pachikara, N., Garg, A., Lawres, L., Toh, J.Y., Voelker, D.R., and Ben Mamoun, C. (2016). Characterization of *Plasmodium* phosphatidylserine decarboxylase expressed in yeast and application for inhibitor screening. Mol Microbiol *99*, 999-1014.
- Choubey, V., Maity, P., Guha, M., Kumar, S., Srivastava, K., Puri, S.K., and Bandyopadhyay, U. (2007). Inhibition of *Plasmodium falciparum* choline kinase by hexadecyltrimethylammonium bromide: a possible antimalarial mechanism. Antimicrob Agents Chemother *51*, 696-706.
- Cobbold, S.A., Vaughan, A.M., Lewis, I.A., Painter, H.J., Camargo, N., Perlman, D.H., Fishbaugher, M., Healer, J., Cowman, A.F., Kappe, S.H., *et al.* (2013). Kinetic flux profiling elucidates two independent acetyl-CoA biosynthetic pathways in *Plasmodium falciparum*. J Biol Chem *288*, 36338-36350.
- Cooke, M., Magimaidas, A., Casado-Medrano, V., and Kazanietz, M.G. (2017). Protein kinase C in cancer: The top five unanswered questions. Mol Carcinog *56*, 1531-1542.

- Crabb, B.S., Rug, M., Gilberger, T.W., Thompson, J.K., Triglia, T., Maier, A.G., and Cowman, A.F. (2004). Transfection of the human malaria parasite *Plasmodium falciparum*. Methods Mol Biol *270*, 263-276.
- de Azevedo, M.F., Gilson, P.R., Gabriel, H.B., Simoes, R.F., Angrisano, F., Baum, J., Crabb, B.S., and Wunderlich, G. (2012). Systematic analysis of FKBP inducible degradation domain tagging strategies for the human malaria parasite *Plasmodium falciparum*. PLoS One *7*, e40981.
- de Koning-Ward, T.F., Gilson, P.R., and Crabb, B.S. (2015). Advances in molecular genetic systems in malaria. Nat Rev Microbiol *13*, 373-387.
- Dechamps, S., Shastri, S., Wengelnik, K., and Vial, H.J. (2010). Glycerophospholipid acquisition in *Plasmodium* - a puzzling assembly of biosynthetic pathways. Int J Parasitol *40*, 1347-1365.
- Denloye, T., Dalal, S., and Klemba, M. (2012). Characterization of a glycerophosphodiesterase with an unusual tripartite distribution and an important role in the asexual blood stages of *Plasmodium falciparum*. Mol Biochem Parasitol *186*, 29-37.
- DeRocher, A.E., Karnataki, A., Vaney, P., and Parsons, M. (2012). Apicoplast targeting of a *Toxoplasma gondii* transmembrane protein requires a cytosolic tyrosine-based motif. Traffic *13*, 694-704.
- Desai, S.A., Bezrukov, S.M., and Zimmerberg, J. (2000). A voltage-dependent channel involved in nutrient uptake by red blood cells infected with the malaria parasite. Nature *406*, 1001-1005.
- Eda, S., and Sherman, I.W. (2002). Cytoadherence of malaria-infected red blood cells involves exposure of phosphatidylserine. Cell Physiol Biochem *12*, 373-384.
- Emoto, K., Kobayashi, T., Yamaji, A., Aizawa, H., Yahara, I., Inoue, K., and Umeda, M. (1996). Redistribution of phosphatidylethanolamine at the cleavage furrow of dividing cells during cytokinesis. Proc Natl Acad Sci U S A *93*, 12867-12872.
- Falkard, B., Kumar, T.R., Hecht, L.S., Matthews, K.A., Henrich, P.P., Gulati, S., Lewis, R.E., Manary, M.J., Winzeler, E.A., Sinnis, P., *et al.* (2013). A key role for

lipoic acid synthesis during *Plasmodium* liver stage development. Cell Microbiol *15*, 1585-1604.

- Flammersfeld, A., Lang, C., Flieger, A., and Pradel, G. (2018). Phospholipases during membrane dynamics in malaria parasites. Int J Med Microbiol *308*, 129-141.
- Flammersfeld, A., Panyot, A., Yamaryo-Botte, Y., Aurass, P., Przyborski, J.M., Flieger, A., Botte, C., and Pradel, G. (2020). A patatin-like phospholipase functions during gametocyte induction in the malaria parasite *Plasmodium falciparum*. Cell Microbiol *22*, e13146.
- Fleige, T., Fischer, K., Ferguson, D.J., Gross, U., and Bohne, W. (2007). Carbohydrate metabolism in the *Toxoplasma gondii* apicoplast: localization of three glycolytic isoenzymes, the single pyruvate dehydrogenase complex, and a plastid phosphate translocator. Eukaryot Cell *6*, 984-996.
- Flores-Diaz, M., Monturiol-Gross, L., Naylor, C., Alape-Giron, A., and Flieger, A. (2016). Bacterial Sphingomyelinases and Phospholipases as Virulence Factors. Microbiol Mol Biol Rev *80*, 597-628.
- Fowler, S.D., and Greenspan, P. (1985). Application of Nile red, a fluorescent hydrophobic probe, for the detection of neutral lipid deposits in tissue sections: comparison with oil red O. J Histochem Cytochem *33*, 833-836.
- Fry, M., and Pudney, M. (1992). Site of action of the antimalarial hydroxynaphthoquinone, 2-[trans-4-(4'-chlorophenyl) cyclohexyl]-3-hydroxy-1,4-naphthoquinone (566C80). Biochem Pharmacol *43*, 1545-1553.
- Fujimori, Y., Kudo, I., Fujita, K., and Inoue, K. (1993). Characteristics of lysophospholipase activity expressed by cytosolic phospholipase A2. Eur J Biochem *218*, 629-635.
- Gardiner, D.L., Skinner-Adams, T.S., Brown, C.L., Andrews, K.T., Stack, C.M., McCarthy, J.S., Dalton, J.P., and Trenholme, K.R. (2009). *Plasmodium falciparum*: new molecular targets with potential for antimalarial drug development. Expert Rev Anti Infect Ther *7*, 1087-1098.

- Gibellini, F., and Smith, T.K. (2010). The Kennedy pathway--De novo synthesis of phosphatidylethanolamine and phosphatidylcholine. IUBMB Life *62*, 414-428.
- Goni, F.M., and Alonso, A. (1999). Structure and functional properties of diacylglycerols in membranes. Prog Lipid Res *38*, 1-48.
- Goodman, C.D., and McFadden, G.I. (2007). Fatty acid biosynthesis as a drug target in apicomplexan parasites. Curr Drug Targets *8*, 15-30.
- Gulati, S., Ekland, E.H., Ruggles, K.V., Chan, R.B., Jayabalasingham, B., Zhou, B., Mantel, P.Y., Lee, M.C., Spottiswoode, N., Coburn-Flynn, O., *et al.* (2015). Profiling the Essential Nature of Lipid Metabolism in Asexual Blood and Gametocyte Stages of *Plasmodium falciparum*. Cell Host Microbe *18*, 371-381.
- Gunther, S., Storm, J., and Muller, S. (2009). *Plasmodium falciparum*: organelle-specific acquisition of lipoic acid. Int J Biochem Cell Biol *41*, 748-752.
- Gunther, S., Wallace, L., Patzewitz, E.M., McMillan, P.J., Storm, J., Wrenger, C., Bissett, R., Smith, T.K., and Muller, S. (2007). Apicoplast lipoic acid protein ligase B is not essential for *Plasmodium falciparum*. PLoS Pathog *3*, e189.
- Hanada, K., Palacpac, N.M., Magistrado, P.A., Kurokawa, K., Rai, G., Sakata, D., Hara, T., Horii, T., Nishijima, M., and Mitamura, T. (2002). *Plasmodium falciparum* phospholipase C hydrolyzing sphingomyelin and lysocholinephospholipids is a possible target for malaria chemotherapy. J Exp Med *195*, 23-34.
- Hay, S.I., Okiro, E.A., Gething, P.W., Patil, A.P., Tatem, A.J., Guerra, C.A., and Snow, R.W. (2010). Estimating the global clinical burden of *Plasmodium falciparum* malaria in 2007. PLoS Med *7*, e1000290.
- Herm-Gotz, A., Agop-Nersesian, C., Munter, S., Grimley, J.S., Wandless, T.J., Frischknecht, F., and Meissner, M. (2007). Rapid control of protein level in the apicomplexan *Toxoplasma gondii*. Nat Methods *4*, 1003-1005.
- Istvan, E.S., Mallari, J.P., Corey, V.C., Dharia, N.V., Marshall, G.R., Winzeler, E.A., and Goldberg, D.E. (2017). Esterase mutation is a mechanism of resistance to antimalarial compounds. Nat Commun *8*, 14240.

- Jackowski, S., Murphy, C.M., Cronan, J.E., Jr., and Rock, C.O. (1989). Acetoacetyl-acyl carrier protein synthase. A target for the antibiotic thiolactomycin. J Biol Chem *264*, 7624-7629.
- Jackson, K.E., Klonis, N., Ferguson, D.J., Adisa, A., Dogovski, C., and Tilley, L. (2004). Food vacuole-associated lipid bodies and heterogeneous lipid environments in the malaria parasite, *Plasmodium falciparum*. Mol Microbiol *54*, 109-122.
- Jefford, C.W. (2001). Why artemisinin and certain synthetic peroxides are potent antimalarials. Implications for the mode of action. Curr Med Chem *8*, 1803-1826.
- Jones, S.M., Urch, J.E., Kaiser, M., Brun, R., Harwood, J.L., Berry, C., and Gilbert, I.H. (2005). Analogues of thiolactomycin as potential antimalarial agents. J Med Chem *48*, 5932-5941.
- Kapoor, M., Dar, M.J., Surolia, A., and Surolia, N. (2001). Kinetic determinants of the interaction of enoyl-ACP reductase from *Plasmodium falciparum* with its substrates and inhibitors. Biochem Biophys Res Commun *289*, 832-837.
- Karnataki, A., Derocher, A., Coppens, I., Nash, C., Feagin, J.E., and Parsons, M. (2007). Cell cycle-regulated vesicular trafficking of *Toxoplasma* APT1, a protein localized to multiple apicoplast membranes. Mol Microbiol *63*, 1653-1668.
- Kaufman, T.S., and Ruveda, E.A. (2005). The quest for quinine: those who won the battles and those who won the war. Angew Chem Int Ed Engl *44*, 854-885.
- Kent, C. (1995). Eukaryotic phospholipid biosynthesis. Annu Rev Biochem *64*, 315-343.
- Kilian, N., Choi, J.Y., Voelker, D.R., and Ben Mamoun, C. (2018). Role of phospholipid synthesis in the development and differentiation of malaria parasites in the blood. J Biol Chem *293*, 17308-17316.
- King (1883). Insects and disease, mosquitoes and malaria. In Popular Sci Monthly.
- Kostrewa, D., Winkler, F.K., Folkers, G., Scapozza, L., and Perozzo, R. (2005). The crystal structure of PfFabZ, the unique beta-hydroxyacyl-ACP dehydratase involved in fatty acid biosynthesis of *Plasmodium falciparum*. Protein Sci *14*, 1570-1580.
- Laveran (1884). In Traité des Fièvres Palustres (Paris), pp. 457.

- Le Roch, K.G., Zhou, Y., Blair, P.L., Grainger, M., Moch, J.K., Haynes, J.D., De La Vega, P., Holder, A.A., Batalov, S., Carucci, D.J., *et al.* (2003). Discovery of gene function by expression profiling of the malaria parasite life cycle. Science *301*, 1503-1508.
- Lehane, A.M., Saliba, K.J., Allen, R.J., and Kirk, K. (2004). Choline uptake into the malaria parasite is energized by the membrane potential. Biochem Biophys Res Commun *320*, 311-317.
- Lim, L., Linka, M., Mullin, K.A., Weber, A.P., and McFadden, G.I. (2010). The carbon and energy sources of the non-photosynthetic plastid in the malaria parasite. FEBS Lett *584*, 549-554.
- Lindner, S.E., Sartain, M.J., Hayes, K., Harupa, A., Moritz, R.L., Kappe, S.H., and Vaughan, A.M. (2014). Enzymes involved in plastid-targeted phosphatidic acid synthesis are essential for *Plasmodium yoelii* liver-stage development. Mol Microbiol *91*, 679-693.
- Louie, T., Goodman, C.D., Holloway, G.A., McFadden, G.I., Mollard, V., and Watson, K.G. (2010). Dimeric cyclohexane-1,3-dione oximes inhibit wheat acetyl-CoA carboxylase and show anti-malarial activity. Bioorg Med Chem Lett *20*, 4611-4613.
- Lykidis, A., and Jackowski, S. (2001). Regulation of mammalian cell membrane biosynthesis. Prog Nucleic Acid Res Mol Biol *65*, 361-393.
- Maeda, T., Saito, T., Harb, O.S., Roos, D.S., Takeo, S., Suzuki, H., Tsuboi, T., Takeuchi, T., and Asai, T. (2009). Pyruvate kinase type-II isozyme in *Plasmodium falciparum* localizes to the apicoplast. Parasitol Int *58*, 101-105.
- Manson (1898). The mosquito and the malaria parasite. Brit Med J *2*.
- Manson, P. (1894). On the Nature and Significance of the Crescentic and Flagellated Bodies in Malarial Blood. Br Med J *2*, 1306-1308.
- Mather, M.W., Henry, K.W., and Vaidya, A.B. (2007). Mitochondrial drug targets in apicomplexan parasites. Curr Drug Targets *8*, 49-60.
- McFadden, G.I., Reith, M.E., Munholland, J., and Lang-Unnasch, N. (1996). Plastid in human parasites. Nature *381*, 482.

- Meissner, M., Krejany, E., Gilson, P.R., de Koning-Ward, T.F., Soldati, D., and Crabb, B.S. (2005). Tetracycline analogue-regulated transgene expression in Plasmodium falciparum blood stages using *Toxoplasma gondii* transactivators. Proc Natl Acad Sci U S A *102*, 2980-2985.
- Mimmi, M.C., Finato, N., Pizzolato, G., Beltrami, C.A., Fogolari, F., Corazza, A., and Esposito, G. (2013). Absolute quantification of choline-related biomarkers in breast cancer biopsies by liquid chromatography electrospray ionization mass spectrometry. Anal Cell Pathol (Amst) *36*, 71-83.
- Mitamura, T., and Palacpac, N.M. (2003). Lipid metabolism in *Plasmodium falciparum*-infected erythrocytes: possible new targets for malaria chemotherapy. Microbes Infect *5*, 545-552.
- Mohammadi, A.S., Li, X., and Ewing, A.G. (2018). Mass Spectrometry Imaging Suggests That Cisplatin Affects Exocytotic Release by Alteration of Cell Membrane Lipids. Anal Chem *90*, 8509-8516.
- Mota, M.M., Pradel, G., Vanderberg, J.P., Hafalla, J.C., Frevert, U., Nussenzweig, R.S., Nussenzweig, V., and Rodriguez, A. (2001). Migration of *Plasmodium* sporozoites through cells before infection. Science *291*, 141-144.
- Mullin, K.A., Lim, L., Ralph, S.A., Spurck, T.P., Handman, E., and McFadden, G.I. (2006). Membrane transporters in the relict plastid of malaria parasites. Proc Natl Acad Sci U S A *103*, 9572-9577.
- Nagel, A., Prado, M., Heitmann, A., Tartz, S., Jacobs, T., Deschermeier, C., Helm, S., Stanway, R., and Heussler, V. (2013). A new approach to generate a safe double-attenuated *Plasmodium* liver stage vaccine. Int J Parasitol *43*, 503-514.
- Nguitragool, W., Bokhari, A.A., Pillai, A.D., Rayavara, K., Sharma, P., Turpin, B., Aravind, L., and Desai, S.A. (2011). Malaria parasite clag3 genes determine channel-mediated nutrient uptake by infected red blood cells. Cell *145*, 665-677.
- Nilsson, S., Angeletti, D., Wahlgren, M., Chen, Q., and Moll, K. (2012). *Plasmodium falciparum* antigen 332 is a resident peripheral membrane protein of Maurer's clefts. PLoS One *7*, e46980.

- O'Brien, S.F., Delage, G., Seed, C.R., Pillonel, J., Fabra, C.C., Davison, K., Kitchen, A., Steele, W.R., and Leiby, D.A. (2015). The Epidemiology of Imported Malaria and Transfusion Policy in 5 Nonendemic Countries. Transfus Med Rev *29*, 162-171.
- Palacpac, N.M., Hiramine, Y., Mi-ichi, F., Torii, M., Kita, K., Hiramatsu, R., Horii, T., and Mitamura, T. (2004). Developmental-stage-specific triacylglycerol biosynthesis, degradation and trafficking as lipid bodies in *Plasmodium falciparum*-infected erythrocytes. J Cell Sci *117*, 1469-1480.
- Pei, Y., Tarun, A.S., Vaughan, A.M., Herman, R.W., Soliman, J.M., Erickson-Wayman, A., and Kappe, S.H. (2010). *Plasmodium* pyruvate dehydrogenase activity is only essential for the parasite's progression from liver infection to blood infection. Mol Microbiol *75*, 957-971.
- Pessi, G., and Ben Mamoun, C. (2006). Pathways for phosphatidylcholine biosynthesis: targets and strategies for antimalarial drugs. Future Lipidology *1*, 173-180.
- Pessi, G., Choi, J.Y., Reynolds, J.M., Voelker, D.R., and Mamoun, C.B. (2005). In vivo evidence for the specificity of *Plasmodium falciparum* phosphoethanolamine methyltransferase and its coupling to the Kennedy pathway. J Biol Chem *280*, 12461-12466.
- Pessi, G., Kociubinski, G., and Mamoun, C.B. (2004). A pathway for phosphatidylcholine biosynthesis in *Plasmodium falciparum* involving phosphoethanolamine methylation. Proc Natl Acad Sci U S A *101*, 6206-6211.
- Prigge, S.T., He, X., Gerena, L., Waters, N.C., and Reynolds, K.A. (2003). The initiating steps of a type II fatty acid synthase in *Plasmodium falciparum* are catalyzed by pfACP, pfMCAT, and pfKASIII. Biochemistry *42*, 1160-1169.
- Prommana, P., Uthaipibull, C., Wongsombat, C., Kamchonwongpaisan, S., Yuthavong, Y., Knuepfer, E., Holder, A.A., and Shaw, P.J. (2013). Inducible knockdown of *Plasmodium* gene expression using the glmS ribozyme. PLoS One *8*, e73783.

- Prudencio, M., Rodriguez, A., and Mota, M.M. (2006). The silent path to thousands of merozoites: the *Plasmodium* liver stage. Nat Rev Microbiol *4*, 849-856.
- Ralph, S.A., van Dooren, G.G., Waller, R.F., Crawford, M.J., Fraunholz, M.J., Foth, B.J., Tonkin, C.J., Roos, D.S., and McFadden, G.I. (2004). Tropical infectious diseases: metabolic maps and functions of the *Plasmodium falciparum* apicoplast. Nat Rev Microbiol *2*, 203-216.
- Ramakrishnan, S., Docampo, M.D., Macrae, J.I., Pujol, F.M., Brooks, C.F., van Dooren, G.G., Hiltunen, J.K., Kastaniotis, A.J., McConville, M.J., and Striepen, B. (2012). Apicoplast and endoplasmic reticulum cooperate in fatty acid biosynthesis in apicomplexan parasite *Toxoplasma gondii*. J Biol Chem *287*, 4957-4971.
- Ramakrishnan, S., Serricchio, M., Striepen, B., and Butikofer, P. (2013). Lipid synthesis in protozoan parasites: a comparison between kinetoplastids and apicomplexans. Prog Lipid Res *52*, 488-512.
- Roberts, V.R.M. (1989). Angewandte Chemie, Vol 102 (Wiley).
- Santiago, T.C., Zufferey, R., Mehra, R.S., Coleman, R.A., and Mamoun, C.B. (2004). The *Plasmodium falciparum* PfGatp is an endoplasmic reticulum membrane protein important for the initial step of malarial glycerolipid synthesis. J Biol Chem *279*, 9222-9232.
- Seeber, F., Limenitakis, J., and Soldati-Favre, D. (2008). Apicomplexan mitochondrial metabolism: a story of gains, losses and retentions. Trends Parasitol *24*, 468-478.
- Sharma, S., Sharma, S.K., Modak, R., Karmodiya, K., Surolia, N., and Surolia, A. (2007). Mass spectrometry-based systems approach for identification of inhibitors of *Plasmodium falciparum* fatty acid synthase. Antimicrob Agents Chemother *51*, 2552-2558.
- Sharma, S., Sharma, S.K., Surolia, N., and Surolia, A. (2009). Beta-ketoacyl-ACP synthase I/II from *Plasmodium falciparum* (PfFabB/F)--is it B or F? IUBMB Life *61*, 658-662.
- Sharma, S.K., Kapoor, M., Ramya, T.N., Kumar, S., Kumar, G., Modak, R., Sharma, S., Surolia, N., and Surolia, A. (2003). Identification, characterization, and

inhibition of *Plasmodium falciparum* beta-hydroxyacyl-acyl carrier protein dehydratase (FabZ). J Biol Chem *278*, 45661-45671.

- Shears, M.J., Botte, C.Y., and McFadden, G.I. (2015). Fatty acid metabolism in the *Plasmodium* apicoplast: Drugs, doubts and knockouts. Mol Biochem Parasitol *199*, 34-50.
- Singh, B., Kim Sung, L., Matusop, A., Radhakrishnan, A., Shamsul, S.S., Cox-Singh, J., Thomas, A., and Conway, D.J. (2004). A large focus of naturally acquired *Plasmodium knowlesi* infections in human beings. Lancet *363*, 1017-1024.
- Singh, P., Alaganan, A., More, K.R., Lorthiois, A., Thiberge, S., Gorgette, O., Guillotte Blisnick, M., Guglielmini, J., Aguilera, S.S., Touqui, L., *et al.* (2019). Role of a patatin-like phospholipase in *Plasmodium falciparum* gametogenesis and malaria transmission. Proc Natl Acad Sci U S A *116*, 17498-17508.
- Sologub, L., Kuehn, A., Kern, S., Przyborski, J., Schillig, R., and Pradel, G. (2011). Malaria proteases mediate inside-out egress of gametocytes from red blood cells following parasite transmission to the mosquito. Cell Microbiol *13*, 897-912.
- Spangenberg, T., Burrows, J.N., Kowalczyk, P., McDonald, S., Wells, T.N., and Willis, P. (2013). The open access malaria box: a drug discovery catalyst for neglected diseases. PLoS One *8*, e62906.
- Srivastava, I.K., Rottenberg, H., and Vaidya, A.B. (1997). Atovaquone, a broad spectrum antiparasitic drug, collapses mitochondrial membrane potential in a malarial parasite. J Biol Chem *272*, 3961-3966.
- Stallmach, R., Kavishwar, M., Withers-Martinez, C., Hackett, F., Collins, C.R., Howell, S.A., Yeoh, S., Knuepfer, E., Atid, A.J., Holder, A.A., *et al.* (2015). *Plasmodium falciparum* SERA5 plays a non-enzymatic role in the malarial asexual blood-stage lifecycle. Mol Microbiol *96*, 368-387.
- Swarnamukhi, P.L., Sharma, S.K., Bajaj, P., Surolia, N., Surolia, A., and Suguna, K. (2006). Crystal structure of dimeric FabZ of *Plasmodium falciparum* reveals conformational switching to active hexamers by peptide flips. FEBS Lett *580*, 2653-2660.

- Tavares, J., Formaglio, P., Thiberge, S., Mordelet, E., Van Rooijen, N., Medvinsky, A., Menard, R., and Amino, R. (2013). Role of host cell traversal by the malaria sporozoite during liver infection. J Exp Med *210*, 905-915.
- Tilley, L., Straimer, J., Gnadig, N.F., Ralph, S.A., and Fidock, D.A. (2016). Artemisinin Action and Resistance in *Plasmodium falciparum*. Trends Parasitol *32*, 682-696.
- Tischer, M., Pradel, G., Ohlsen, K., and Holzgrabe, U. (2012). Quaternary ammonium salts and their antimicrobial potential: targets or nonspecific interactions? ChemMedChem *7*, 22-31.
- Usui, M., Prajapati, S.K., Ayanful-Torgby, R., Acquah, F.K., Cudjoe, E., Kakaney, C., Amponsah, J.A., Obboh, E.K., Reddy, D.K., Barbeau, M.C., *et al.* (2019). *Plasmodium falciparum* sexual differentiation in malaria patients is associated with host factors and GDV1-dependent genes. Nat Commun *10*, 2140.
- van Meer, G., Voelker, D.R., and Feigenson, G.W. (2008). Membrane lipids: where they are and how they behave. Nat Rev Mol Cell Biol *9*, 112-124.
- Vance, J.E., and Tasseva, G. (2013). Formation and function of phosphatidylserine and phosphatidylethanolamine in mammalian cells. Biochim Biophys Acta *1831*, 543-554.
- Vaughan, A.M., O'Neill, M.T., Tarun, A.S., Camargo, N., Phuong, T.M., Aly, A.S., Cowman, A.F., and Kappe, S.H. (2009). Type II fatty acid synthesis is essential only for malaria parasite late liver stage development. Cell Microbiol *11*, 506-520.
- Venugopal, K., Hentzschel, F., Valkiunas, G., and Marti, M. (2020). *Plasmodium* asexual growth and sexual development in the haematopoietic niche of the host. Nat Rev Microbiol *18*, 177-189.
- Vial, H.J., Thuet, M.J., and Philippot, J.R. (1982). Phospholipid biosynthesis in synchronous *Plasmodium falciparum* cultures. J Protozool *29*, 258-263.
- Vielemeyer, O., McIntosh, M.T., Joiner, K.A., and Coppens, I. (2004). Neutral lipid synthesis and storage in the intraerythrocytic stages of *Plasmodium falciparum*. Mol Biochem Parasitol *135*, 197-209.

- Waller, R.F., Keeling, P.J., Donald, R.G., Striepen, B., Handman, E., Lang-Unnasch, N., Cowman, A.F., Besra, G.S., Roos, D.S., and McFadden, G.I. (1998). Nuclear-encoded proteins target to the plastid in *Toxoplasma gondii* and *Plasmodium falciparum.* Proc Natl Acad Sci U S A *95*, 12352-12357.
- Waller, R.F., Ralph, S.A., Reed, M.B., Su, V., Douglas, J.D., Minnikin, D.E., Cowman, A.F., Besra, G.S., and McFadden, G.I. (2003). A type II pathway for fatty acid biosynthesis presents drug targets in *Plasmodium falciparum*. Antimicrob Agents Chemother *47*, 297-301.
- Waters, N.C., Kopydlowski, K.M., Guszczynski, T., Wei, L., Sellers, P., Ferlan, J.T., Lee, P.J., Li, Z., Woodard, C.L., Shallom, S., *et al.* (2002). Functional characterization of the acyl carrier protein (PfACP) and beta-ketoacyl ACP synthase III (PfKASIII) from *Plasmodium falciparum*. Mol Biochem Parasitol *123*, 85-94.
- Wein, S., Ghezal, S., Bure, C., Maynadier, M., Perigaud, C., Vial, H.J., Lefebvre-Tournier, I., Wengelnik, K., and Cerdan, R. (2018). Contribution of the precursors and interplay of the pathways in the phospholipid metabolism of the malaria parasite. J Lipid Res *59*, 1461-1471.
- WHO (2019). World Malaria Report
- Witola, W.H., El Bissati, K., Pessi, G., Xie, C., Roepe, P.D., and Mamoun, C.B. (2008). Disruption of the *Plasmodium falciparum* PfPMT gene results in a complete loss of phosphatidylcholine biosynthesis via the serine-decarboxylase-phosphoethanolamine-methyltransferase pathway and severe growth and survival defects. J Biol Chem *283*, 27636-27643.
- Wrenger, C., and Muller, S. (2004). The human malaria parasite *Plasmodium falciparum* has distinct organelle-specific lipoylation pathways. Mol Microbiol *53*, 103-113.
- Yao, J., and Rock, C.O. (2013). Phosphatidic acid synthesis in bacteria. Biochim Biophys Acta *1831*, 495-502.
- Yu, M., Kumar, T.R., Nkrumah, L.J., Coppi, A., Retzlaff, S., Li, C.D., Kelly, B.J., Moura, P.A., Lakshmanan, V., Freundlich, J.S., *et al.* (2008). The fatty acid

biosynthesis enzyme FabI plays a key role in the development of liver-stage malarial parasites. Cell Host Microbe *4*, 567-578.

- Zhang, M., Wang, C., Otto, T.D., Oberstaller, J., Liao, X., Adapa, S.R., Udenze, K., Bronner, I.F., Casandra, D., Mayho, M., *et al.* (2018). Uncovering the essential genes of the human malaria parasite *Plasmodium falciparum* by saturation mutagenesis. Science *360*.
- Zidovetzki, R., Sherman, I.W., Prudhomme, J., and Crawford, J. (1994). Inhibition of *Plasmodium falciparum* lysophospholipase by anti-malarial drugs and sulphydryl reagents. Parasitology *108 (Pt 3)*, 249-255.

Publications

Research Articles

- **Pradeep Kumar**, Monika, Vandana Thakur and Asif Mohmmed. *Glm*S mediated knock-down of a phospholipase expedite alternate pathway to generate phosphocholine required for phosphatidylcholine synthesis in *Plasmodium falciparum.* **Biochem J (under peer review)**

- **Pradeep Kumar**, Yoshiki Yamaryo-Botté, Vandana Thakur, Mudassir M. Banday, Cyrille Y. Botté and Asif Mohmmed. A *Plasmodium* lysophospholipase localized in parasitophorous vacuole plays essential role in schizogony and proliferation of asexual stages. **(Manuscript under preparation)**

- Photosensitized INA-Labelled protein 1 (PhIL1) is novel component of the inner membrane complex and is required for *Plasmodium* parasite development. Ekta Saini, Mohammad Zeeshan, Declan Brady, Rajan Pandey, Gesine Kaiser, Ludek Koreny, **Pradeep Kumar**, Vandana Thakur, Shreyansh Tatiya, Nicholas J. Katris, Rebecca Stanway Limenitakis, Inderjeet Kaur, Judith L. Green, Andrew R. Bottrill, David S. Guttery, Ross F. Waller, Volker Heussler, Anthony A. Holder, Asif Mohmmed, Pawan Malhotra & Rita Tewari. **Scientific Reports**; volume 7, Article number: 15577 (2017)

- Unravelling a novel PhIL1-glideosome associated complex in *Plasmodium falciparum* IMC that is essential for merozoite invasion of RBCs. Ekta Saini, **Pradeep Kumar**, Vaibhav Sharma, Inderjeet Kaur, Asif Mohmmed and Pawan Malhotra. **(Manuscript under preparation)**

Book Chapter

- Asad M, Muneer A, **Kumar P**, Thakur V, Rathore S, Malhotra P, Mohmmed A. 2019. Road towards development of new anti-malarials: Organelle associated metabolic pathways in *Plasmodium* as drug- targets and discovery of lead drug candidates. In Hameed, S, Zeeshan, F (eds), **Pathogenicity and Drug Resistance of Human Pathogens: mechanisms and novel Approaches. Springer, Singapor**e